Structural studies in the Southern Province, south of Sudbury, Ontario

by

Daniel J. Redmond

A Thesis

submitted to the Department of Geological Sciences

in partial fulfillment of the requirements

for the degree of

Master of Science

October 1992

Brock University

St. Catharines, Ontario

Abstract

Rocks correlated with the Hough Lake and Quirke Lake Groups of the Huronian Supergroup form part of a northeasterly trending corridor that separates 1750 Ma granitic intrusive rocks of the Chief Lake batholith from the 1850 Ma mafic intrusive rocks of the Sudbury Igneous Complex. This corridor is dissected by two major structural features; the Murray Fault Zone (MFZ) and the Long Lake Fault (LLF). Detailed structural mapping and microstructural analysis indicates that the LLF, which has juxtaposed Huronian rocks of different deformation style and metamorphism grade, was a more significant plane of dislocation than the MFZ. The sense of displacement along the LLF is high angle reverse in which rocks to the southeast have been raised relative to those in the northwest. South of the LLF Huronian rocks underwent ductile deformation at amphibolite facies conditions. The strain was constrictional, defined by a triaxial strain ellipsoid in which $X > Y > Z$. Calculations of a regional k value were approximately 1.3. Penetrative ductile deformation resulted in the development of a preferred crystallographic orientation in quartz as well as the elongation of quartz grains to form a regional southeast-northwest trending, subvertical lineation. Similar lithologies north of the LLF underwent dominantly brittle deformation under greenschist facies conditions. Deformation north of the LLF is characterized by the thrusting of structural blocks to form angular discordances in bedding orientation which were previously interpreted as folds. Ductile deformation occurred between 1750 and 1238 Ma and is correlated with a regional period of south over north reverse faulting that effected much of the southern Sudbury region.

Post dating the reverse faulting event was a period of sedimentation as a conglomerate unit was deposited on vertically bedded Huronian rocks. Rocks in the study area were intruded by both mafic and felsic dykes. The 1238 Ma mafic dykes appear to have been offset during a period of dextral strike slip displacement along the major faults. Indirect evidence indicates that this event occurred after the thrusting at 950 to 1100 Ma associated with the Grenvillian Orogeny.

Acknowledgements

First and foremost I would like to thank Dr. Frank Fueten for his committed supervision, guidance and most of all patience through these last three years. It was a true pleasure to work with you Frank. Also I wish to thank Dr. Rich Cheel, Dr Greg Finn and Dr Jack Henderson for service on my committee and their input towards the completion of this thesis.

To Chris Kimmerly (co founder of the PreCambrian Think Tank and number 1 pub crawl partner), Paula MacKinnon and Rich (the scale suit) Seabright, I wish to convey my thanks and gratitude for their assistance. I also want to express a very special thank you to Kristen Booth and her family. Getting to know you all was one of the great pleasures of the last 2 years. Kristen I hope you enjoy your Masters as much as I did, Good Luck!

Finally and most importantly, I dedicate this thesis to my parents and family who have always been their for me and knew that I was capable of great things, Thank you!

Table of Contents

List of Figures

List of Tables

Chapter 1

Introduction

Metasedimentary and metavolcanic rocks of the Huronian Supergroup form a northeast trending corridor that separates the Proterozoic granitoid suites of the Grenville Front Tectonic Zone to the southeast from the intrusive rocks of the Sudbury Igneous Complex to the northwest (Figure 1.1).

The geology of the area is structurally complex. The rocks have been influenced by the effects of several deformational events including the Penokean Orogeny (Brocoum and Dalziel 1974; Van Schmus 1976; Card et al. 1984), the 1850 Ma Sudbury Event (Krogh et al. 1982), Post-Sudbury event deformation (1600 to 1300 Ma.) (Shanks and Schwerdtner 1989, Henderson 1972) and the 1000-1200 Ma Grenvillian orogeny (Davidson 1986).

Based on field observations the Huronian rocks in the study area are more intensely deformed than their equivalents in the Espanola region to the southwest and the Coniston area to the northeast. The area is structurally interesting because of its location with respect to the Grenville Front and the Sudbury Structure. The area is also cut by the Murray Fault (MF) which is a major structural feature in the Southern Province.

The area examined in this study encompasses approximately 170 km^2. It is bounded to the north by Highway 17 and the city of Sudbury. To the south the area extends to the contact between the Chief Lake batholith and the Huronian metasedimentary rocks. To the west the study area is bounded by the eastern border of the Whitefish Lake Indian Reserve and extends to the eastern tip of McFarlane Lake in the east.

A detailed geological map of the area was developed based on data collected during

quartz c-axis fabrics and deformed grain shape analysis using computer based Autocorrelation Function. Structural petrology provided insight into the intensity and style of deformation along the major faults.

The objectives of this study are to; 1) correlate the lithologic units in the area with formations of the Huronian Supergroups, 2) document the type and intensity of deformation in the area, 3) determine the sense of displacement along the major faults in the area, 4) determine the timing of the different deformational and metamorphic events that have effected the rocks in the study area and 5) discuss implications of deformation in the area that effect regional tectonic synthesis of the Sudbury area.

The rocks in the study area have been correlated with the Hough Lake Group and the lower Quirke Lake Group. The metasedimentary rocks which were deposited between 2500 and 2219 Ma (Corfu and Andrews 1986) have been intruded by 2219 Ma Nipissing gabbro rocks as well as 1238 Ma (Krogh et al. 1987) olivine diabase dykes and rhyolitic felsic dykes of unknown age. Although deformation has disrupted the stratigraphy, the rocks are progressively higher in the stratigraphic order from north to south. Rocks in the study area have been metamorphosed to between middle greenschist and middle amphibolite facies. The study area is transected by two major structural features: the previously examined Murray Fault Zone (MFZ) (Card and Hutchinson 1972; Zolnai et al. 1984) and the previously unrecognized Long Lake Fault (LLF) (Figure 1-1). Much of the deformation in the area can be attributed to displacement along these faults.

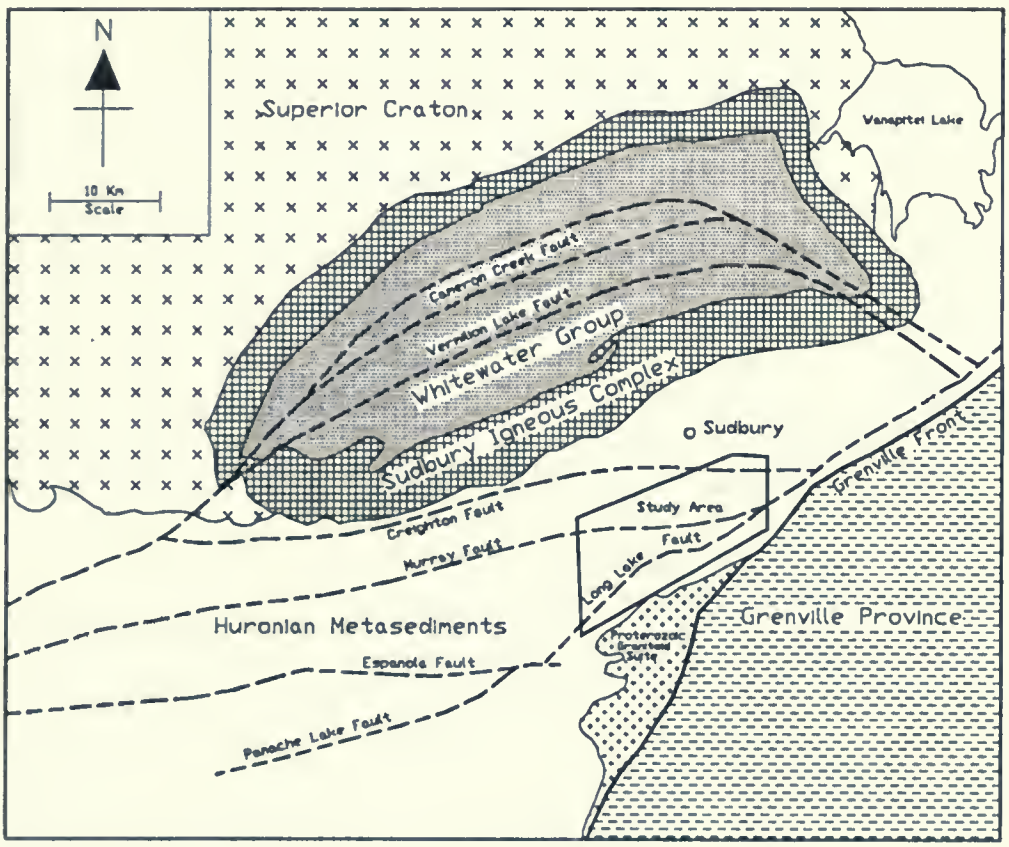

Figure 1-1: Map of the Sudbury region showing the location of the major geological features and the location of the study area.

Chapter 2

Stratigraphy and Petrology

Rocks of the Huronian Supergroup form an early Proterozoic assemblage of volcanics and dominantly terrestrial clastic sedimentary rocks. The sediments were deposited between 2500 Ma and 2219 Ma (Corfu and Andrews 1986; Card et al. 1977) and are characterized by a cyclical repetition of conglomerate, mudstone and quartz-feldspar arenite which form a Group. Based on the development of 4 repeating cycles the Huronian Supergroup has been subdivided in ascending order into four groups, namely the Elliot Lake, Hough Lake, Quirke Lake, and Cobalt groups. Rocks in the study area have been correlated with the Hough Lake Group and the lower Quirke Lake Group (Table 2-1).

2.1 Ramsay Lake Formation (Hough Lake Group)

Conglomerates correlated with the Ramsay Lake Formation are exposed in several locations along the northwestern perimeter of the study area and consist of matrix supported, polymictic conglomerates with clasts of white quartz, white granites and mafic greenstone. The size distribution is bimodal with 5 to 10 cm clasts forming the large fraction within a matrix containing quartz microclasts which are 2 to 10 mm in size. The matrix is composed of muscovite and fine grained quartz with minor amounts of biotite and chlorite (Figure 2-1). The unit displays random sorting and bedding is rare (Figure 2-2).

North of Robinson Lake, the conglomerate has been tectonically brecciated. In this area, the Ramsay Lake Formation is up to 500 m thick.

Table 2-1. Stratigraphy of the Huronian Supergroup (from Debicki, 1990)

Cobalt Group	Bar River Formation	sandstone, siltstone
	Gordon Lake Formation	siltstone argillite, sandstone
	Lorrain Formation	sandstone, minor conglomerate and siltstone
	Gowganda Formation	conglomerate, argillite, siltstone, sandstone
	Local Disconformity	
Quirke Lake Group	Serpent Formation	sandstone, siltstone, limestone, conglomerate
	Espanola Formation	limestone, dolostone,siltstone, sandstone
	Bruce Formation Lauzon Member	conglomerate, sandstone, siltstone
	Local Disconformity	
Hough Lake Group	Mississagi Formation	sandstone, siltstone, argillite conglomerate
	Pecors Formation	siltstone, argillite, sandstone
	Ramsay Lake Formation	conglomerate, sandstone, siltstone
	Local Disconformity	
Elliot Lake Group	McKim Formation	argillite, siltstone, sandstone
	Matinenda Formation	sandstone, siltstone, argillite conglomerate
	Copper Cliff Formation	rhyolite, dacite felsic intrusions, porphyry, crystal tuff, pyroclastic, minor meta-basalt and metasediments
	Stobie Formation	metabasalt, fragmental mafic metavolcanic, mafic schist
	Salmay Lake Formation	metabasalt, fragmental mafic metavolcanics, metasediments
	Elsie Mountain Formation	metabasalt, minor metasediments

2.2 Pecors Formation

Quartz-rich pelites of the Pecors Formation conformably overlie the Ramsay Lake Formation. The mineralogy of the Pecors Formation is dominated by muscovite and/or

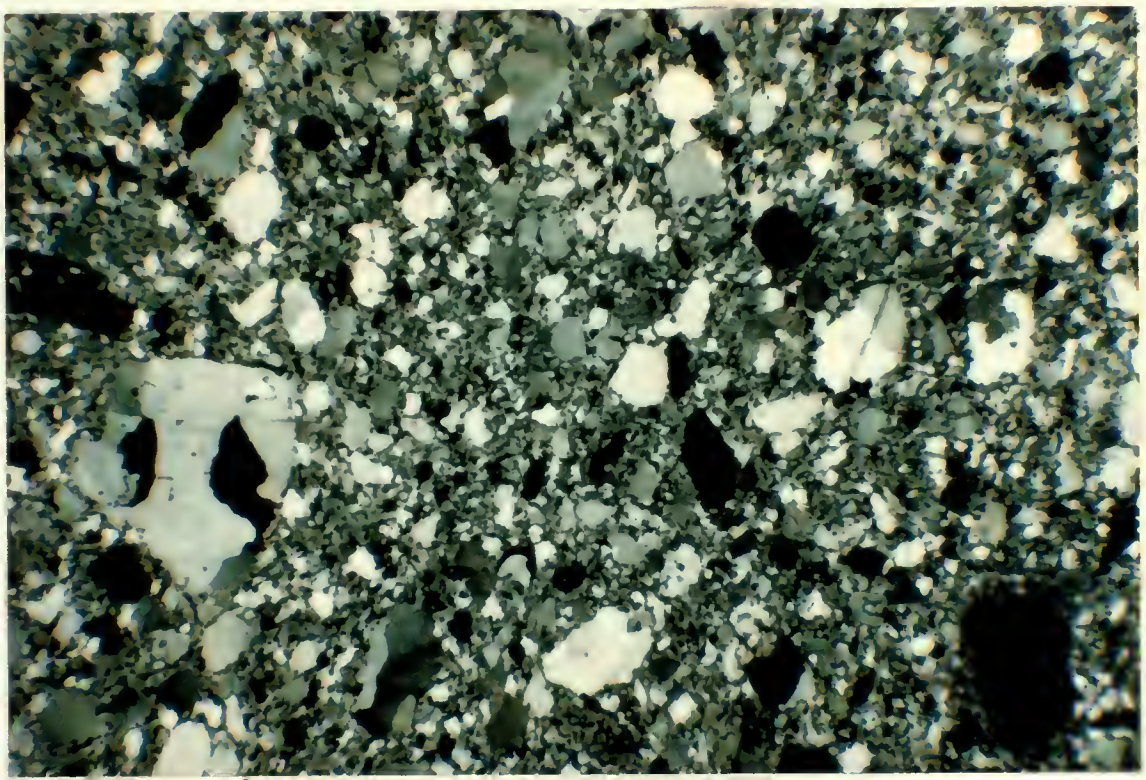

Figure 2-1 (top): Photomicrograph of Ramsay Lake Formation Conglomerate (crossed polars). Bottom of photo is 10 mm in length.

Figure 2-2 (left): Remnant bedding in the Ramsay Lake Conglomerate.

biotite, fine grained quartz, chlorite and minor amounts of plagioclase feldspar (Figure 2-3). The unit displays a well developed slaty cleavage and small scale sedimentary structures, including climbing ripples and small scale trough cross strata. The contact with the underlying Ramsay Lake Formation is gradational over several metres and is marked by the disappearance of large clasts. In the map area, the Pecors Formation ranges in thickness from 10 m to 100 m.

2.3 Mississagi Formation

Feldspathic quartzite correlated with the Mississagi Formation is the dominant rock type in the map area and comprises approximately 80% of the total exposure. The Mississagi Formation consists of 50 to 60% quartz, 20 to 30% feldspar and 5 to 10% biotite and/or muscovite (Figure 2-4). Fresh surfaces range in colour from dull grey to pale green. Bedding is well developed with bed thickness ranging from a few centimetres up to one metre (Figure 2-5). In most instances, cross-bedded quartzite beds are separated by thin (1 to 5 cm) pelitic interbeds. The Mississagi Formation also includes lenses of finer grained greywacke to subgreywacke. Thicknesses of these lenses ranges from 2 to 20 metres. These units are stratigraphically bound within the coarser grained planar crossbedded quartzites more typical of the Mississagi Formation.

Primary sedimentary structures are generally preserved in the Mississagi Formation, although many have been deformed. Planar crossbedding is the dominant sedimentary structure with lesser common, 10 cm scale trough crossbedding (Figure 2-6). The contact with the underlying Pecors Formation is abrupt but conformable. Within the lower 50 metres of the Mississagi Formation, thick (1 to 2 metres) lenses of greywacke are common.

Due to the structural complexities, the total thickness of the formation cannot be

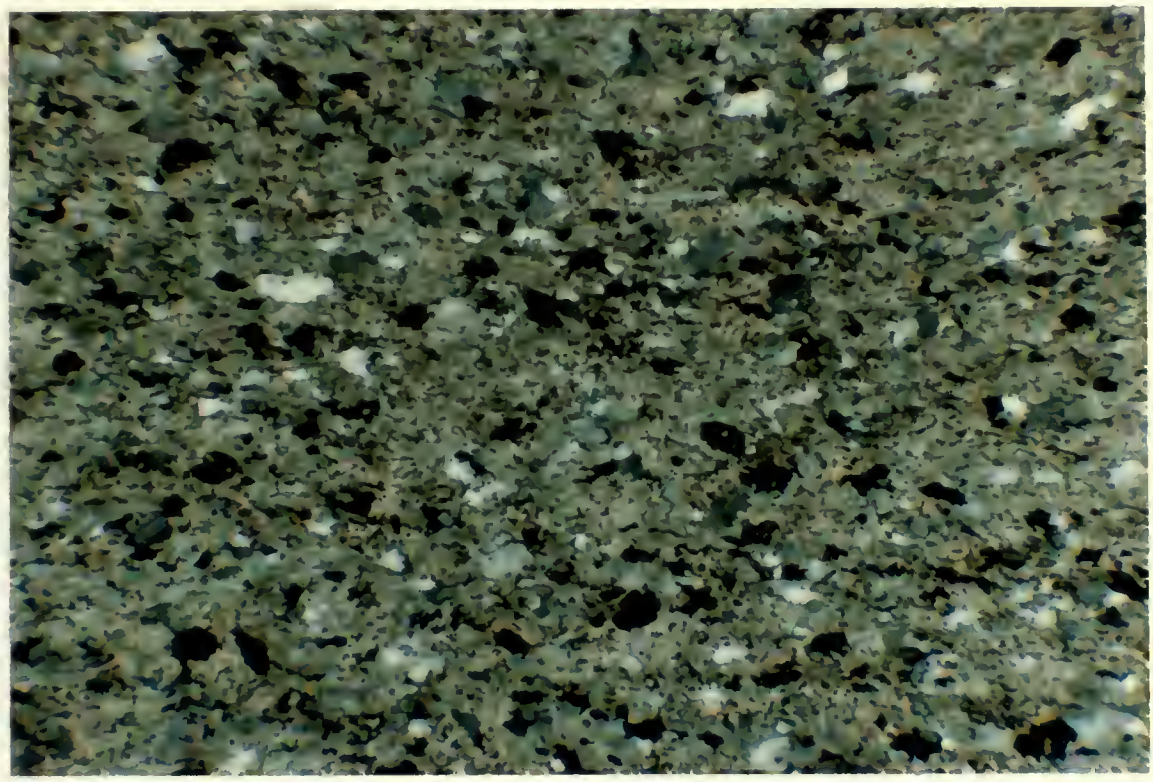

Figure 2-3: Photomicrograph of Pecors Formation pelites (crossed polars). Bottom of photo is 4 mm in length.

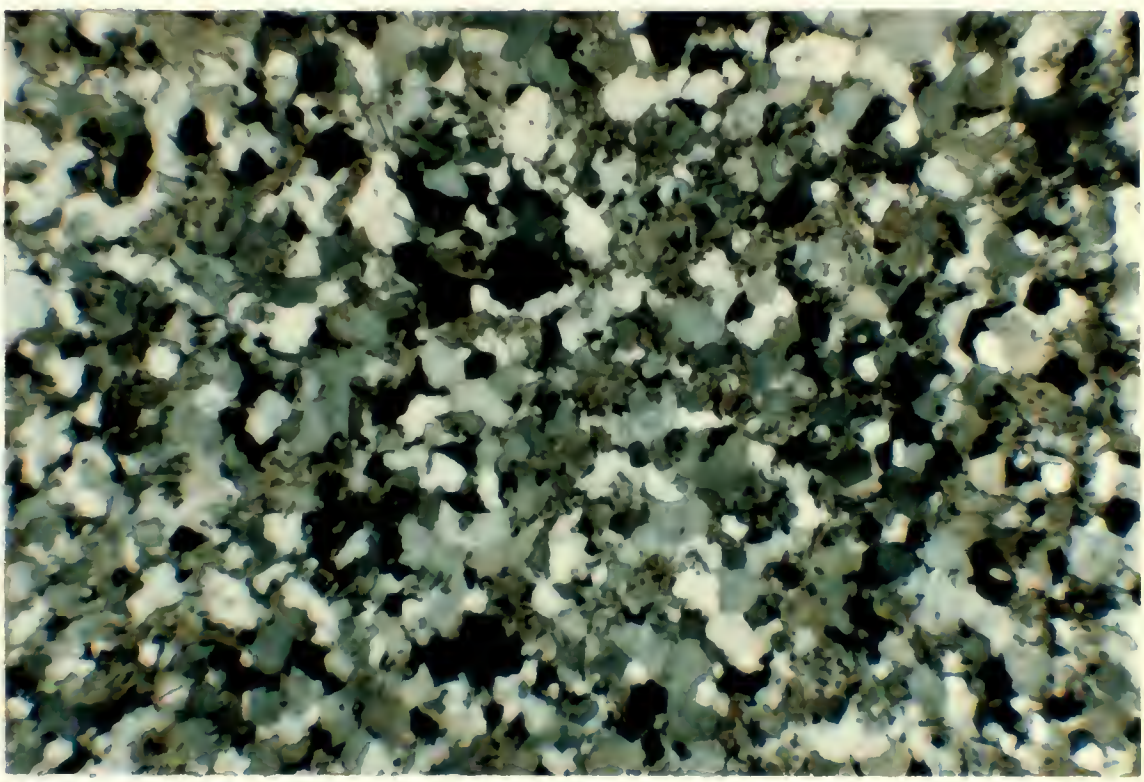

Figure 2-4: Photomicrograph of Mississagi Formation Quartzite (crossed polars). Bottom of photo is 10 mm in length.

Figure 2-5: Photo of vertical bedding in Mississagi Formation quartzite south of the Murray Fault.

Figure 2-6: Photo of well developed planar crossbedding in Mississagi Formation quartzites.

determined in the map area. Estimates of the total thickness of the unit vary considerably from less than 425 m to 3000 m (Dressler 1984b).

2.4 Bruce Formation (Quirke Lake Group)

Pebbly greywacke to conglomerate forms a large outcrop in the southwestern corner of the map area and has been identified as belonging to the Bruce Formation by several workers (Card et al. 1977; Henderson 1967; Collins 1938). In the map area this conglomerate can be described as a matrix supported, polymictic conglomerate with clast size ranging from 1 to 10 cm on average with a few as large as 50 cm in diameter. The unit is massive and displays no apparent sorting of clast size or type. Clast types include both white and yellow quartzite, coarse grained white granite and minor amounts of greenstone. Clasts range from well rounded to angular depending on size with the larger clasts, dominantly white granite being typically angular whereas the smaller quartzite clasts are generally well rounded. The matrix is composed of equal proportions of fine grained quartz and muscovite with lesser amounts of biotite (Figure 2-7). In outcrop fresh surfaces the matrix is blueish grey while weathered surfaces are rusty red. The matrix contains abundant well rounded micro-clasts (dominantly quartzite).

The outcrop of Bruce Formation is bound by southerly-dipping Mississagi Formation. The contact with the Mississagi Formation is sharp and appears unconformable. The southern limit of the conglomerate is delineated by a large shear zone. The southwestern edge of the Bruce Formation outcrop has been intruded by Nipissing gabbro. At the northeastern edge of the outcrop, the conglomerate is intruded by a pink granite believed to be a phase of the Chief Lake batholith (Henderson 1967) dated at 1750 Ma by Krogh (1970). In the area the maximum thickness of the Bruce conglomerate is 800 m. Henderson (1967) proposed that

this outcrop is the location of syncline fold axis with Bruce Formation in the core. The discontinuity of the Bruce Formation in the area is more likly the result faulting and the unconformity between the Bruce and Mississagi is a tectonic one.

2.5 Conglomerates not Formally Assigned

Conglomerate not formally assigned to a Huronian formation crops out in several locations north and at one location on the south shore of Long Lake. The conglomerates closely resemble the Bruce Formation described south of Long Lake, with a few notable exceptions. Pink granite clasts from 5 cm to 2 m in diameter are dispersed throughout the conglomerate (Figure 2-8). These granites may be loosely categorized as coarse grained or fine grained varieties and vary from unfoliated to poorly foliated. Pink granite has rarely been reported from the lower formations of the Huronian Supergroup, with the notable exception documented by Long (1977). The conglomerate also contains quartzite clasts, possibly derived from the Mississagi Formation, as large as 15 m in diameter (Figure 2-9). Based on petrological examination the matrix of the conglomerate is gritty and contains less muscovite and more quartz than the matrix of Huronian conglomerates of the Bruce or Ramsay Lake Formations (Figure 2-10). The conglomerate unconformably overlies Mississagi Formation, but the nature of the unconformity is uncertain (Figure 2-11). Olivine diabase dykes of the Sudbury Swarm (1238 Ma; Krogh et al. 1987) intrude the conglomerate. Several hypotheses for the origin of these conglomerates can be advanced:

1. The conglomerate outcrops are located along strike with an extensive chain of Bruce conglomerate that extends westward along the north shore of Panache Lake. This conglomerate is similar to that of the Bruce Formation in the southwest corner of the study area. However, no pink granite clasts were identified in the Bruce Formation where it crops

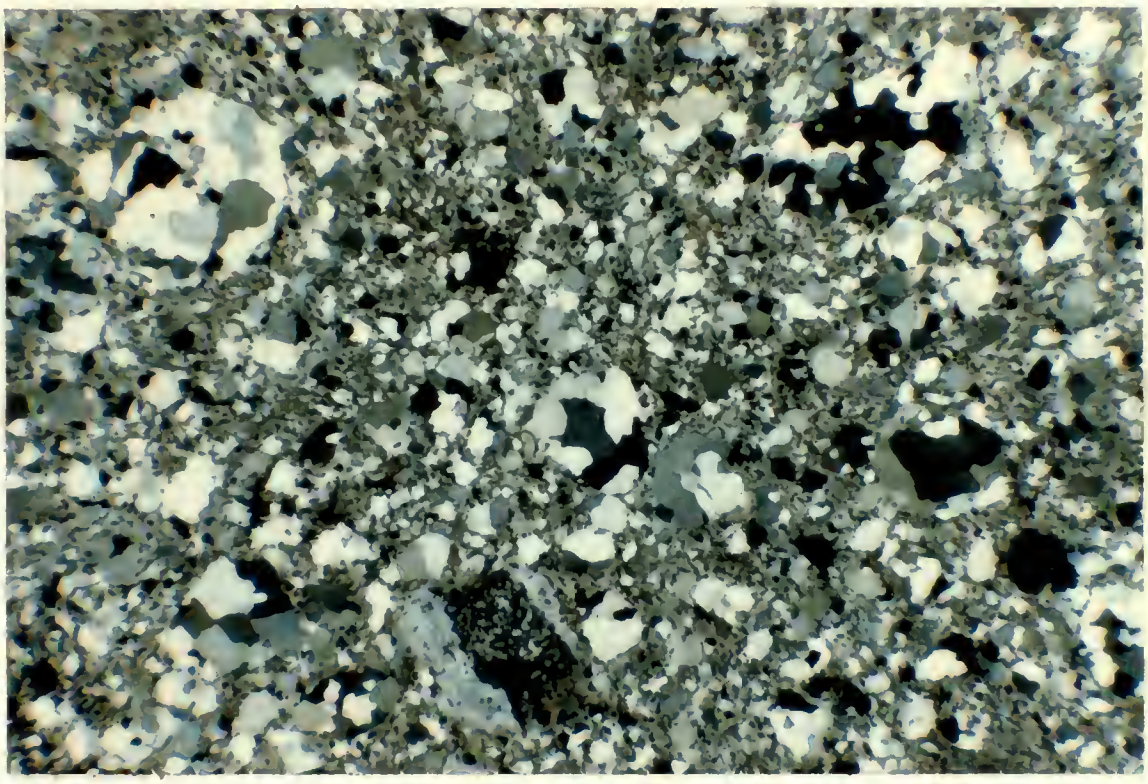

Figure 2-7: Photomicrograph of Bruce Formation Conglomerate (crossed polars). Bottom of the photo is 14 mm in length.

Figure 2-8: Photo of large pink granite clasts in conglomerate north of Long Lake. Mr Seabright is calibrated into 10 cm intervals for scale.

Figure 2-9: Photo of large quartzite clast within the conglomerate north of Long Lake. The clasts area believed to be part of the Mississagi Formation. The person is standing near the contact of a 15 m long clast. Note the smaller quartzite clast to the left.

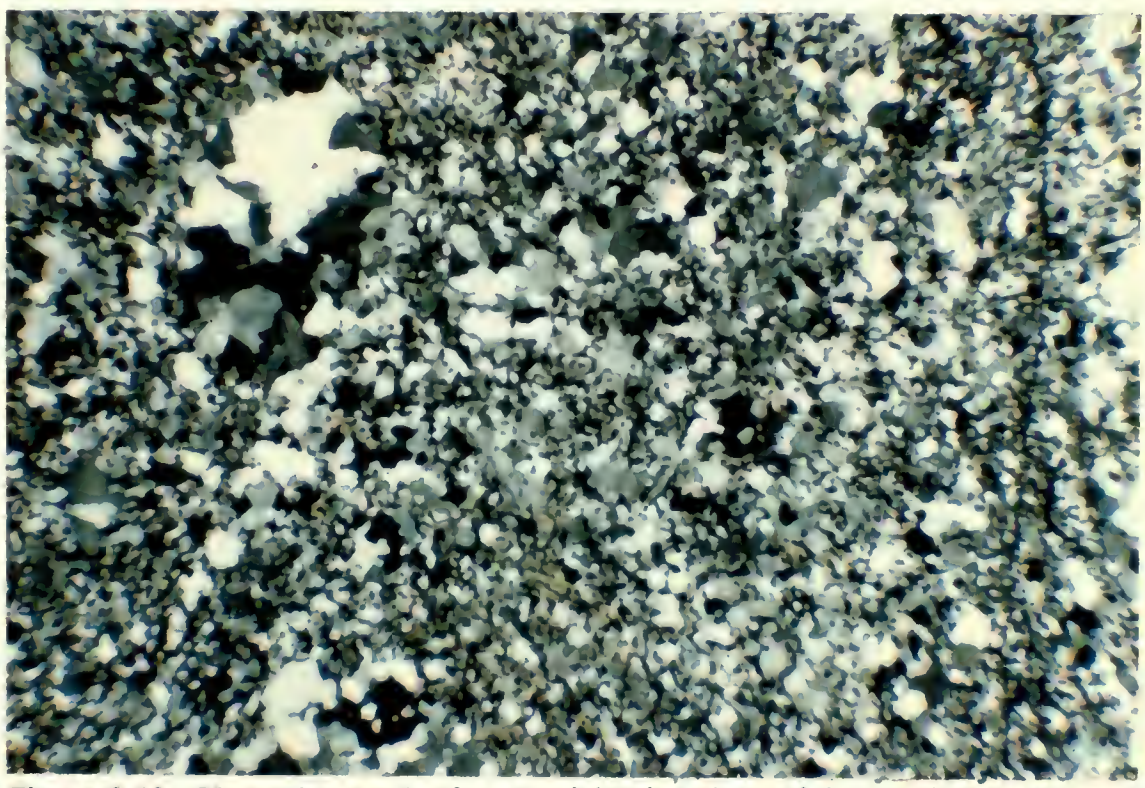

Figure 2-10: Photomicrograph of quartz rich mineralogy of the conglomerate north of Long Lake (crossed polars). Bottom of photo is 14 mm in length.

out south of Long Lake. If these conglomerates are part of the Bruce Formation, an explanation for the pink granite clasts may be that the northern and southern outcrops of the Bruce Formation have different source regions, or else the deformation has resulted in juxtaposing different horizons of the Bruce Formation.

2) Conglomerates described as Ramsay Lake Formation have been reported by Collins (1938) and Davidson (1992) near the shore of Richard Lake. These outcrops are roughly on strike with the unassigned conglomerates. Davidson's (1992) Ramsay Lake Formation is conformably overlain by a conformable Pecors Formation, which in turn is conformably overlain by feldspathic quartzites of the Mississagi Formation. This stratigraphic correlation is in contrast to that of the undefined conglomerates described above in which gritty conglomerates unconformably overly Mississagi Formation.

While quartz pebbles are commonly reported within the Ramsay Lake Formation, large quartzite clasts have not been reported. The large clasts present in the unassigned conglomerate would have to be of some unit other than Mississagi Formation, as the Mississagi Formation is younger than the Ramsay Lake Formation.

3) Thompson (1962) mapped the gritty conglomerates described above as intraformational members within the Wanapitei unit (now Mississagi Formation) of the Sudbury Group. He was unconvinced that the conglomerate represented either the Ramsay Lake or Bruce Formations as it was bound by atypical Mississagi feldspathic quartzites.

Following a detailed examination of the upper Mississagi and Bruce Formation contact, Long (1977) described intraformational conglomerate units associated with the transition between shallow water sedimentation responsible for deposition of the Mississagi Formation and glacial deposition of the overlying Bruce Formation. The unit comprises a sequence of resedimented conglomerates (the Lauzon Member) which unconformably overlies

planar crossbedded quartzites of the Mississagi Formation. Conglomerates of the Lauzon Member are in turn overlain by horizontally laminated quartzite. The Lauzon Member is a boulder to pebble conglomerate with a very poorly sorted matrix including both white and red-pink granite, quartzite and a lesser component of greenstone. Clasts are generally subrounded to well rounded. In an undeformed state, most clasts are approximately equidimensional so no preferred clast orientation is apparent (Long 1977). Conglomerates of the Lauzon Member were likely deposited from sediment gravity flows within a series of subaqueous fans or fan head valleys which may have been initiated by normal fault movement along the MF system at the onset of Bruce glaciation (Long, 1977).

4) Another explanation for these conglomerates is that they represent a post-Huronian sedimentation event. The source of the pink granites may be the Chief Lake batholith (1750 Ma, Krogh 1970) which is located less than a kilometre south of the conglomerate exposure. To test this hypothesis pink granite clasts were collected for U-Pb geochronology at the Royal Ontario Museum. Zircons extracted from the clasts yield an age > 2640 Ma (Heaman, 1992, pers.com.) making the source of these clasts clearly Archean. The presence of Archean pink granite clasts, which where not observed in the Ramsay Lake Formation, provide a strong correlation between this conglomerate and those described as the Lauzon Member at the base of the Bruce Formation by Long (1977).

Based on field relationships, mineralogy and clast types, these outcrops of conglomerate are considered to be part of the Lauzon Member of the Lower Bruce Formation. This is supported by the unit's sharp contact with the underlying Mississagi Formation. There is no appearance of the greywacke similar to the Pecors Formation separating the conglomerate from the Mississagi Formation. The presence of possible clasts of Mississagi quartzite indicate that the conglomerate postdates deposition of the Mississagi Formation and

that the Mississagi Formation was lithified prior to the depostion of the Lauzon Member. Long (1977) documented that clasts of both the Ramsay Lake and Pecors Formations were present in the Lauzon Member. The debris flow model attributed to the deposition of the Lauzon Member would provide a sufficient transport mechanism to explain the 15 m diameter clasts of Mississagi quartzite in the conglomerate. The mineralogy of this unit is more quartz-rich than either the Ramsay or Bruce Formations in the study area. This study was the first to identify conglomerates of the Lauzon Member as far east as Sudbury.

2.6 Unconformable Conglomerate

A small outcrop of conglomerate is located 500 m north of McFarlane Lake. The total area of the outcrop is less than 100 m^2. This subhorizontal conglomerate unconformably overlies vertically bedded Mississagi Formation. The unit can be described as a monomictic, unimodal matrix to very locally clast supported conglomerate. The single clast type present is white quartz that may be either vein quartz or very clean quartzite. Quartz clasts range in size from 1 to 3 cm in diameter, and are generally angular in shape. The matrix consists of quartz, plagioclase and lesser amounts of biotite and muscovite; quartz and plagioclase have undergone some recrystallization (Figure 2-12). The clast supported constituent of the unit appears to develop in narrow channels which form in the shallow gullies between vertical beds of Mississagi Formation. The contact with the Mississagi Formation is erosional and the conglomerate is no more than 0.5 m thick, giving it the appearance of a thin blanket (Figure 2-13, 2-14). The conglomerate is foliated but is less deformed than the underlying Mississagi Formation. Based on the configuration of the conglomerate-quartzite contact and the development of cross cutting structures, this unit is unlikely a Huronian aged channel that cut through horizontal Mississagi Formation rocks (R. Cheel, 1992, pers. com.).

Figure 2-11: Photo of the sharp contact between the Lauzon Member Conglomerate (top and the Mississagi Formation quartzite).

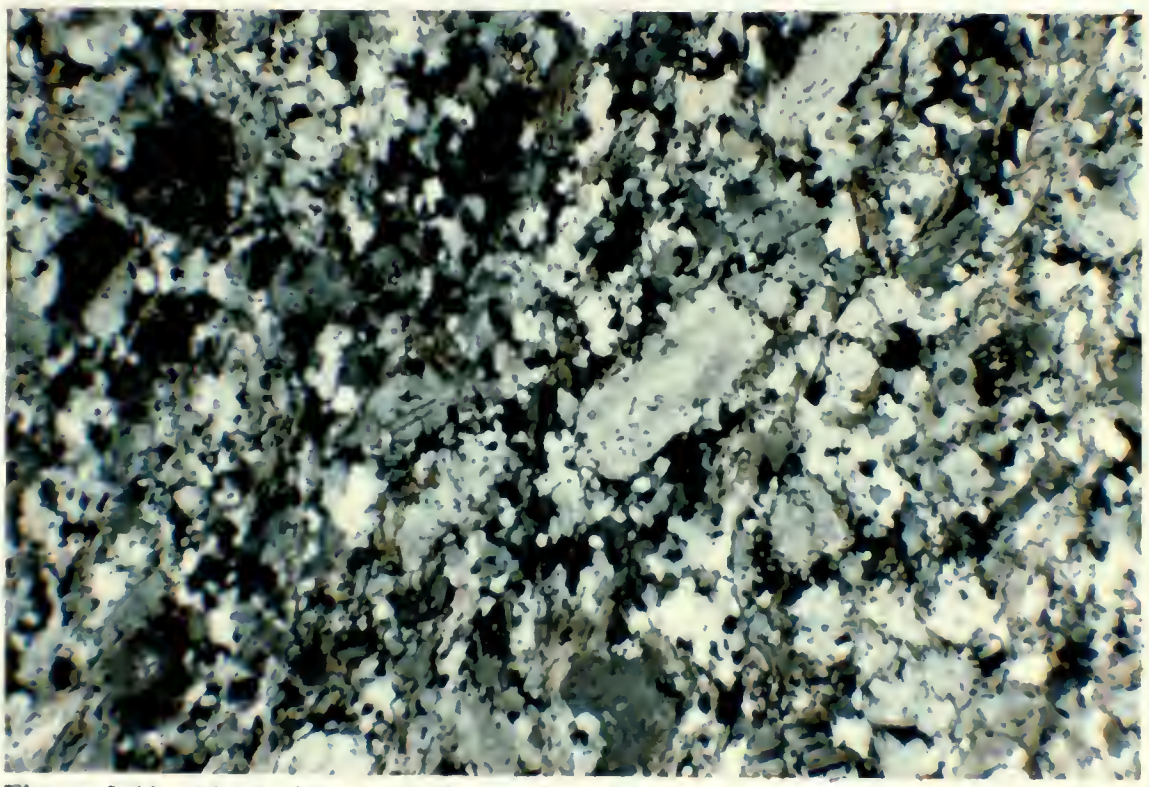

Figure 2-12: Photomicrograph of unconformable conglomerate (crossed polars). Bottom of the photo is 8 mm in length.

Figure 2-13: Photo of sharp erosional contact between the Unconformable conglomerate and the Mississagi quartzite.

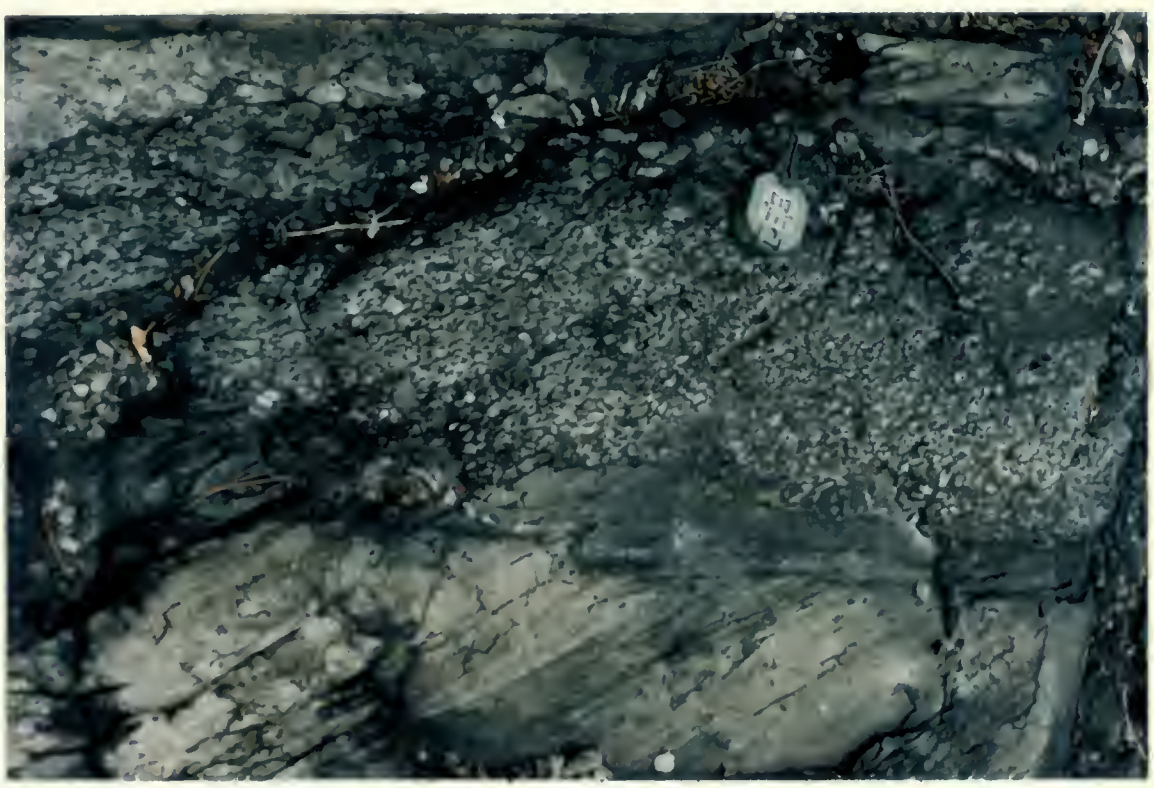

Figure 2-14: Photo of thin blanket of Unconformable conglomerate overlying vertically bedded Mississagi quartzite. Note the well developed planar crossbedding in the quartzite.

This conglomerate appears to have formed during a post-Huronian sedimentation event. Based on the monomictic nature and limited occurrence it appears to be locally constrained event. No similar conglomerates have been reported in the region and no other outcrops of this conglomerate occur in the map area.

2.7 Nipissing gabbro

Nipissing gabbro (2219 Ma; Corfu and Andrews 1986) intrudes Huronian metasedimentary rocks in many locations and is the second most dominant lithology in the area. Nipissing gabbroic rocks can range in occurrence from large intrusive masses hundreds of metres in diameter to dykes several metres in width. In most cases, gabbro outcrops trend in a southwest-northeasterly direction. It is unclear whether this is the original intrusive configuration or is due to tectonic displacement. This trend is most notable south of Long Lake. The gabbroic rocks are more resistant to erosion than the surrounding metasediments.

Nipissing gabbro is dull green on fresh surfaces. In an unaltered state, Nipissing gabbro consists of coarse grained plagioclase, clinopyroxene, hornblende, magnetite and pyrite (Figure 2-15). In several locations the gabbro has been brecciated.

2.8 Olivine Diabase Dykes

Olivine diabase dykes of the Sudbury Swarm (1238 Ma; Krogh et al., 1987) cut all rock types in the area. The dykes trend in a northwest direction and range in width from 30 cm to 5 m. Several of these dykes crop out along Long Lake road, near Long Lake. They consist of anhedral grains of olivine, plagioclase, and clinopyroxene (Figure 2-16). Phenocrysts of plagioclase are as large as 3 cm in length. It has not been possible to trace any of these dykes across the Murray Fault.

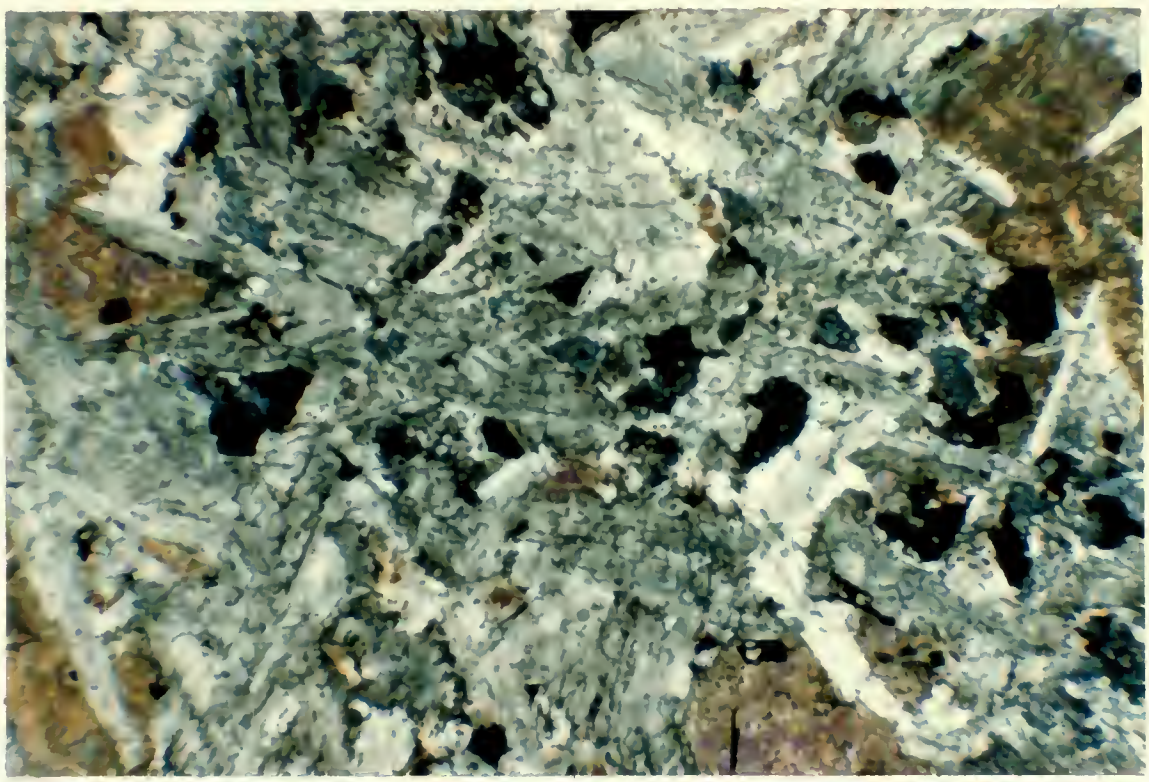

Figure 2-15: Photomicrograph of Nipissing Gabbro (crossed polars). Bottom of photo is 10 mm in length.

Figure 2-16: Photomicrograph of coarse grained olivine diabase dyke (crossed polars). Bottom of the photo is 10 mm in length.

2.9 Late Rhyolitic Felsic Dykes

In several locations, felsic dykes with a rhyolitic composition cut the Mississagi Formation. The most notable outcrop is located in a road cut on Long Lake Road near Silver Lake. The dyke trends in a southwesterly direction and is approximately 1 m wide. Similar outcrops of felsic dykes were found on the south shore of Crooked Lake and the north shore of Long Lake. It appears from the outcrop locations that this is a single dyke. The dyke is composed of phenocrysts of quartz, zoned plagioclase and orthoclase in a fine grained matrix of quartz, biotite and muscovite (Figure 2-17).

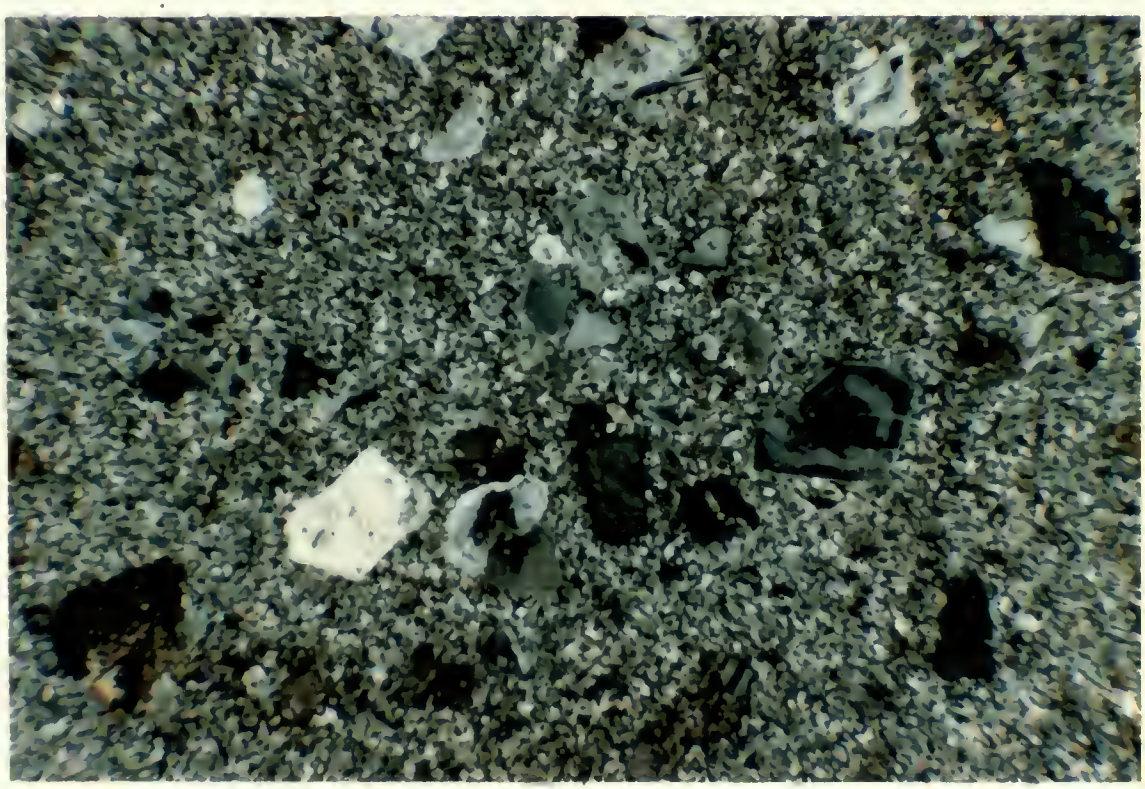

Figure 2-17: Photomicrograph of Rhyolitic felsic dyke (crossed polars). Bottom of the photo is 8 mm in length.

Chapter 3

Metamorphic History

3.1 Introduction

The study area can be divided into two metamorphic zones with Long Lake and McFarlane Lake as the boundary reflecting variation in metamorphic facies. Determination of the metamorphic facies in each area is based on the presence of specific metamorphic minerals. Rock units south of Long Lake and McFarlane Lake display metamorphic mineral assemblages characteristic of lower to middle amphibolite facies while the rocks north of the lakes display mineral assemblages more characteristic of middle greenschist facies. Classification of P-T conditions for metamorphic facies follows that of Turner (1980) (Figure 3-1).

In discussing metamorphism, lithologic units have been divided into two groups, namely pelitic to semipelitic and quartzofeldspathic lithologies and are considered separately. No detailed investigation of the mafic intrusives (Nipissing gabbro) was performed. Interpretation of metamorphic history is based on thin section petrology and field observations.

3.2 Amphibolite facies rocks

Lithologies south of the Long Lake and McFarlane Lake have been ductilely deformed and petrological evidence indicates they were metamorphosed at lower to middle amphibolite facies. The following mineral associations were observed in quartzofeldspathic rocks:

1) quartz - plagioclase - alkali feldspar - muscovite - biotite - chlorite - epidote
2) quartz - plagioclase - alkali feldspar - muscovite - biotite - chlorite
3) quartz - plagioclase - alkali feldspar - muscovite - biotite
4) quartz - plagioclase - alkali feldspar - muscovite - chlorite
5) quartz - plagioclase - alkali feldspar - muscovite
6) quartz - muscovite - biotite
7) quartz - plagioclase - alkali feldspar - biotite - garnet

Within the lithologies south of Long Lake and McFarlane Lake, garnet was only observed in two thin sections (Figure 3-2). Feldspar grains (both plagioclase and alkali feldspar) in most cases have partially altered to phyllosilicates and/or epidote; however primary twinning can still be distinguished. The following mineral associations were observed in pelitic to semipelitic rocks south of the Long Lake:

1) staurolite - andalusite - muscovite - quartz - biotite - chlorite
2) staurolite - muscovite - quartz - biotite - chlorite
3) muscovite - chlorite - quartz - biotite
4) muscovite -quartz - epidote - plagioclase - biotite

The appearance of staurolite is widespread in the pelitic rocks south of Long Lake and McFarlane Lake. Staurolite grains up to 1 cm in size were observed in the field, most notably in the pelitic rocks along the south shore of McFarlane Lake (Figure 3-5). In thin section, original staurolite grains were observed to be partially to completely replaced by fine grained retrograde muscovite proportions (Figure 3-3, 3-4). The occurrence of andalusite grains is far more restricted than that of staurolite. Large elongated grains, up to 5 cm in length were observed in only one outcrop south of the McFarlane Lake (Figure 3-5). These grains are similar to staurolite in that they have nearly completely been replaced by muscovite and chlorite.

The coexistence of staurolite and andalusite occurs at temperature between 520 and 600°C and pressures between 2 and 4 Kbars according to petrogenetic grid for pelitic rocks of Yardley (1989) (Figure 3-6). This places the rocks in the low pressure phase of the middle amphibolite facies as defined by Turner (1980). A similar conclusion was arrived at by Card (1978) in his regional study on the metamorphism of the eastern Southern Province.

The regional foliation is deflected around the porphyroblasts of staurolite and andalusite developing well defined pressure shadows indicating that amphibolite facies metamorphism was pre-or early syntectonic. (Figure 3-3). Phyllosilicates surrounding the

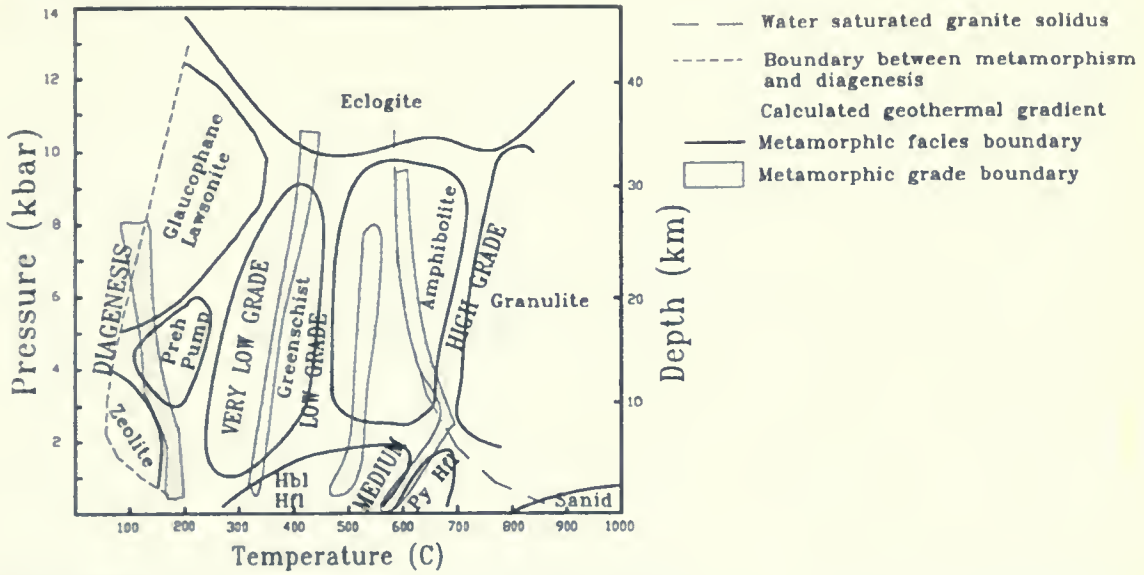

Figure 3-1: Inferred P-T conditions of metamorphic facies of Turner (1980) and metamorphic grade of Winkler (1974).

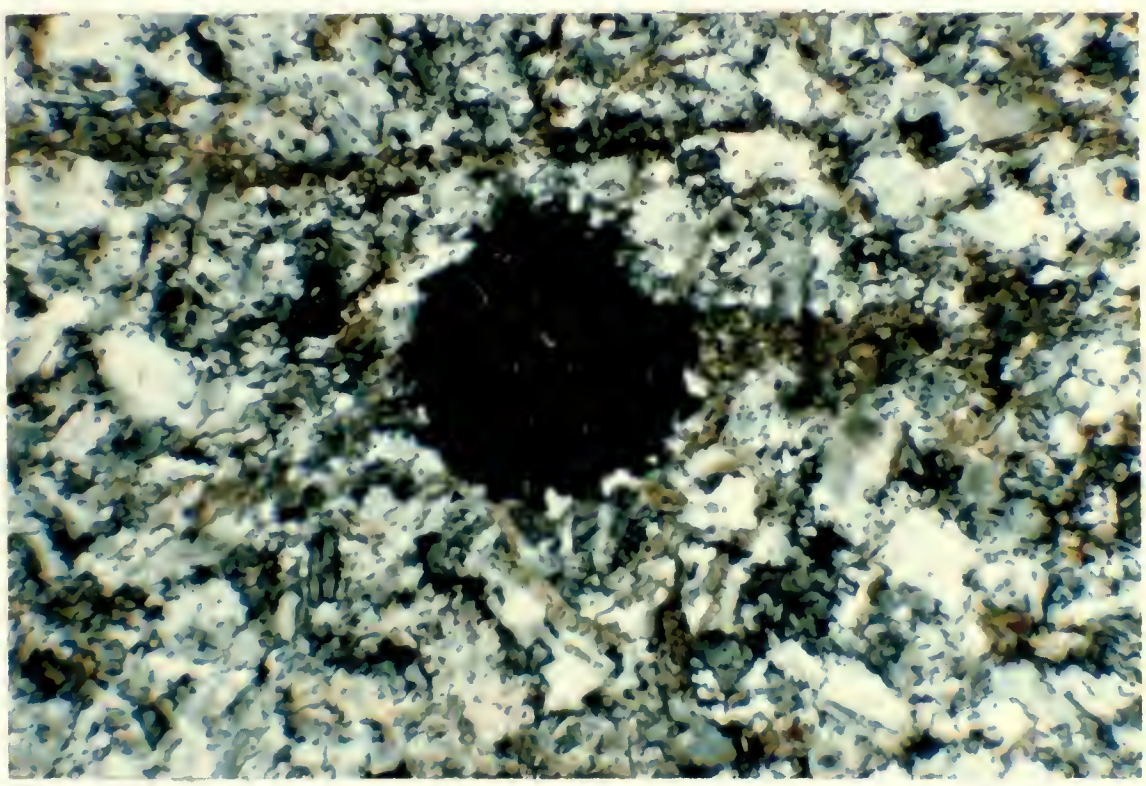

Figure 3-2: Photomicrograph of garnet porphyroblast in metamorphosed Mississagi quartzite (crossed polars). Bottom of photo is 3 mm in length.

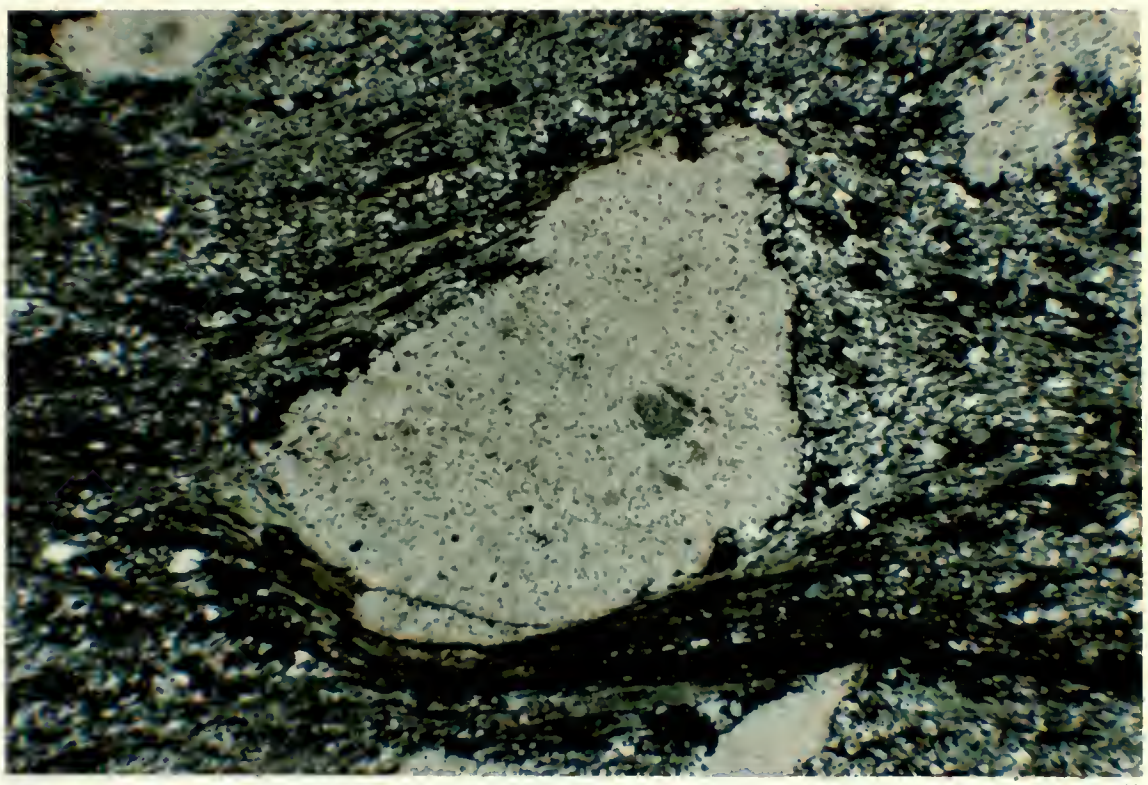

Figure 3-3: Photomicrograph of foliation wrapping around remnant staurolite porphyroblast (crossed polars). Note the small core of staurolite. Bottom of the photo is 15 mm in length.

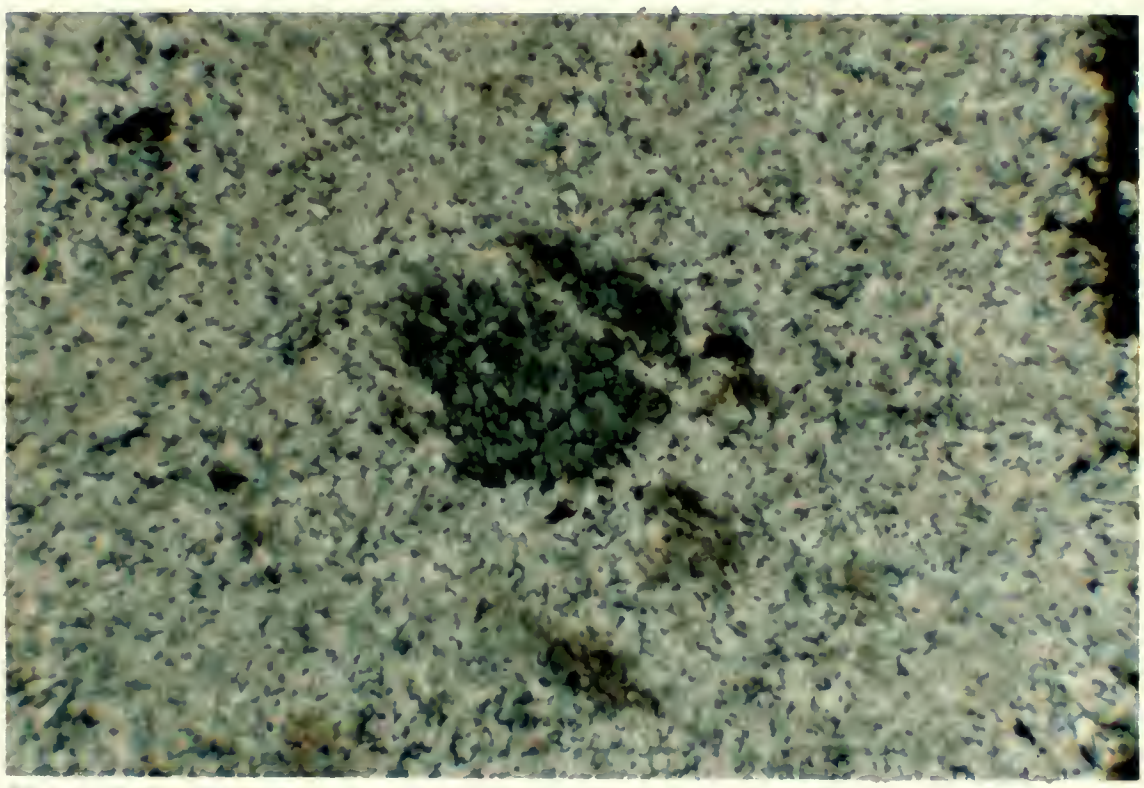

Figure 3-4: Photomicrograph of close up of grain in Figure 3-3 showing the remnant staurolite core surrounded by retrograde muscovite (crossed polars). Bottom of the photo is 3 mm in length.

Figure 3-5: Photo of remnant staurolite and andalusite grains in pelitic rocks south of McFarlane Lake.

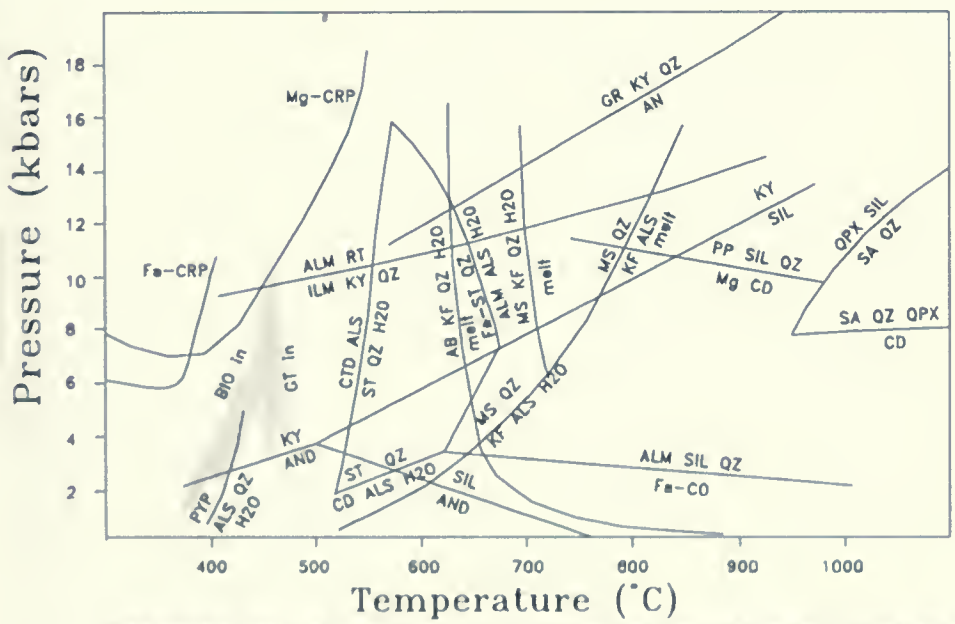

Abbreviations used are: AB=albite; ALM=Al-silicate; AN=anorthite; AND=andalusite; BIO=biotit; CD=cordierite; CRP=carpholite; CTD= chloritoid; GR= grossular; GT= garnet; ILM=ilmenite; KF=K-feldspar; KY=kyanite; MS=muscovite; OPX=orthopyroxene; PP=pyrope; PYP= pyrophyllite; QZ=quartz; RT=rutile; SA=sapphirine; SIL=sillimanite; ST=staurolite.

Figure 3-6: Petrogenitic grid for pelitic metasediments (from Yardley, 1989).

porphyroblasts are elongated in the plane of the foliation and parallel the southeast plunging lineation. Overprinting the primary foliation defined by the alignment of the phyllosilicates is a secondary crenulation cleavage. In contrast the muscovite which formed as a result of alteration of staurolite and andalusite displays no alignment of grains or development of the secondary crenulation cleavage, indicating that retrograde metamorphism postdated deformation. Olivine diabase dykes south of Long Lake have not been metamorphosed indicating that metamorphism predated intrusion of the dykes and is therefore pre-Grenvillian.

It is unclear whether the development of amphibolite facies metamorphic mineral assemblages in this zone results from either contact metamorphism in response to the intrusion of the Chief Lake Batholith or regional metamorphism prior to the deformation in the region. Card (1978) noted that the coexistence of staurolite and andalusite indicates regional metamorphism at low pressure and temperature conditions corresponding to the low pressure intermediate type of Misyashiro (1961). In contrast the development of staurolite has been reported as forming in a contact aureole around the Creighton Pluton in McKim township (Dressler 1984b) to the north of the study area.

3.3 Middle to Upper Greenschist Zone

Lithologies north of Long Lake and McFarlane Lake display middle to upper greenschist facies mineral associations. Associations observed in quartzo feldspathic rocks include:

1) quartz - plagioclase - alkali feldspar - muscovite - biotite - chlorite
2) quartz - plagioclase - alkali feldspar - muscovite - chlorite
3) quartz - plagioclase - alkali feldspar - muscovite - biotite
4) quartz - plagioclase - alkali feldspar - muscovite

The following mineral associations were observed in pelitic to semi pelitic rocks.

1) muscovite - quartz - plagioclase - alkali feldspar - biotite - chlorite
2) muscovite - quartz - plagioclase - alkali feldspar - biotite
3) muscovite - quartz - chlorite
4) muscovite - biotite - quartz - chlorite

No variation in metamorphic association was observed across the Murray Fault.

3.4 Summary of Metamorphism

Long Lake and McFarlane Lake appear to form a boundary that separates medium grade metamorphic rocks to the southeast from low grade rocks to the northwest. Pelitic rocks south of chain record evidence of metamorphism at lower to middle amphibolite facies, corresponding to temperatures between 520 and 600 °C and pressures between 2.5 and 4 Kbars, based on the coexistence of staurolite and andalusite. Amphibolite facies metamorphism was followed by a period of deformation and retrograde metamorphism. Rocks north of Long Lake and McFarlane Lake have undergone regional metamorphism at middle to upper greenschist facies corresponding to temperatures between 300 to 400°C and pressures between 2 and 4 Kbars. It is unclear weather the amphibolite facies assemblages south of Long Lake and McFarlane Lake resulted from contact or regional metamorphism but metamorphism predates intrusion of the Sudbury dykes and is therefore pre-Grenvillian.

Chapter 4

Structural Geology

4.1 Introduction

Rocks in the study area have undergone extensive deformation. The style of deformation ranges from ductile flow producing a stretching lineation to brittle fracturing and accompanying brecciation. A geologic map (Figure 4-1) has been produced based on structural features observed in the field.

Two major structural features cross the map area (Figure 4-1). The Murray Fault (MF) which has long been considered a major structural feature and can be traced across much of the Southern Province. The term Murray Fault Zone (MFZ) will be used to incorporate the splay faults that extend off the major break of the MF. The second major structural feature is the recently identified Long Lake Fault (LLF);(Fueten and Redmond 1992). The LLF joins with the MFZ near Richard Lake to the northeast of the study area and is inferred to link with the Lake Panache and Espanola Faults to the southwest. It therefore can be considered as part of the regional east-west trending fault system of the Southern Province. The structural geology will be discussed in context to the LLF and MFZ.

4.2 Murray Fault Zone

Card and Hutchinson (1972) suggested that the MFZ system originated prior to Huronian sedimentation and was initially part of a graben system forming the depositional basin for Huronian sediments. During later activity the MFZ became a southerly dipping thrust fault (Cooke 1946; Zolnai et al. 1984) with considerable right lateral displacement (Cooke 1946; Yates 1948; Card 1968; Zolnai et al. 1984). Zolnai et al. (1984) concluded that 10-15 km of south side up structural relief exists across the MFZ south west of the Sudbury

Structure and attributed late brittle right-lateral movement on the MFZ to result from northwest-southeast compression during the Grenvillian Orogeny.

In outcrops of Huronian metasedimentary rocks near or within the MFZ, bedding is invariably steeply south-dipping to vertical (Figure 4-1). Angular discordances between beds are common, as is intense fracturing. No shear sense indicators were found in the field to indicate a movement direction and no markers have been found that could be traced across the MFZ. Two olivine diabase dykes have been found both north and south of the MFZ. Unfortunately there is nothing distinctive about the dykes which would allow correlation across the MF. Davidson (1992) reports a distinctive pair of olivine diabase dykes immediately east of the study area which have a 1 km dextral offset across the MFZ. If the dykes found in the study area are similar in age to those of Davidson (1992) the sense and approximate magnitude of offset would be the same as reported by Davidson (1992) and would further support a late movement with a dextral component. In the study area there is no direct evidence for the 10-15 km of structural relief, suggested by Zolnai et al. (1984). In the northern section of the map area, outcrops of Ramsay Lake and Pecors Formation appear to have been juxtaposed by a complex series of displacments along the individual faults of the MFZ.

The Huronian rocks to the north and the south of the MFZ display relatively little deformation. Bedding orientations vary with both northerly and southerly dips common; however no complete folds could be traced (Figure 4-1). The rocks display little fracturing and sedimentary structures are preserved.

4.2.1 Anastomosing Shear Zones in the MFZ

In several localities rocks of the Mississagi Formation are cut by a network of

Figure 4-2: Photo of anastomosing shears cutting through Mississagi quartzite in the Murray Fault Zone.

anastomosing fractures and narrow shear zones, which outline lozenges ranging in size from metres to several millimetres (Figure 4-2). The long dimensions of the lozenges lie within local bedding planes which control lozenge formation. The long axes of the lozenges were measured on several outcrops along the MFZ, using the method outlined by Gapais et al. (1987). The technique was originally developed to determine the bulk kinematics in homogenous rocks, however in the Mississagi Formation the kinematic XZ plane was constrained to lie perpendiclar to the bedding plane. The orientation of the X and Y axes and any variation in the X/Y ratios may provide valuable information related to the larger scale kinematics of the MFZ.

Detailed analysis of these anastomosing shear zones was performed by Seabright (1992) in conjunction with this study. Six occurrences of macro scale anastomosing shear zones were measured along the MFZ. At each occurrence 100 measurements were taken. Bedding for the six sites dipped subvertially. Poles of shear planes were plotted and contoured on lower hemisphere equal area stereo nets. Contoured plots and corresponding statistical data for each site are given in Figure (4-3).

In order to compare fabrics, Seabright (1992) calculated the orientation of eigenvectors (E1, E2 and E3) corresponding to the kinematic X long, Y intermediate and Z short axes. Seabright (1992) assumed that the Z axis lies perpendicular to the plane of bedding, the corresponding trends of the X axis lies to the south west in 4 sites and to the north east in two sites. The plunge of the X axis varies from 20 to 70 degrees with an average for the 6 sites of 43 degrees. To quantify the three dimensional shape of lozenges defined by the anastomosing shears, eigenvalues ($\lambda 1$, $\lambda 2$, $\lambda 3$) were calculated. Eigenvalues are a measure of how well the data clusters around a specific kinematic eigenvector. The larger the eigenvalue the less clustering of shear plane poles around a corresponding eigenvector.

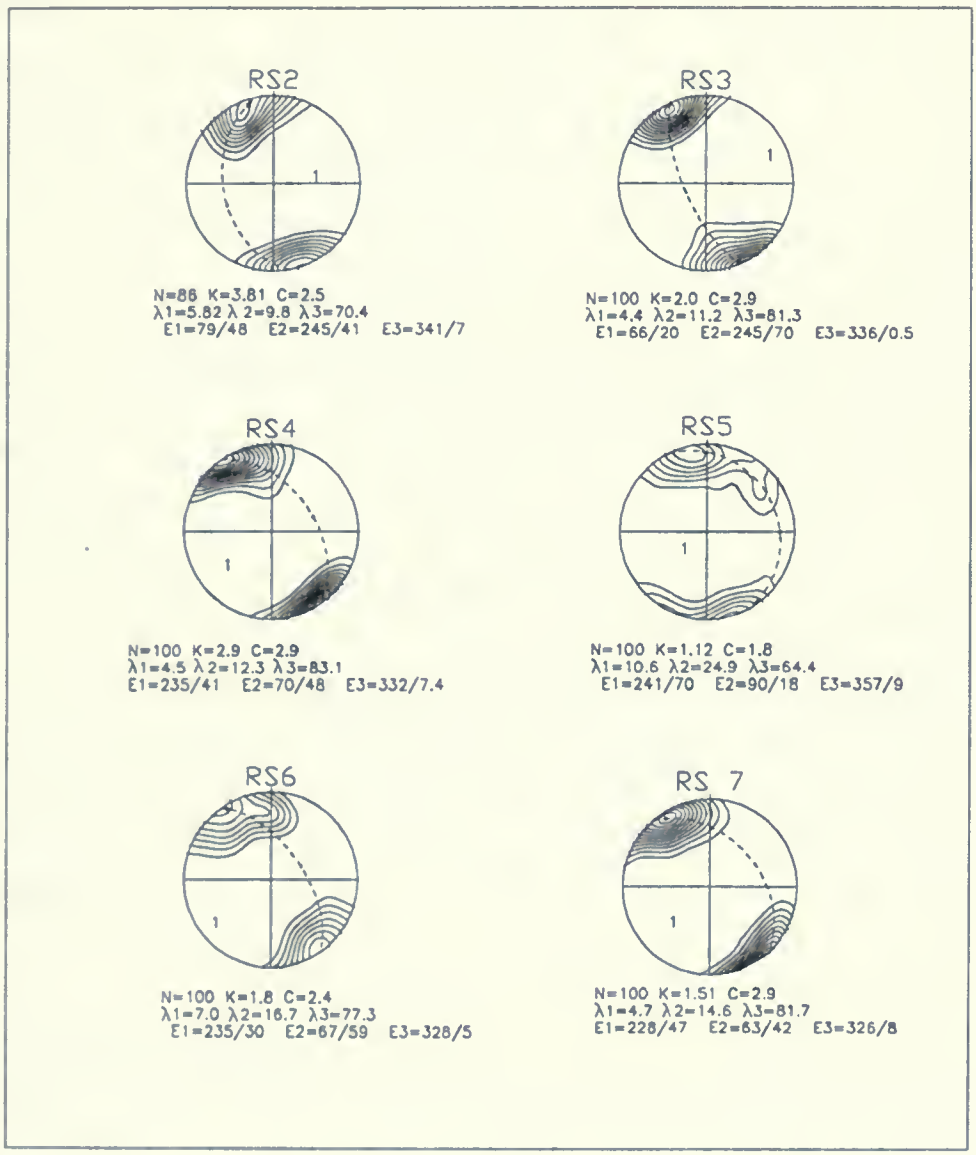

Figure 4-3: Contoured plots and corresponding statistical data for each site of anastomosing shears in the MFZ

Because the eigenvalues measure the clustering of data points about the eigenvector they can be used to quantify various fabric qualities, such as shape and significance of preferred orientation. Two such parameters used to describe the distribution of data are C and K (Woodcock 1977). K is defined as [ln(λ3/λ2)/ln (λ2/λ1)] and measures the shape of the fabric. C is defined as [ln(λ3/λ1)] and measures the significance of the fabric. Data from each site are plotted on a modified Flinn diagram (Figure 4-4).

K values for the six sites range from 1.12 to 3.81 which places them in the cluster field ($1 < K < \infty$) as described by Woodcock (1977). C values for the six sites range from 1.8 to 2.93 placing them in the moderately well developed field (Woodcock 1977). With respect to k values as defined in a normal Flinn diagram, the lozenges defined by the array of anastomosing shears are uniaxial oblate as a result of flattening strain.

Unfortunately no accurate regional reference frame, such as a consistent lineation, could be found in the field to coordinate the orientation of the X, Y and Z kinematic axes of the lozenges. Therefore the orientation of the lozenges could not be correlated with a regional sense of shear along the MFZ even though a consistent lozenge shape was found in all 6 sites along the MFZ.

4.3 Long-Lake Fault

The LLF is a system of numerous steep southerly dipping shear zones. Individual shear zones tend to be on the order of one metre wide and may cut across bedding, separating lenses of less deformed rock (Figure 4-5). Within quartz rich bands in the shear zones a dip-parallel stretching lineation is well developed (Figure 4-6). This lineation trends between 110° and 140° and plunges between 60° and 80° (Figure 4-1). The sandstones of the Mississagi Formation do not readily produce shear sense indicators and hence the sense of

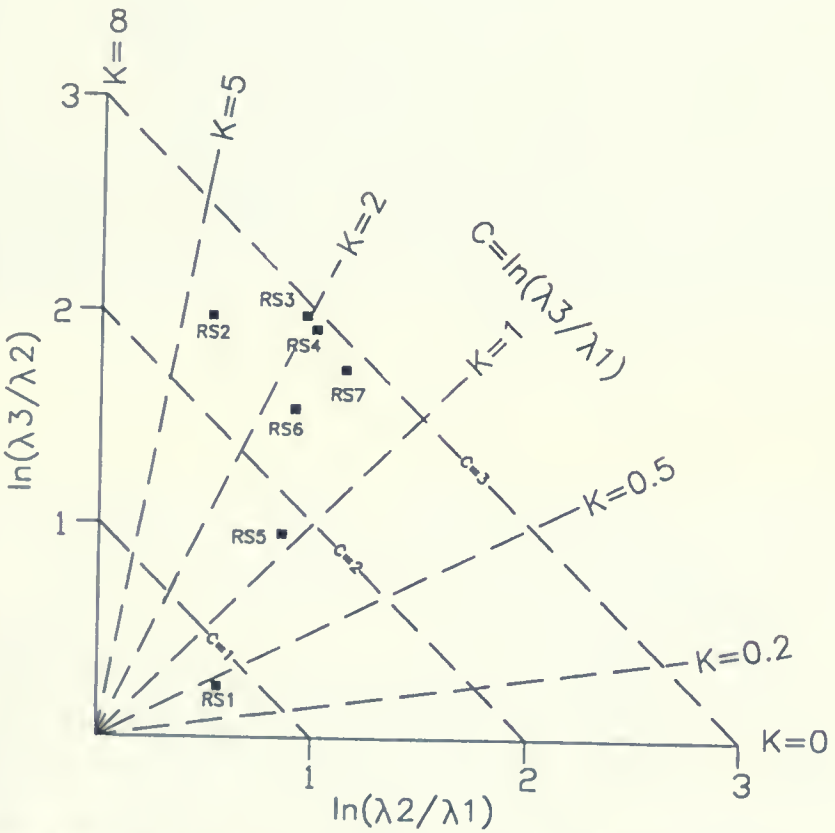

Figure 4-4: 2-axis plots of anastomosing shear fabrics for the 6 sites in the MFZ. Modified Flinn diagram after Woodcock (1977).

Figure 4-5: Photo of intensely sheared Mississagi quartzite between Long Lake and McFarlane Lake. Shear zones are dipping to the southeast.

Figure 4-6: Photo of quartz rich mylonite bands in Long Lake.

movement on the fault cannot be deduced directly in the field. Nippissing gabbros for the most part display little deformational features. However in outcrops between Long Lake and McFarlane Lake the gabbro is intensely foliated. This foliation strikes northeast and dips to the south at about 70°.

As on the MFZ, a dextral component of displacement has been found on the LLF. On one conglomerate outcrop within Long Lake, granite clasts are rotated in a dextral sense (Figure 4-7). It is unknown whether this represents a separate late dextral deformation event or if motion was oblique with a dextral component.

Conglomerates to the south of the LLF display a well developed foliation defined by the alignment of phyllosilicates. The clasts have a preferred elongation direction which plunges to the southeast. South of the LLF quartzites of the Mississagi Formation are foliated and lineated. The lineation is defined by the elongation of quartz grains. The regional trend of the mineral lineation is in a south to south east direction and plunge angles are subvertical. The rocks south of the LLF have not been intensely fractured.

Conglomerate units immediately north of the LLF display only a weak development of a foliation and clast are generally spherical in shape. Immediately north of Long Lake, rocks of the Mississagi Formation display brittle deformational features as the rocks are intensely fractured. A southerly dipping foliation appears to cross cut vertically bedded Mississagi quartzite. Limited evidence of a ductile stretching lineation was observed in rocks north of LLF.

Evidence argues that the LLF is a high angle reverse fault with a south over north sense of displacement which produced the down-dip stretching lineation. This is based on the fact that it has brought into contact amphibolite facies rocks that had undergone dominantly ductile deformation to the south with similar rocks that underwent middle

greenschist facies metamorphism and dominantly brittle deformation to the north. No kinematic indicators were found in the field to confirm this.

4.4 Folding

Large regional folds are present within the Huronian Supergroup to the west of the study area and smaller folds are observed to the east of the area (Davidson 1992). Several fold axes are indicated on previously published maps of the study area (Grant et al. 1962; Card et al. 1977; Dressler 1984a). The axial trace of an anticline syncline pair of folds has been previously mapped as cutting across Crooked Lake and the axis of a major anticline has been placed through the centre of Long Lake. No direct field evidence was found to support the existence of these fold structures. Long Lake is the site of a major fault discussed above. This fault may have started through the limb or hinge of a major fold but there is no direct evidence remaining for folding. The angular discordances of bedding near Crooked Lake which led to their interpretation as folds are due to faulting which has juxtaposed shallow and steeply dipping rocks of the Mississagi Formation (Figures 4-8, 4-9, 4-10). This relationship was observed in several locations between the LLF and MFZ in the eastern half of the study area where the faults converge. Determination of bedding facing direction is hampered by deformation of planar crossbedding structures. Only trough cross bedding was used as a tops indicator.

Bedding orientations north of the MFZ (Figure 4-1) and in the area between the MFZ and LLF in the western half of the study area have both northerly and southerly dips. While it was impossible to map out complete fold closures in these relatively undeformed areas, folds may be present. Davidson (1992) reports a major syncline east of Ramsey Lake in the

Figure 4-7: Photo of dextrally rotated granite clast in conglomerate outcrop on the south shore of Long Lake. The compass is pointing north.

Figure 4-8: Photo of angularly juxtaposed blocks of Mississagi quartzite near Crooked Lake. The arrow points to the central block in which bedding dips in the opposite direction to the blocks on either side.

Figure 4-9: Photo displaying the angular discordant nature of bedding orientation in the rocks north of the Long Lake Fault. This area was previously interpreted as syncline on the map by Thompson (1962).

Figure 4-10: Photo displaying the steep over shallow bedding orientation on the southwest shore of Crooked Lake. Similar bedding relationships were observed in lithologies north of the Long Lake Fault.

relatively undeformed area north of the MFZ.

Macro scale folds were observed in several locations adjacent to the major faults. Folds range in size from centimetre to a metre scale and appear to have developed during later strike slip movement along the major faults. However, they could have been produced prior to strike slip displacement and then rotated into their present configuration. The fold axes are generally subvertical and the asymmetry of the folds allowed for determination of a shear sense.

Several of these folds were observed between the MF to the north and the Naughton Fault to the south. All folds in this area render a sinistral sense of shear (Figures 4-11, 4-12). This is in direct contrast to the dextral component of strike slip movement commonly attributed to the MF.

Within the LLF quartz rich mylonites have been folded. The down-dip mineral lineation which developed during ductile deformation has been incorporated in the folding indicating that folding associated with strike slip movement postdated the development of the stretching lineation. All folds within LLF have subvertical fold axes and their sense of asymmetry indicates development resulting from a dextral strike slip movement. Folds could have developed during a minor component of strike slip movement during the dip slip shearing along the LLF or could be the result of a separate, post-ductile deformational event.

4.5 Brecciation

The Huronian rocks in the study area host several types of cataclastic brecciation. The origin of breccias associated with the Sudbury Structure remains the subject of considerable debate. Macro scale breccias within the area have been classified into two groups, Sudbury-Type breccia (as described by Dressler 1984b) and cataclastic breccia associated with brittle

Figure 4-11 (top) and 4-12 (bottom): Photos of sinistral drag folds in Mississagi quartzite between the Naughton Fault and the Murray Fault. The handle of the hammer points north and the hammer lies to the west of the fold in both photos.

deformation along the major faults in the area.

4.5.1 Sudbury-Type Breccia

The formation of Sudbury-Type breccia is widely believed to have occurred during the Sudbury event. Sudbury-Type breccia is abundant throughout much of the study area, appearing as linear or irregularly shaped bodies. These bodies can range in size from several hundreds of metres in diameter to thin centimetre wide veins. The relationships between the breccia bodies and the surrounding host rock are inconsistent. Breccia bodies can crosscut primary bedding but in several locations it appears to be contained within sedimentary bedding. Many bodies of Sudbury-type breccia are elongated and strike between 45 and 70 degrees.

Breccia clasts range in size from centimetre scale to as large as several metres in diameter. Clasts are generally well rounded and often have an elongate shape as a result of the sedimentary layering of the host material. Where outcrops have undergone little post brecciation deformation, clasts often appear in a jigsaw puzzle fashion as clasts can be visually pieced back together (Figure 4-13). This indicates that transport of clasts was often minimal. Clast type generally reflect that of the host rock however exotic clast types (often Nipissing gabbro) have been observed in breccia bodies with significant distance from any surface exposures of possible source rocks. Occurrences of Sudbury-Type breccias have been reported as far as 80 km from the Sudbury Structure however no outcrops of Sudbury-Type breccia were observed south of the LLF. The limited outcrops of Sudbury breccia previously mapped south of LLF (Thompson 1962) have been identified as xenoliths of Mississagi Formation contained within Nippising gabbroic rocks or Chief Lake batholith.

To examine the extent of post Sudbury event deformation, the long axis of Sudbury-type breccia clasts was measured on a horizontal surface at several outcrops within the study

Figure 4-13: Photo of "jigsaw puzzle" Sudbury breccia clasts in Mississagi quartzite north of Robinson Lake.

Figure 4-15: Photo of cataclastic fault breccia in the Murray Fault.

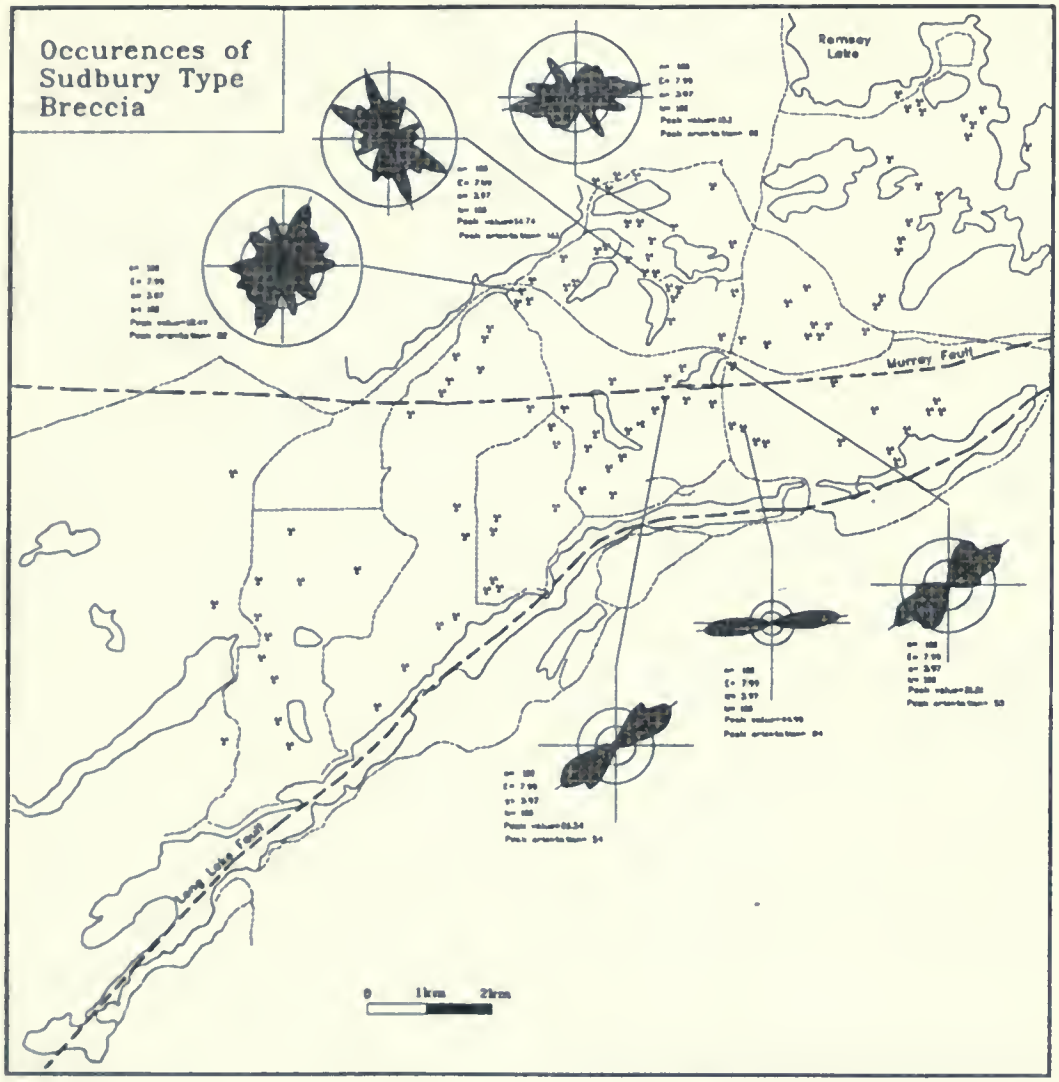

Figure 4-14: Map of the study area indicating the location of circular histogram diagrams which plot the long axis orientation of Sudbury breccia clasts.

area. Corresponding data are plotted on Figure (4-14). Sudbury breccia clast north of the MFZ have a random distribution of long axis orientation indicating that the rocks have undergone little deformation after the formation of the breccia. Approaching the MFZ, breccia clasts display an increased preferred orientation, with long axis oriented approximately 55 degrees. South of the MFZ, clasts display a strong preferred orientation of the long axis which strikes at 85 degrees.

4.5.2 Fault Breccia

Within the plane of the MF, host rocks have been intensely brecciated. Clasts are angular in shape and range in size from a few millimetres to several centimetres in diameter (Figure 4-15). Thin section analysis indicates a wide variety of source materials have been incorporated into the breccia. Quartzite clasts display elongate quartz grains which have undergone ductile deformation and dynamic recrystallization. The orientation of the stretching lineation for individual clasts is random, indicating that the quartzites underwent ductile deformation prior to the brittle cataclastic brecciation (Figure 4-16). Clasts of mafic volcanic rocks display well preserved igneous textures that have not been deformed. Large pseudomorphs of high temperature beta quartz are present. These have undergone extensive intracrystaline ductile deformation and display well developed undulose extinction. Also present in the breccia are rock fragments composed of epidote, muscovite and olivine. The latter may indicate that olivine diabase dike material has been incorporated into the breccia. Clasts of Nipissing gabbro are also present, as the breccia body is located in close proximity to a large outcrop of the diabase.

4.6 Summary of Deformation

Both the MFZ and the LLF record ductile as well as brittle deformation. Based on

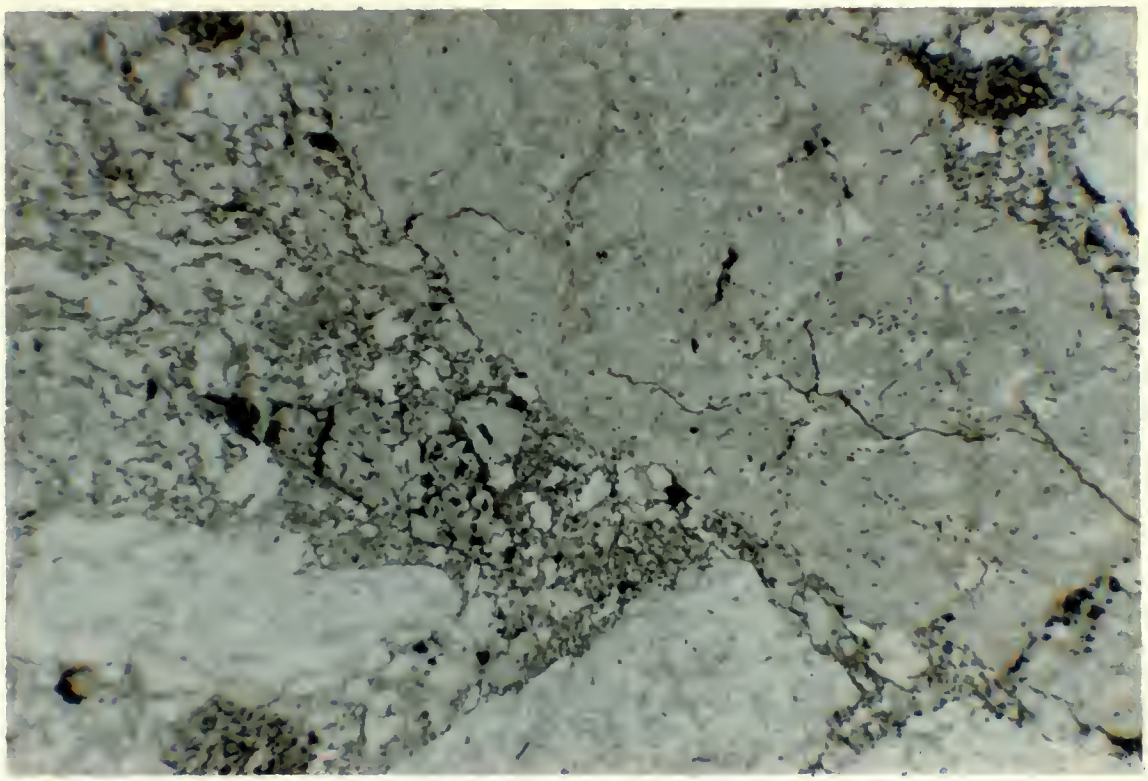

Figure 4-16: Photomicrograph of fault breccia in Murray fault (plane light). Bottom of the photo is 17 mm in length.

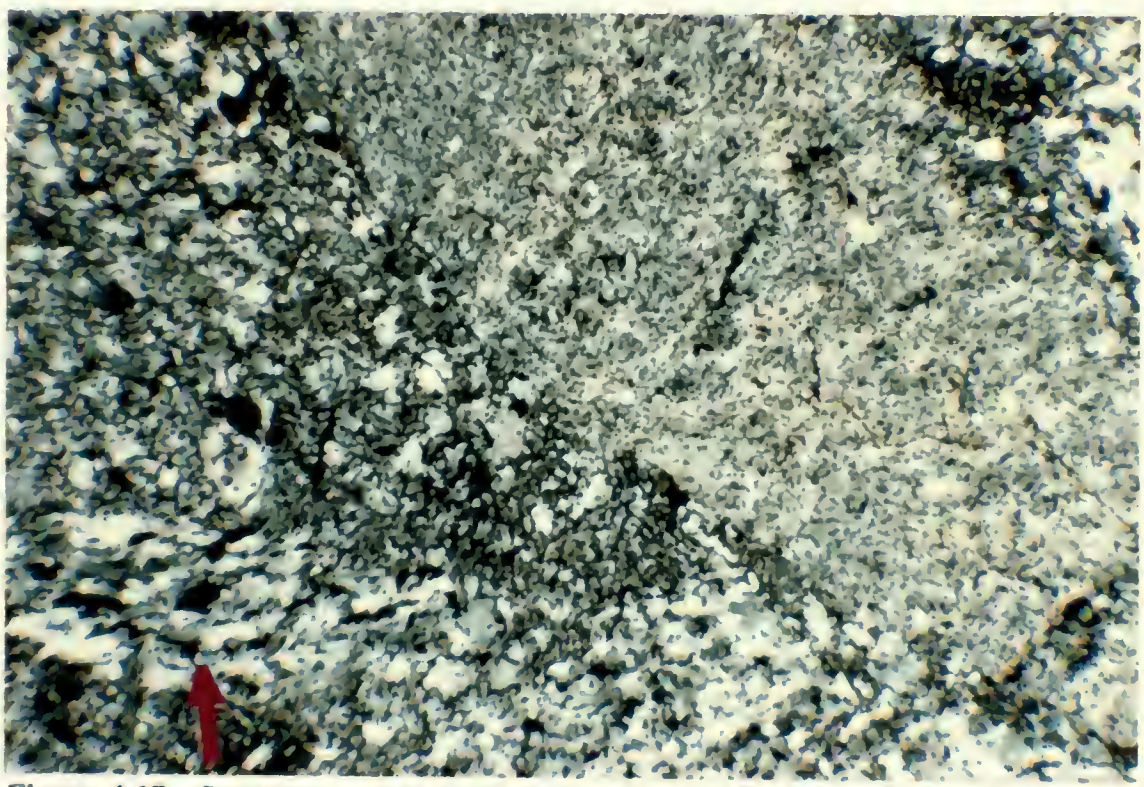

Figure 4-17: Same thinsection as Figure 4-16 but under crossed polars. Note the red arrow that points to a quartzite clasts of ribboned quartz grains.

the change in deformational style across the LLF, it can be considered to be structurally more significant than the MFZ in this area. Overall the rocks of the Huronian Supergroup become progressively younger from north to south indicating that the regional stratigraphy dips to the southeast. If the plane of the LLF dips at a similar angle to that of stratigraphy, significant amounts of vertical displacement can occur on the LLF without a change in the rock type across the fault. Although limited occurrences of a ductile lineation were found in the MFZ, no variation in deformation or metamorphism was observed across the MFZ.

Evidence for late movement with at least a dextral and possibly a sinistral component is present for both faults. While the timing of the dextral motion is uncertain, there is evidence that this motion took place after 1238 Ma. One may be tempted to speculate that a dextral transgressive event is associated with the Grenvillian Orogeny as suggested by Zolnai et al. (1984) as it post-dated the dyke intrusion.

The large regional folds which exist to the southeast and northwest of this area cannot be documented here and several previously interpreted fold axes are the result of faulting. Rocks north and south of the MF are relatively undeformed with attitudes which are likely the result of folding in the Southern Province, i.e. northerly as well as southerly dips exist.

The overall deformation in the area appears to be much more intense than to the southwest or northeast of the area. The MFZ and LLF converge to form a "triangle zone" and it may well be that a room problem, created during motion on these faults, is responsible for the greater amount of deformation where these two faults are in close proximity with each other. Alternatively, intrusion of the Chief Lake batholith to the south, or the close proximity of the area to the Grenville Front and associated Grenvillian deformation may be responsible.

Chapter 5

Quartz C-axis Fabrics

5.1 Introduction

As the quartzite rocks of the Mississagi Formation did not produce any kinematic indicators which could be observed in the field, the proposed south over north reverse sense of shear along the LLF could not be confirmed. To provide greater insight into the ductile deformational history of the major faults in the area, a study on the regional variation of quartz c-axis fabrics was performed on samples of Mississagi quartzite. Asymmetric development of quartz c-axis fabrics can be used as a kinematic indicator to evaluate the shear sense along the major faults. Fabric analysis allowed for direct comparison of variations in intensity of deformation across the study area. The activation of distinct glide systems in quartz which are directly related to the development of a preferred crystallographic orientation can be related to changes in P-T conditions during deformation.

Intracrystaline plastic deformation involves mechanical processes such as dislocation glide, climb and twinning. These processes, combined with the effects of mineral recrystallization and grain boundary slip results in the development of characteristic crystallographic preferred orientation fabrics in polycrystaline materials. In quartz, dislocation glide is considered to be the most significant method to accommodate imposed strain (Price 1985). Although clear glide planes are not obvious, studies on the dislocation of quartz have shown that glide along specific crystallographic planes is more common than others. The most commonly reported glide planes involve either the basal plane c={0001}, the prism m={1010} the positive rhomb r={1011}, or the negative rhomb z={0111} (Price 1985). All of these glide planes accommodate slip in both the a and c directions (Figure 5-1).

Recrystallization processes are known to modify c-axis fabrics significantly, making

them different from those developed without recrystallization (Price 1985). However in situations where recrystallization operates while the deformation is continuing (dynamic recrystallization), observed fabrics are similar to those in rocks without significant recrystallization. Observations by Hobbs (1968) and Ransom (1971) demonstrate that new quartz grains developing about an older deformed crystal tend to grow with their c-axes within 20-40° to that of their host. This relationship can be important to the developing fabric as temporal recrystallization can produce strong domain grouping of small grains with similar orientations, the domain sizes, shapes, and orientations being strongly influenced by the size, shape, and orientation of the older deformed grains (Price 1985).

5.2 Technique

The orientation of quartz c-axis were determined from 25 samples of Mississagi quartzite. Thirteen of the samples were from south of the LLF and the remaining 12 were from varied locations north of the LLF. Thin sections were cut parallel to the observed lineation and perpendicular to foliation. When no lineation was observed in the field, a vertical section was cut perpendicular to the bedding as observed lineations in most cases where down-dip and the foliation generally was parallel to the orientation of bedding. The strike of the plane of the thin section ranged from 130 to 180° with a dip of 90°. Sections cut in this orientation would permit documentation of the extent of the penetrative ductile deformation directed from the southeast. All c-axis diagrams are orientated such that the north-south axis of the net represents the great circle of the observed foliation. Lineation, when developed, plots at the intersection of the north-south foliation axis and the perimeter of the net. The kinematic Y axis for all fabrics is located at the centre of the net. The X axis is located at the top of the net and the Z axis at the intersection of the east-west axis

perimeter. The fabrics are viewed looking from the southwest (Figure 5-2).

The presence of a preferred crystallographic orientation was initially determined by insertion of a gypsum plate and subsequently confirmed by universal stage measurements. A total of 150 grains were measured for each thin section. Grains were measured along traverses perpendicular to the foliation. This technique provides a random sample set of quartz grains over the area of the thin section.

Lower hemisphere equal area plots were contoured. The contouring method uses a continuous spherical Gaussian counting function described by Robin and Jowett (1986). In all plots the kurtosis (k) was chosen such that $E=3\sigma$ where E represents the expected value of the counts for N data points and σ is the expected standard deviation of the counts if the N data points are drawn randomly from an isotropic population. Statistical information for each net is given in Appendix 2.

Classification of c-axis fabrics follows the point maxima system originally developed by Fairbairn (1949) and later modified by Lister and Dornsiepen (1982). Positions of point maxima (Figure 5-3) correspond to crystallographic orientations within a quartz crystal with the c-axis at the Y position. Point maxima classification provides an exact means to describe the orientation of peaks within a fabric diagram. In several samples the crossed girdle system of fabric description developed by Lister and Williams (1980) is employed as it best describes fabric development (Figure 5.4; Fueten 1992). This will allow for comparison of the fabric in the study with that of other similar studies.

Single girdle fabrics comparable to that displayed by sample DR210 (Figure 5.5) are characterized by the lowest contour following a single steeply dipping girdle across the net. Several distinct maxima may exist within the great circle of the net. The presence of a single girdle fabric has been interpreted as indicating the dominance of activation of a single glide

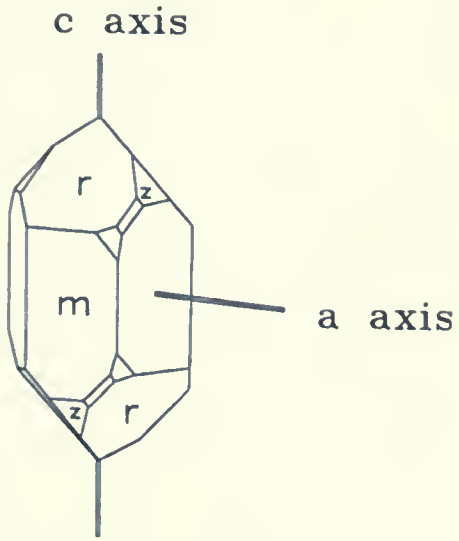

Figure 5-1: Line drawing of ideal quartz crystal showing the direction of the crystallographic axis and the crystallographic planes

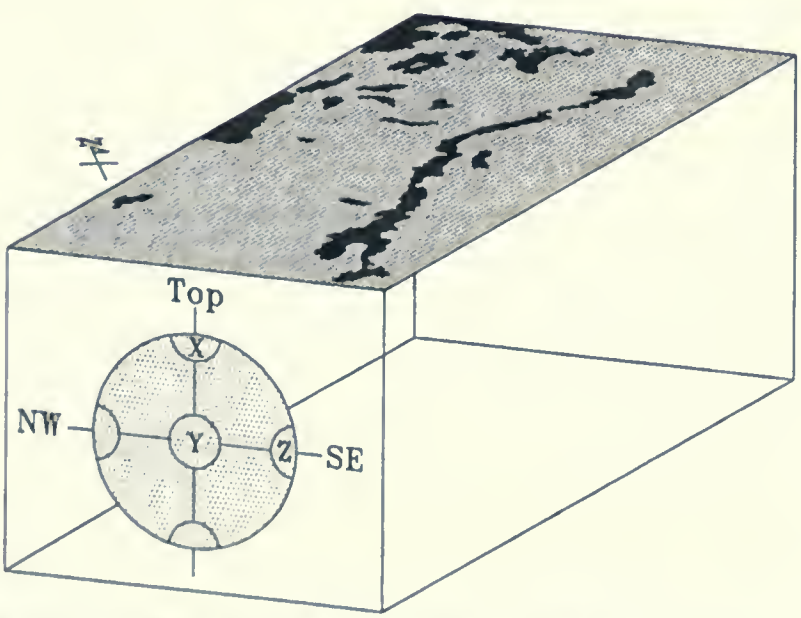

Figure 5-2: 3-D orientation of quartz c-axis fabric diagrams with respect to the map area.

system to accommodate an imposed strain (Urai et al. 1986). During deformation the active glide plane will align itself parallel to the shear plane.

Crossed girdle fabrics can be subdivided into Type I crossed girdle and Type II crossed girdles (Lister and Williams (1980). Skeletal diagrams displaying the classification of crossed girdles can be seen in Figure (5-4). Type II crossed girdles are characterized by two crossing arms that bisect at the Y axis position. In a well developed Type II crossed girdle there should be no connection of the arms along the perimeter on the net. The lowest contour should extend across the centre of the net to the adjacent Maxima III position. This gives the fabric the look at well defined cross with arms that are near a 45° angle to the north-south and east-west axis of the stereo net (Figure 5-4).

In contrast the individual arms of the Type I crossed girdle intersect away from the Y position. Such a fabric can appear as two shallow dipping girdles along the side perimeter of the net that join the north and south Maxima III positions in each half of the fabric.

5.3 Results

5.3.1 Domain 1

The study area has been divided into three domains based on similarities in quartz c-axis fabrics (Figure 5-5). Domain 1 consists of the metasedimentary rocks south of the LLF. In the field rocks display a well developed down-dip stretching lineation defined by elongate quartz grains. A penatrative foliation parallels the southeasterly dipping bedding plane of the quartzite.

In thin section feldspar grains (both plagioclase and microcline) have partially altered to muscovite, however primary twinning is generally well preserved and appears undeformed. Quartz grains display a pronounced preferred elongation direction parallel to the lineation and

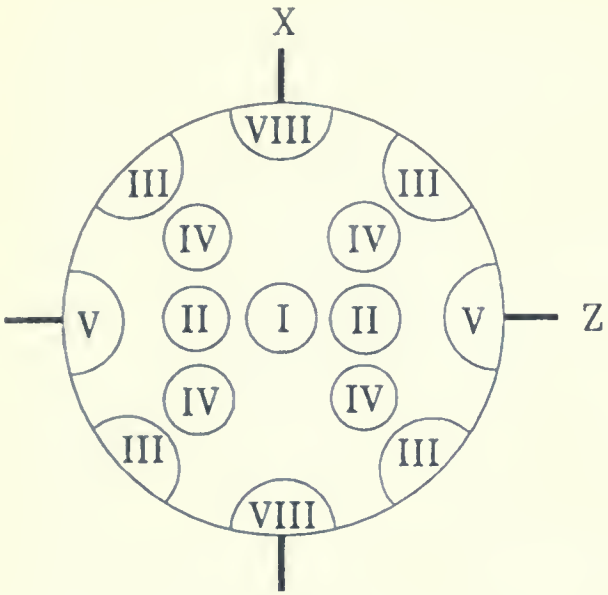

Figure 5-3: Position of the point maxima in a quartz c-axis fabric.(taken from Fueten et al. 1992)

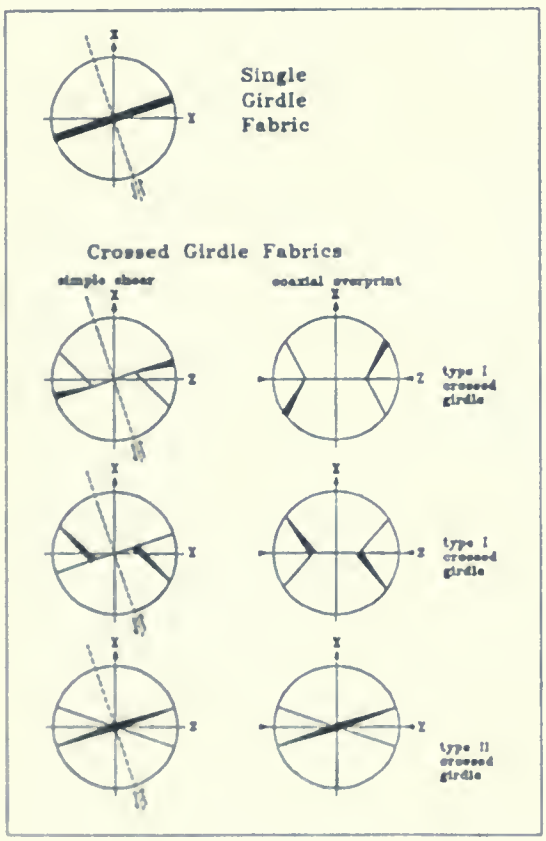

Figure 5-4: Fabric skeletons used for single and crossed girdle classification, from Fueten (1992). These area idealized skeletons for a sinistral sense of shear on the indicated shear plane.

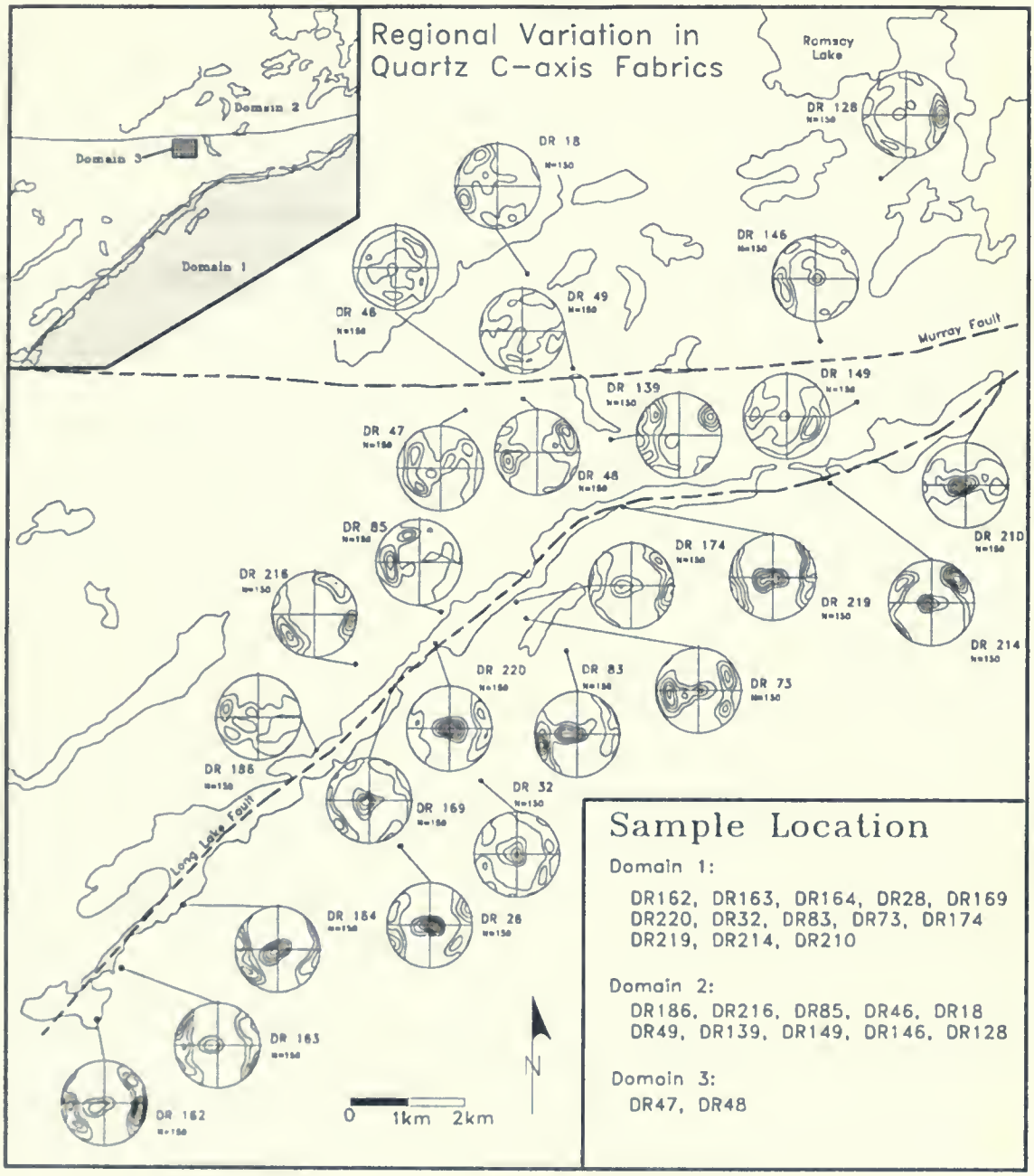

Figure 5-5: Map of the study area indicating the variations in quartz c-axis fabric from 25 samples of Mississagi quartzite. All fabrics are oriented similar to that described in Figure 5-2.

have been flattened in the plane of the foliation (Figure 5-6). Minor subgrain development is present but primary quartz grains still dominate the fabric. Quartz displays extensive undulose extinction and grain boundaries are irregular in shape and are commonly sutured.

In rocks within the shear zones that define the LLF feldspar grains are intensely fractured and deformation has resulted in the dislocation and kinking of primary feldspar twins. Quartz grains have a pronounced elongation direction that parallels the lineation. The development of subgrains resulting from recrystallization is more pronounced than in rocks south of the fault. In most samples primary grains can still be observed, however several samples have completely recrystallized to an array of subgrains.

In several samples, elongate quartz grains display deformation lamellae (Figure 5-7). These lamellae are generally oriented at 45° to the long axis of the grain. The development of deformation lamellae in quartz is restricted to rocks within shear zones of the LLF.

Overprinting the ductile deformation is a later brittle event. Subhorizontal fracturing and microbrecciation cut across and often offset ductilely deformed quartz grains that define the subvertical mineral lineation (Figure 5-8). Evidence of later brittle deformation was not observed in the rocks south of the LLF as they appear unfractured or unbrecciated.

C-axis fabrics from 13 samples taken from Domain 1 all display a characteristic development of a strong Maxima I position. The majority of fabrics have moderate development of the Maxima III positions. On each side of the net, the Maxima III positions are connected by a shallow girdle along the perimeter. This shallow girdle does not extend around the top or bottom of the net to join adjacent Maxima III positions in the north and south halves of the net. In most of the samples the lowest contour does not cross the net to join the Maxima I and III positions to form a cross.

Many of the fabrics display an asymmetry in the development of adjacent Maxima III

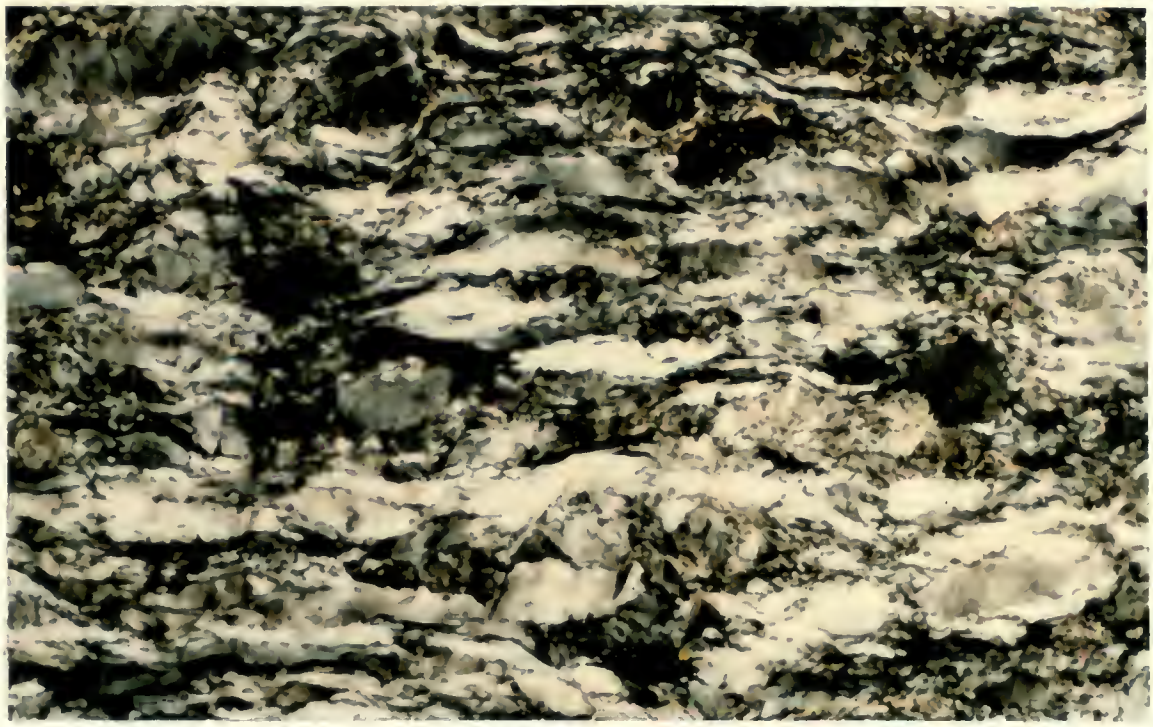

Figure 5-6: Photomicrograph of elongated quartz grains in sample south of Long Lake (sample DR219) (crossed polars). Section is cut parallel to lineation and perpendicular to foliation. Bottom of photo is 8 mm in length.

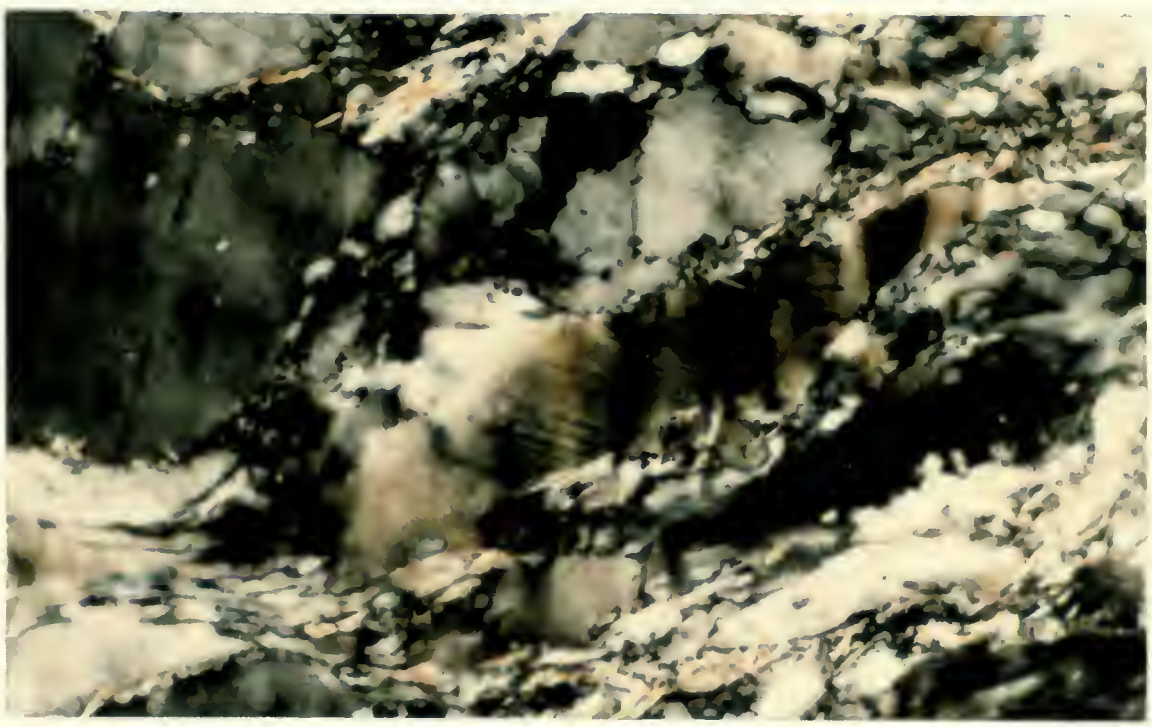

Figure 5-7: Photomicrograph of deformation lamellae in quartz grain (crossed polars). Bottom of photo is 0.26 mm in length.

positions. Samples DR28, DR73, DR83, DR214, DR219 and DR220 all display asymmetric development of the Maxima III position with a more pronounced peak in the northeast and southwest quadrants (Figure 5-5). In the southwest section of Domain 1, samples DR 162 and DR 163 display the dominant development of the northwest-southeast Maxima III positions. These two samples also have a weaker development of the Maxima I position than any other fabric in Domain 1. Samples DR32, DR164, DR169 and DR174 display a symmetric or weakly developed Maxima III position. In the northeastern section of Domain 1, sample DR 210 displays a well developed Maxima I single girdle fabric.

5.3.2. Domain 2

Domain 2 consists of the rocks north of the LLF. In the field quartzite displays no apparent mineral lineation. The development of a foliation in the Mississagi Formation was restricted to the shale interbeds except for rocks immediately adjacent to the MFZ. Deformation associated with the major faults in Domain 2 is dominantly brittle in nature characterized by intense fracturing and cataclastic brecciation.

In thin section quartz appears as irregular shaped grains with little elongation. Grain extinction is sharp and grain boundaries display minor suturing. This is more pronounced in the vertically bedded Mississagi Formation than in the shallower dipping units of the Formation. Quartz grains have not undergone any significant recrystallization. Vertically bedded Mississagi Formation which occurs dominantly between the MFZ and the LLF commonly display extensive fracturing and microbrecciation similar to that observed in the rocks adjacent to the LLF.

In contrast to quartz c-axis fabrics in Domain 1, the rocks north of the LLF have very poorly developed to unrecognizable c-axis fabrics. None of the samples displays any significant development of the Maxima I position which dominates in fabric south of the

LLF. Two of the samples (DR139 and DR216) taken from the vertically bedded quartzites just north of the LLF display an orthorhombic Maxima III position. The rest of the samples from Domain 2 show no recognizable fabric development.

5.3.2 Domain 3

Domain 3 is a small section of ductilely deformed rocks south of the MFZ, west of Crooked Lake, where the quartzite displays a steep southerly down dip lineation. In thin section quartz grains display a preferred elongation direction parallel to the lineation and have undergone flattening in the plane of the foliation. Quartz has undergone significant dynamic recrystallization to an array of subgrains, however primary grains still define the fabric (Figure 5-9). Grains display a strong undulose extinction with irregular grain boundaries and significant suturing. The rocks in Domain 3 display little fracturing at the microscopic scale.

Two samples taken from within the MFZ, just west of Crooked Lake (DR47 and DR48, Figure 5-5) display asymmetric development of the Maxima III position. In both samples the northeast and southwest Maxima III positions are developed. The dominant Maxima III postions are connected by a dominant northeast-southwest trending steep dipping arm across the girdle. A mutually perpendicular arm that trends northwest-southeast is only weakly developed and is truncated and offset at the Y position on the net. Although other samples were taken along the MFZ, these were the only samples which displayed a mineral lineation and a recognizable quartz c-axis fabric. The two samples, DR47 and DR48 from Domain 3 have been interpreted as being Type I crossed girdles.

5.4 Discussion

5.4.1 Domain 1

Fueten et al. (1991) propose a model to explain the presence of the well developed

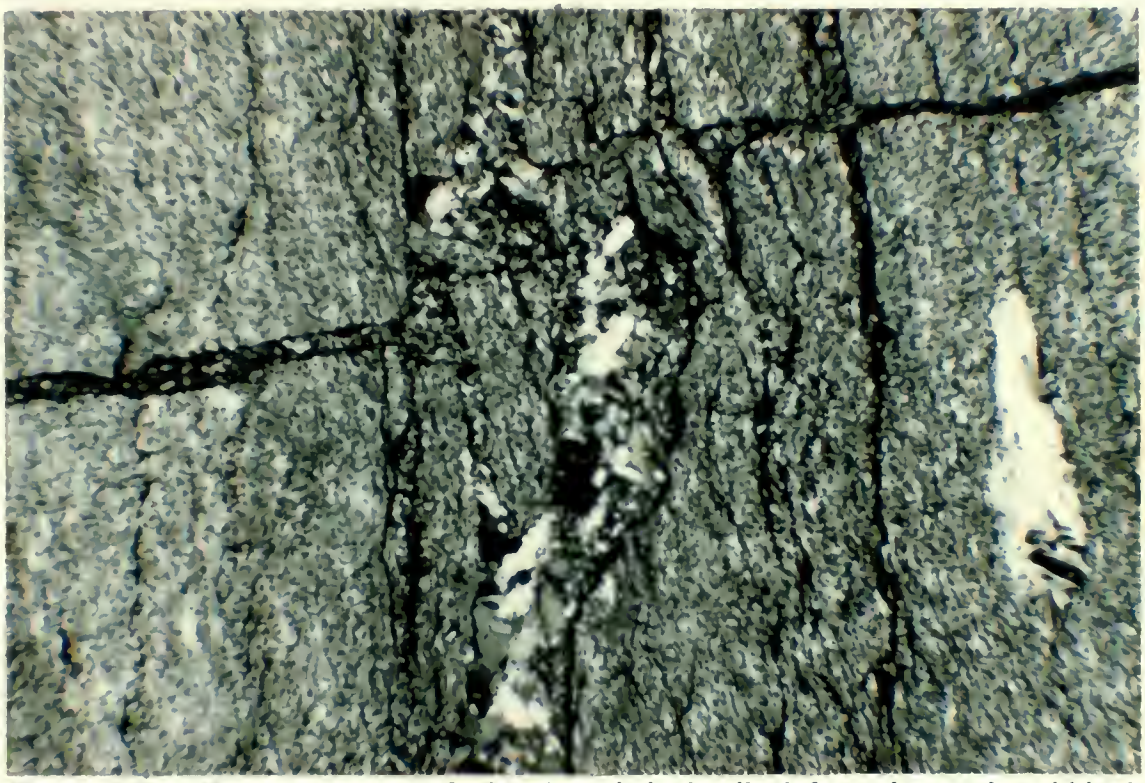

Figure 5-8: Photomicrograph of micro breccia in ductile deformed quartzite within the Long Lake Fault (crossed polars). Bottom of photo is 10 mm in length.

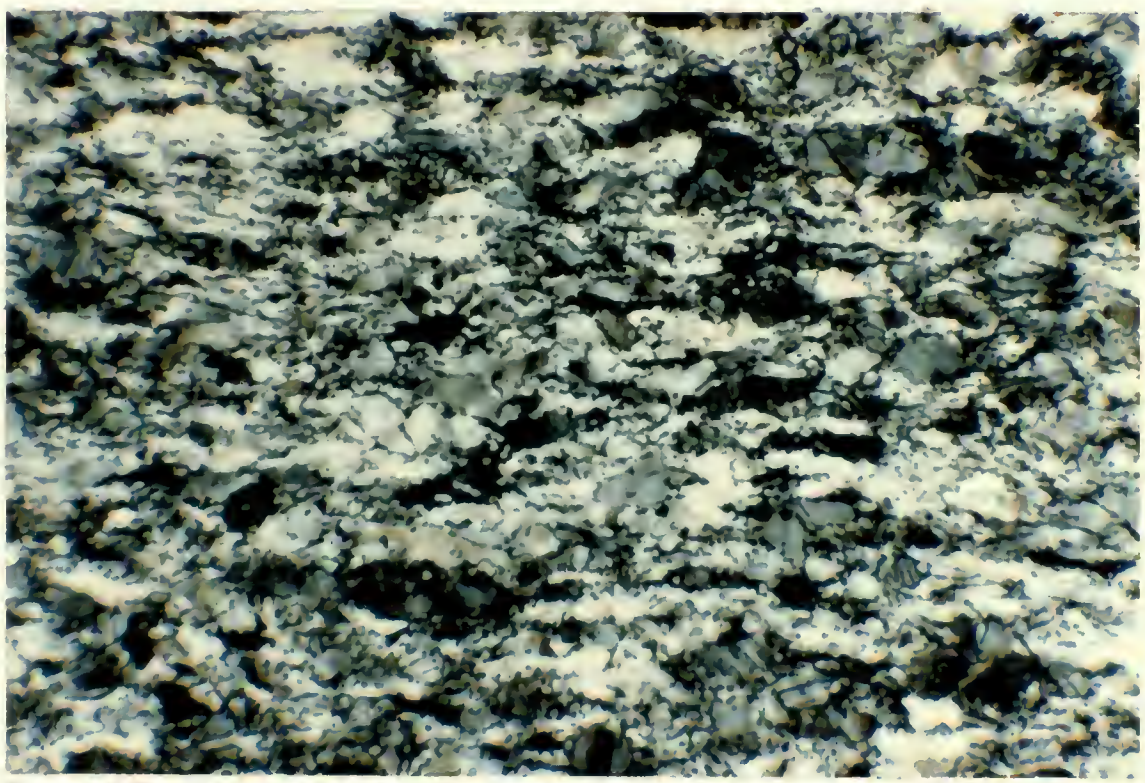

Figure 5-9: Photomicrograph of elongated quartz grains in sample DR 48 from the Murray Fault Zone (crossed polars). Section cut parallel to lineation and perpendicular to foliation. Bottom of photo is 6 mm in length.

Maxima I and III positions as opposed to development of intermediate positions in the fabric. According to their model, quartz grains in a deforming rock minimize their internal strain energy by accommodating the imposed strain along an "easy" glide plane. If the "easy" glide plane is the basal plane in the <a> direction, then grains at the Maxima III would be aligned with their basal plane striking in the same direction as the foliation plane but dipping 45° away from the foliation plane. In such an orientation, the shear stress on the basal glide system would be maximized for a shear that was perpendicular to the plane of foliation and the lineation.

In terms of girdle classification, quartz c-axis fabrics in Domain 1 have two possible interpretations. Similar fabrics to those in Domain 1 have been interpreted as Type II crossed girdle fabric even though the maxima are not joined to form the arms of the cross (Fueten 1992) and (Lister and Dornsiepen 1982).

The second interpretation of these fabrics is that they are Type I crossed girdles similar to samples DR47 and DR48. However unlike the DR47 and DR48, samples south of the LLF have a strong Maxima I position and not a weak girdle across the net. In most of the samples the southeast-northwest arm has been bisected and displaced away from the central Y position on the net while the southwest-northeast arm is more dominant. This interpretation can account for the weak girdle which joins the Maxima III positions on each side of the net and the lack of a similar girdle along the top and bottom of the net. It is clear that active glide along the prism plane resulting in a strong Maxima I position was the dominant plane of glide in all samples south of the LLF and that active glide along the basal plane in the <a> direction was less significant. Based on the configuration of the c-axis fabrics south of the LLF they are more likely type I crossed girdles with a corresponding strong Maxima I position.

In the rocks in Domain 1, northeast-southwest quadrant Maxima III positions are more significant than northwest-southeast quadrant Maxima III positions. In type I crossed girdle fabrics this asymmetric development of the Maxima III positions indicates that the rocks underwent a south over north sense of shear (Figure 5-4). The kinematic interpretation of most of the c-axes fabrics in Domain 1 supports the south over north sense of shear determined from the metamorphic facies boundaries.

Based on quartz c-axis fabric analysis from samples in Domain 1, the rocks have undergone ductile deformation indicated by the fact that they all display a well developed crystallographic preferred orientation fabric. In all the samples in Domain 1, the fabric is dominated by the strong development of the Maxima I position which is commonly attributed to active prism <a> glide. Fabrics in Domain 1 can best be classified as Type I crossed girdles even though the connecting girdle between the maxima positions is often absent and the kinematic interpretation of most of the fabrics supports the south over north shear sense.

5.4.2 Domain 2

Most of the samples from Domain 2 display quartz c-axis fabrics that are unidentifiable, however two samples (DR216 and DR139) from the vertically bedded rocks north of the LLF, display the development of at least two of the four Maxima III positions. No asymmetry in the fabric development could be used as a kinematic indicator in Domain 2.

The interesting feature of Domain 2 is the almost complete absence of the Maxima I position which dominated the fabrics south of the LLF. The development of the Maxima III position is widely attributed to result from active glide along the basal plane; however, the development of the Maxima III positions is inconsistent across the domain. In Domain 2 there is no significant evidence of active glide along the prism plane in the <a> axis

direction.

5.4.3 Domain 3

The 2 samples from Domain 3 both display the development of Type I crossed girdles defined by the development of the Maxima III and a weak development of the northeast-southwest girdle across the net. The northwest-southeast arm is bisected away from the Y position on the net, resulting in the connection of the two Maxima III on each side of the net. The location of the 2 samples is immediately adjacent to a splay fault of the MFZ. The fault (named the Naughton Fault; Card, 1964) may have been the more active shear plane. This would explain the apparent absence of ductile fabrics along the MF as defined by Thompson (1962) and Card (1964).

As with the rocks in Domain 2 which enclose Domain 3, samples from Domain 3 display no evidence of the Maxima I which is commonly interpreted as evidence for active glide along the prism plane in the <a> direction. Although the rocks in Domain 3 are similar in appearance and have undergone similar deformation to those in Domain 1, in Domain 3 active glide along the basal plane in the <a> direction dominated over glide along the prism planes in the <a> direction. The asymmetric development of the these fabrics indicates that the rocks adjacent to the MFZ underwent south over north reverse shear (Figure 5-10).

5.6 Summary of Quartz c-axis fabrics

Based on the development of preferred crystallographic orientation of quartz, the LLF appears to be a boundary between quartzite that has undergone extensive ductile deformation and quartzite that has undergone only minor ductile deformation. In all domains there is evidence for active glide along the basal plane in the <a> axis direction (although limited in Domain 2) however active glide along the prism plane in the <a> axis direction is limited to

rocks south of the LLF. Evidence for significant penetrative ductile deformation was found in a small section of the MFZ restricted to the plane of the Naughton Fault. Kinematic interpretation of quartz c-axis fabrics from south of LLF as well as the MFZ both indicate a south over north reverse sense of shear.

Extensive recrystallization does not appear to have influenced the crystallographic orientation of quartz grains in Domain 1. Sample DR214 has undergone extensive recrystallization and displays a similar fabric to samples like DR219 which have undergone far less recrystallization. It is apparent that recrystallization was dynamic and occurred in conjunction with deformation.

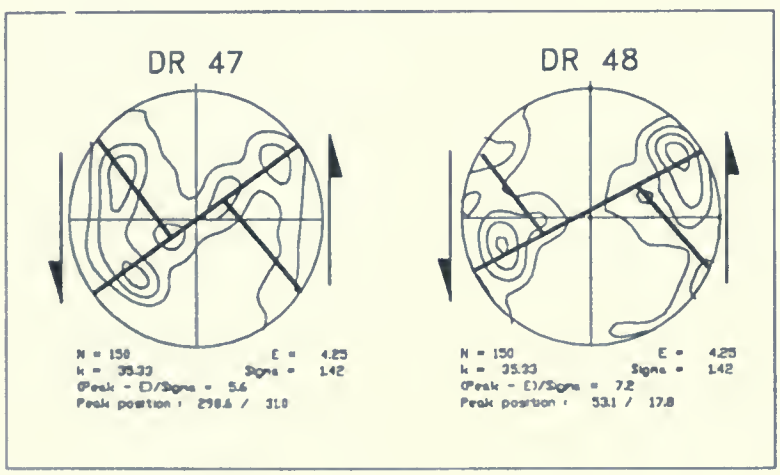

Figure 5-10: Kinematic interpretation of samples DR47 and DR48 as Type II crossed girdles. Both fabrics indicate a south over north sense of shear.

Chapter 6

Fabric Analysis using the Autocorrelation Function

6.1 Introduction

The autocorrelation function (ACF) is a powerful tool to study fabric development in deformed rocks in which the overall fabric is defined by the shape of individual grains. In rocks with a single dominant mineralogy such as the Mississagi Formation, ACF analysis can be used to determine the average grain shape and size. If grain shape has been influenced by deformation, the ACF analysis can provide an estimated value of the finite strain ellipse. This allows for easy strain calculations in rocks where no other visible strain markers such as clasts or fossils are available. Although convincing results of marker analysis using the ACF have been obtained using computer generated black and white markers (Heibronner 1992), the reliability of ACF analysis on naturally deformed rocks has not been determined.

In this chapter the ACF analysis of naturally deformed rocks will be evaluated. A comparison of ACF grain shape and size values for three samples of variably deformed quartzites of the Mississagi Formation is compared with results obtained by the Inertia Tensor Method (ITM) as described by Robin (in prep.).

6.2 Description of the Autocorrelation Function

The ACF is a computer based method that can be used to determine the average preferential direction and elongation ratios from a sample of distinct close packed markers. In the case of deformed quartz-rich rocks, quartz grains represent a population of closed markers which are optically distinguished by changes in greytones.

A greytone image can be described as a continuous variation in greylevels directly related to specific positions in an X-Y coordinate system. To process such an image by

computer, the continuous range of greylevels must be transformed into fixed greylevel values which are constant over small areas (pixels in the case of a computer monitor). Once an image is transformed a quantitative comparison of variations in greylevels in relation to directions defined by changes in the X,Y coordinate position can be performed. If a specific marker has a round shape, the distance from the centre to the marker perimeter (the location of greylevel variation) will be equal in all directions in the X-Y coordinate system. In contrast markers with a elongate shape the distance from centre to perimeter will have a direction of maximum greylevel consistency and a mutually perpendicular direction of minimum greylevel consistency. When interpreting the ACF it is important to distinguish between objects and images. The human brain will interpret a photograph of a thin section as being made up of a series of individual grains. In contrast the ACF interprets the same photo as a series of grey level variations without recognition of individual objects. ACF output is in the form of a series of contours which represent changes in overall greylevel intensity as an image is offset in a series of directions. Heilbronner (1992) determined that in theory the 0.5 contour should mimic the average size and shape of the sample of markers being analyzed.

In theory a video image of a thin section of quartzite can be analyzed using the ACF as the outline of an individual quartz grain is represented by a change in greylevel value. ACF analysis can provide a method for which the average shape and size of quartz grains in a rock can be determined. Such information can be used as a strain marker in deformed rocks.

6.3 Advantages and limitations of ACF analysis on deformed rocks

The ACF method of fabric analysis has several advantages over other methods used to evaluate grain shape and size. ACF requires no preliminary segmentation of the image such as defining the grain boundaries, fitting the best ellipse or defining the centre point of individual grains and therefore eliminates operator bias. A second advantage of the ACF is the relative speed and simplicity with which an analysis can be performed. Once the image has been captured, all that is required is several minutes of automated computer processing before outputting the information. The ACF can be used to: 1) define the average grain shape in terms of axial ratio; 2) determine the orientation of the average grain long axis; 3) give a confident average grain size value and; 4) Provide a value for the finite stain ellipse if average grain shape and size are the direct result of deformation.

Criteria must be fulfilled to ensure an accurate interpretation of the ACF output. Grain boundaries should be defined by significant variations in greylevel. Secondly, greylevel values over the surface of an individual grain should vary less than values between grains. Finally linear features such as fractures, shear zones, c-s fabrics or scratches on the surface of the slide should not appear in the ACF sampling area.

Minerals which display well developed twinning such as plagioclase and microcline can greatly distort ACF output values. Samples containing quartz ribbons with a strong preferred crystallographic orientation can produce errors in the ACF output for both average shape and size calculations.

For an accurate ACF analysis the analyzed area must contain a significant amount of grains to allow for a representative sample set. However the resolution of individual grains must be high enough to allow for accurate interpretation of variation in greylevels from one grain to another. The resolution and corresponding accuracy of the ACF improves with a

higher number of greylevels and a smaller analysis area (i.e. higher number of greylevels in the sampling area). There are several available means to obtain the above requirements on a wide range of images from thin sections to polished slabs.

The use of ACF analysis on deformed rocks has some limitations. The first is that variations in grain shape determined using ACF represents a minimum estimate for the finite strain ellipse. The possible effects of pressure solution and/or grain boundary sliding will not be represented in the change of grain shape. The second limitation of ACF analysis is that the estimate value of the finite strain ellipse can only be accurately determined in rocks with a single dominant mineralogy (in this case quartz). As the extent of shape change in a specific mineral grain is strongly influenced by the rheology of that mineral, ACF analysis on a polymineralic rock would give an average overall grain shape which would be difficult to interpret in terms of the finite strain ellipse.

6.4 Description of the Inertia Tensor Method (ITM)

The ITM described by Robin (in prep.) is a computer based analysis that allows for the calculation of average size, shape and orientation of a series of markers (quartz grains in this case). It is based on the digitizing of individual marker outlines from a population set. The area enclosed by an individual closed marker can be characterized by a two dimensional inertia tensor. The inertia tensor for one sectional marker yields the principal directions of extension and shortening for which a best fit ellipse can be calculated. The sum of a sufficient number of inertia tensors from an isotropic population of grains reveals the average marker shape, size and orientation (Robin in prep.). The best fit ellipse for a grain can be easily calculated from a closed line segment which defines the outline of the grain. This can be done by digitizing a statistically significant number of points on the grain boundary. The

ITM is similar to ACF in that it eliminates much of the operator bias. It is however a far more time consuming process as the outlines of a significant number of grains must be digitized to provide a sufficient sample set.

6.5 Methodology

Three samples of variably deformed Mississagi quartzite were chosen. Sample DR1 was taken from the undeformed rocks north of the MF, DR2 was take immediately adjacent to the LLF and DR3 was taken just north of the MF. Photomosaics were produced for a 5 mm^2 area in each thin section and the dimensions of the area measured. Grain boundaries where then traced on a piece of clear overlay. Outlines were then digitized and processed using the computer program SM (unpublished software by F. Fueten, Department of Geological Sciences, Brock University, St Catharines, Ont.) and the sum inertia tensor calculated. The average grain shape (long and short axis), orientation of the long axis in X-Y coordinate space as an angle σ and the average grain area were determined for each sample.

From the same area of each thin section two video images were captured and the ACF analysis performed. The output is in the form of a series of peak greylevel contours. The O.5 contour was digitized using the inertia tensor program. The 0.5 contour should theoretically mimic the average grain shape and size assuming that markers are close packed and the void space between grains is minimal which is the case in these samples (Panozzo, 1992). ACF output for the three samples are given in Figures 6-1, 6-2, 6-3. The ACF analysis output area was converted to millimetres so that the scale of the contour output would equal that of the photomosaics used for the ITM. The ellipse shape, size and orientation could then be calculated. The data from the two ACF outputs for each sample are then averaged. The grain size, shape and orientation data for both the ITM and ACF

Figure 6-1: ACF output for sample DR1

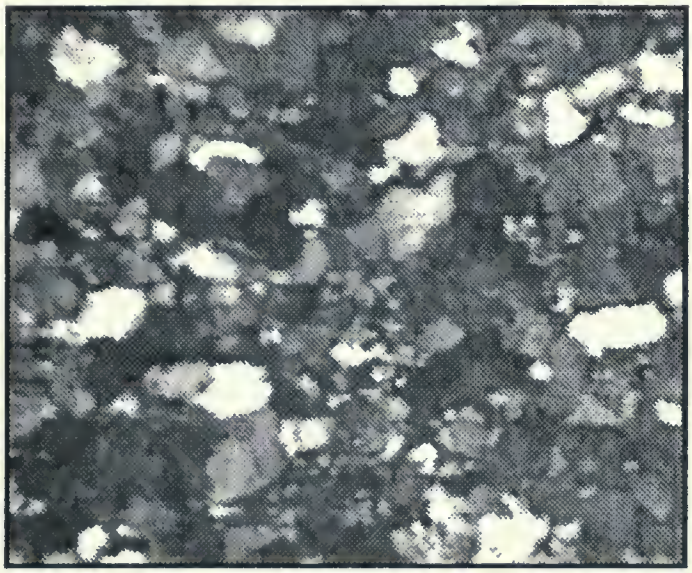

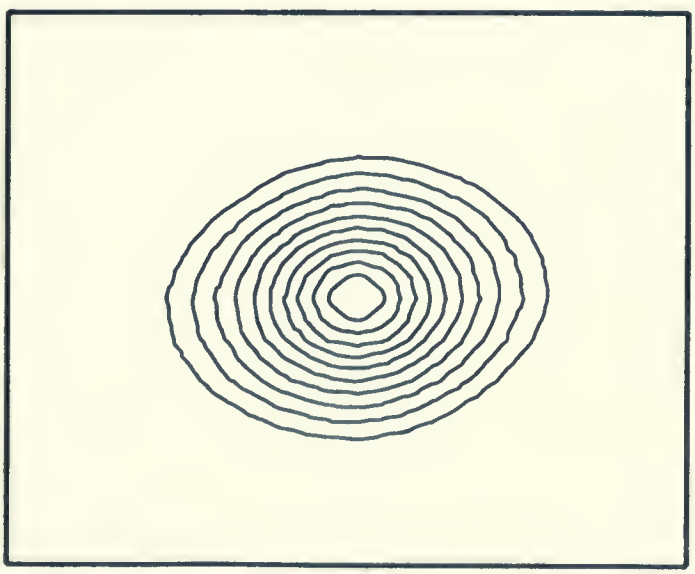

Auto-correlation of above image. Current Window: 28 X 28
Contour lines descending from 0.95 in intervals of 0.05.

Figure 6-2: ACF output for sample DR2

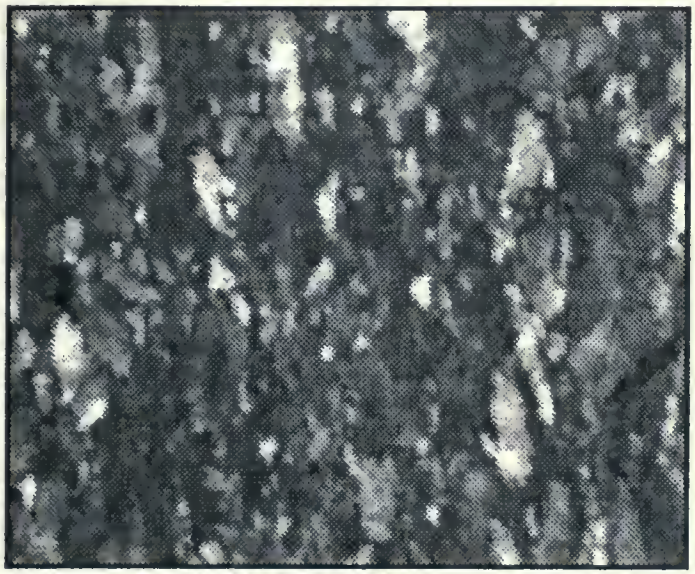

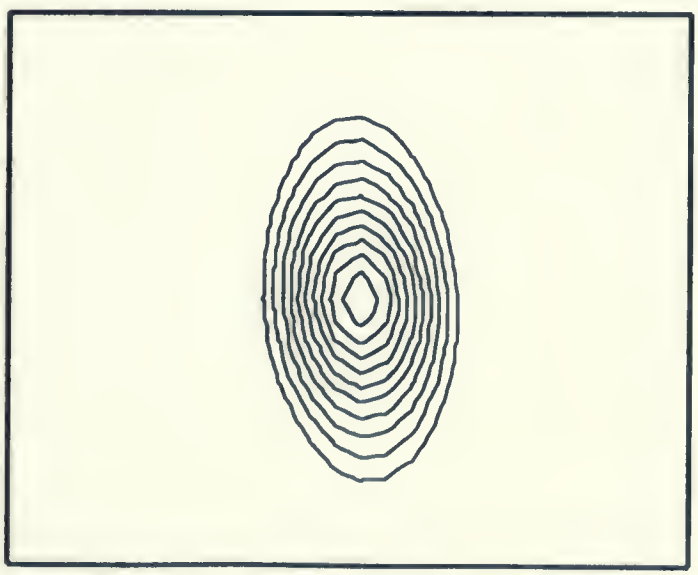

Auto-correlation of above image. Current Window: 28 X 28
Contour lines descending from 0.95 in intervals of 0.05.

Figure 6-3: ACF output for sample DR3

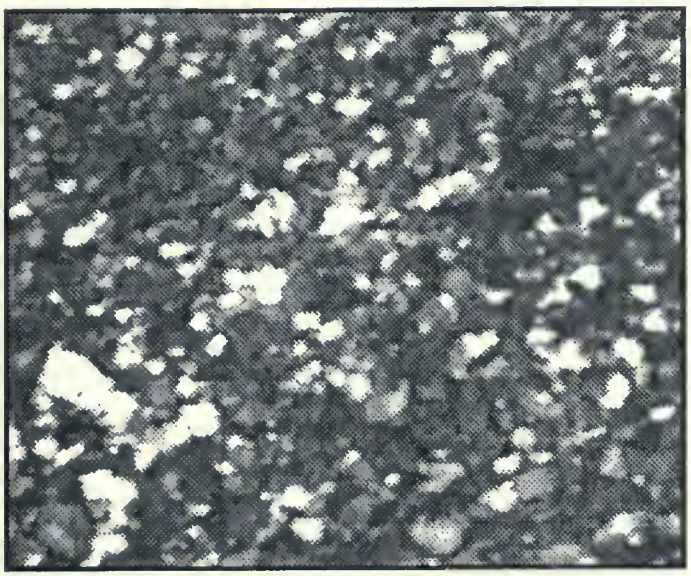

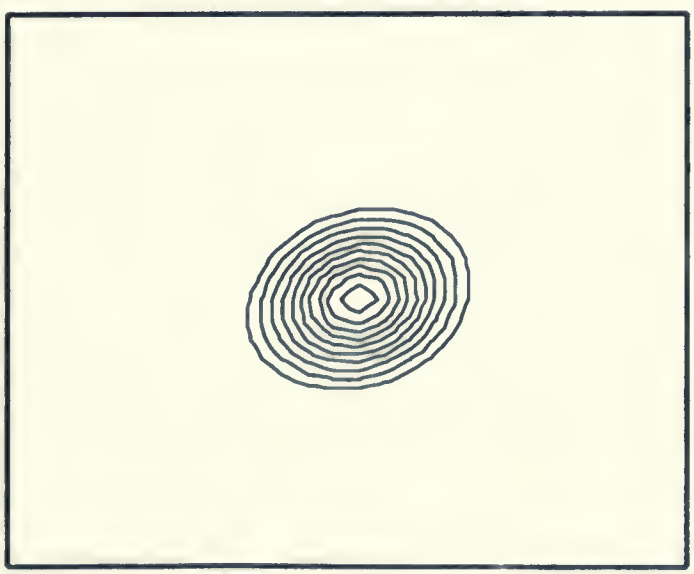

Auto-correlation of above image. Current Window: 28 X 28
Contour lines descending from 0.95 in intervals of 0.05.

methods are given in Table 6-1. For a detailed description of the mathematical procedures and software used, the reader is referred to Pfeiderer (1992).

Table 6-1: ACF test data.

Sample		Units	Inertia Tensor Method	ACF Method	Accuracy %
	Average Area	mm^2	0.065 (N=164)	0.064	2.4%
DR1	Average Axial Ratio	Amax/Bmin	1.115	1.177	5.5%
	Long Axis Orientation	Angle	14.360	-9.720	*
	Average Area	mm^2	0.022 (N=185)	0.024	6.7%
DR2	Average Axial Ratio	Amax/Bmin	2.014	2.102	4.3%
	Long Axis Orientation	Angle	84.790	83.966	*
	Average Area	mm^2	0.019 (N=169)	0.023	20.21%
DR3	Average Axial Ratio	Amax/Bmin	1.357	1.347	0.075%
	Long Axis Orientation	Angle	19.040	16.060	*

6.6 Comparison of Results

6.6.1 Average Grain Size

Average grain size values for the three samples ranged from 0.065 to 0.019 mm^2. Samples DR1 (coarse grained quartzite) and DR3 (fine grained quartzite) were autocorrelated at the same magnification. Both samples displayed little fabric development. Sample DR2 with an average grain size similar to that of DR3 was autocorrelated at a magnification twice that of the other samples. From the results in Table 6-1 the average grain size calculations determined from the ACF are similar to those determined from the ITM. Samples DR1 and DR2 have less than 7% difference in average grain size values between the two methods and do not exceed 0.002 mm^2. The 20.2% difference in values between results for sample DR3 is most likely the result of the grain size being too small for the greylevel resolution of the ACF program. If such is the case then the individual grain size should fall between 0.5 and

1.0 percent of the total ACF analysis area to ensure adequate results. In the case of a 256 by 256 pixel analysis window, which was used in this study, the area undergoing ACF should be 10 to 15 grains in width. Similar conclusions were made by Heilbronner (1992).

6.6.2 Average Axial Ratio

Average axial ratios (defined as the long axis divided by a mutually perpendicular short axis) determined using the ITM for the three samples ranged from 1.1 to 2.0. ACF analysis of the three samples gave very similar values to those obtained using ITM. For all three samples the percentage of difference was never greater than 5.5%. The most important of these trials is sample DR2 were the initially more spherical grains now display a preferred elongation as a result of deformation. Average axial ratio determined by ITM have a value of 2.01 and the corresponding ACF analysis gave a value of 2.10.

6.6.3 Long Axis Orientation

If grains have developed a preferred long and short axis as a result of deformation, then the orientation of the average grain long axis can be determined. The accurate determination of the average long axis orientation for a population of grains becomes increasingly more difficult as the grains have a more spherical shape. ACF analysis was performed on several samples of different axial ratio to determine the minimum axial ratio value for which an accurate angle of elongation could be determined. This was done by first determining the axial ratio and long axis orientation of a thin section. The thin section was then rotated through a known arbitrary angle on the microscope stage and ACF analysis was performed on the same area of the thin section. This was done on several samples with different axial ratios to determine at what minimum axial ratio the ACF value could accurately track the known angle of rotation of the thin section. The data are presented in Table 6-2. It was determined that for average axial ratios greater or equal to 1.3 the

orientation of the long axis could be accurately determined within a few degrees. The accuracy of the long axis orientation increases with the average axial ratio value.

Table (6-2) Long axis orientation test using ACF

Sample #	Axial Ratio (long/short)	Rotation of Microscope stage from 0°	Corresponding rotation of ACF output long axis	Difference between values
DR 18	1.10	70°	37.2°	32.8
		160°	142.8°	17.8
DR 141	1.21	70°	61.3°	8.7
		160°	169.8°	9.8
DR 49	1.30	70°	72.2°	2.2
		160°	157.6°	2.4
DR 181	1.40	70°	71.6°	1.6
		160°	157.3°	2.7
DR 73	1.50	70°	68.5°	1.5
		160°	160.9°	0.9

Long axis orientation determined by ACF for sample DR1 (axial ratio=1.1) varied from the value determined by ITM by approximately 25°. Differences between long axis orientation values for sample DR3 (axial ratio=1.35) was 3° and for sample DR2 (axial ratio=2.1) was less than 1°.

6.7 Conclusions

From the results of comparison tests between fabric analysis using the ACF and ITM, it is concluded that an accurate determination of average grain size, shape and orientation can be obtained from samples of the Mississagi Formation using the ACF method. Several

criteria must be met to ensure the accuracy of the ACF output. To determine the average grain size there should be between 100 to 200 individual grains in the analysis area. ACF can be used to calculate the average grain shape in terms of axial ratio (long/short). If the development of elliptical axial ratio (long > short) occurred as a result of deformation of original detridal grain shapes, the average grain axial ratio can be used as a value for the finite strain ellipse.

In samples where the average axial ratio is greater the 1.3, the orientation of the long and short axis can be determined by the ACF.

Chapter 7

Regional Grain Shape Analysis using the Autocorrelation Function

7.1 Introduction

In Chapter 6 it was established that the ACF method could accurately determine values for the average grain size, average axial ratio and the orientation of the long axis in thin section samples of Mississagi quartzite. If changes in the shape of grains are the direct result of deformation, the determination of regional variations in average grain size, shape and orientation can provide minimum values for changes in the finite strain ellipse. In a regional structural analysis it is better to use a technique that can obtain a large number of data points over a method in which a few data points are used (Ramsay et al. 1983).

A regional grain shape analysis using the autocorrelation function (ACF) was performed on 65 thin section samples of Mississagi quartzite to measure changes in regional grain shape and use them as strain markers. The main advantage of the ACF method is the simplicity and speed with which it can be performed.

7.2 Method

Thin sections were cut parallel to the observed lineation and perpendicular to foliation. North of the LLF, where no lineation was observed sections were cut perpendicular to the strike of the bedding plane. In most cases this placed them in the same plane as thin sections in the lineated rocks. The 25 thin section samples used for c-axis fabric evaluation were also used in the ACF fabric analysis.

ACF analysis was performed on each thin section at the same magnification. From the ACF output, the average grain shape properties were determined. Corresponding elliptical

symbols for the average grain shape were at the field locations of each sample (Figure 7-1). In Chapter 6 it was determined that ACF could accurately determine the long axis orientation of grains with an average axial ratio greater or equal to 1.3. Samples were divided into two groups based on the value of the axial ratio. Samples with an axial ratio less than 1.3 were given a symbol that did not indicate the long axis orientation but was representative of the average grain size. Samples with an axial ratio greater than 1.3 were give a separate symbol. The symbol indicates the average grain size and shape as well the trend and plunge of the long axis. All statistical information for each sample is given in Table 7-1.

7.3 ACF Analysis Results

7.3.1 Grain Size

ACF values for average grain size for rocks south of the LLF range from 0.015 to 0.04 mm^2 with an average of 0.025 mm^2 (Figure 7-2). Smaller average grain sizes were observed in the highly sheared rocks within the LLF and are attributed to increased amounts of dynamic recrystallization.

ACF determination of average grain size for non-elongated samples north of the LLF is equal to 0.0289 mm^2 and for the elongated samples was 0.0234 mm^2. The reduction in grain size in the elongated samples is attributed to the partial recrystallization of deformed primary quartz grains.

The data indicate that while there is a reduction in average grain size south of the LLF, the elongation of quartz grains has occurred with only a minor reduction of size. This would indicate that elongation of grains occurred as a result of stretching of more originally spherical grains and not by a) removal of silica on the short axis sides of the grain or b) loss of volume by removal of subgrains during dynamic recrystallization or c) deformation of new

Table 7-1: Statistical Data for ACF analysis of 65 samples of Mississagi Quartzite

Sample #	Grain Area (mm2)	Axial Ratio		Trend	Plunge	Length (mm)	Amax (mm)	Bmin (mm
D6	0.0119	1.09				0.3897	0.0641	0.0591
D18	0.0429	1.10				0.7375	0.1228	0.1112
D21	0.0250	1.22				0.5666	0.0987	0.0807
D23	0.0371	1.09				0.6855	0.1133	0.1043
D25	0.0206	1.08				0.5108	0.0841	0.0779
D28	0.0172	1.68	*	118	80	0.4916	0.0959	0.0572
D29	0.0165	2.23	*	165	64	0.5167	0.1083	0.0486
D32	0.0178	1.72	*	135	75	0.5030	0.0987	0.0575
D34	0.0316	2.24	*	150	76	0.7138	0.1501	0.0670
D43	0.0212	1.26				0.5235	0.0922	0.0732
D45	0.0270	1.34	*	155	80	0.5945	0.1072	0.0803
D46	0.0378	1.23				0.6974	0.1219	0.0988
D47	0.0397	1.63	*	135	67	0.7405	0.1434	0.0881
D48	0.0203	2.07	*	182	82	0.5594	0.1157	0.0560
D49	0.0201	1.30				0.5103	0.0911	0.0702
D51	0.0133	1.04				0.4109	0.0664	0.0639
D55	0.0195	1.12				0.4982	0.0834	0.0745
D57	0.0700	1.08				0.9430	0.1548	0.1439
D63	0.0154	1.71	*	160	82	0.4657	0.0914	0.0536
D65	0.0278	1.24				0.5984	0.1046	0.0847
D66	0.0351	1.33	*	112	83	0.6757	0.1219	0.0917
D67	0.0192	1.05				0.4929	0.0802	0.0762
D68	0.0208	1.49	*	172	90	0.5288	0.0992	0.0667
D73	0.0111	1.50	*	161	62	0.3869	0.0727	0.0485
D78	0.0297	1.36	*	144	73	0.6244	0.1134	0.0835
D83	0.0195	1.57	*	120	88	0.5158	0.0987	0.0628
D85	0.0328	1.13				0.6470	0.1089	0.0960
D97	0.0248	1.08				0.5609	0.0923	0.0856
D98	0.0153	1.18				0.4418	0.0758	0.0642
D99	0.0215	1.02				0.5206	0.0837	0.0816
D101	0.0230	1.28				0.5447	0.0967	0.0757
D114	0.0238	1.29				0.5559	0.0993	0.0763
D115	0.0199	1.83	*	178	76	0.5373	0.1076	0.0588
D121	0.0352	1.37	*	168	86	0.6797	0.1240	0.0904
D128	0.0304	1.11				0.6215	0.1038	0.0933
D130	0.0248	1.09				0.5602	0.0926	0.0852
D132	0.0274	1.12				0.5902	0.0989	0.0881
D138	0.0373	1.25				0.6924	0.1219	0.0973
D139	0.0229	1.08				0.5389	0.0889	0.0822
D141	0.0347	1.21				0.6673	0.1155	0.0955
D145	0.0300	1.15				0.6191	0.1051	0.0910
D146	0.0143	1.66	*	170	88	0.4478	0.0870	0.0523
D147	0.0382	1.23				0.7003	0.1221	0.0996
D148	0.0455	1.05				0.7583	0.1235	0.1171
D149	0.0217	1.13				0.5267	0.0882	0.0784
D162	0.0236	2.48	*	134	85	0.6338	0.1363	0.0550
D163	0.0140	1.63	*	128	64	0.4399	0.0851	0.0523
D164	0.0129	1.92	*	142	54	0.4398	0.0888	0.0462
D169	0.0323	1.18				0.6420	0.1102	0.0933
D174	0.0270	1.38	*	145	83	0.5961	0.1089	0.0790
D175	0.0232	1.50	*	148	67	0.5588	0.1054	0.0701
D178	0.0263	1.62	*	134	48	0.6033	0.1164	0.0719
D181	0.0115	1.40	*	180	87	0.3911	0.0717	0.0512
D183	0.0254	1.09				0.5683	0.0940	0.0861
D186	0.0163	1.29				0.4603	0.0818	0.0635
D188	0.0192	1.20				0.4972	0.0857	0.0714
D189	0.0172	1.25				0.4715	0.0827	0.0663
D194	0.0119	1.06				0.3898	0.0634	0.0600
D198	0.0187	1.08				0.4865	0.0802	0.0742
D199	0.0269	1.06				0.5837	0.0953	0.0899
D210	0.0316	1.80	*	184	86	0.6766	0.1344	0.0749
D214	0.0097	1.78	*	200	43	0.3724	0.0740	0.0416
D216	0.0167	1.28				0.4698	0.0860	0.0620
D219	0.0178	1.81	*	191	87	0.5070	0.1012	0.0559
D220	0.0165	1.51	*	134	83	0.4732	0.0891	0.0590

Samples denoted with a * have axial ratios >= 1.3

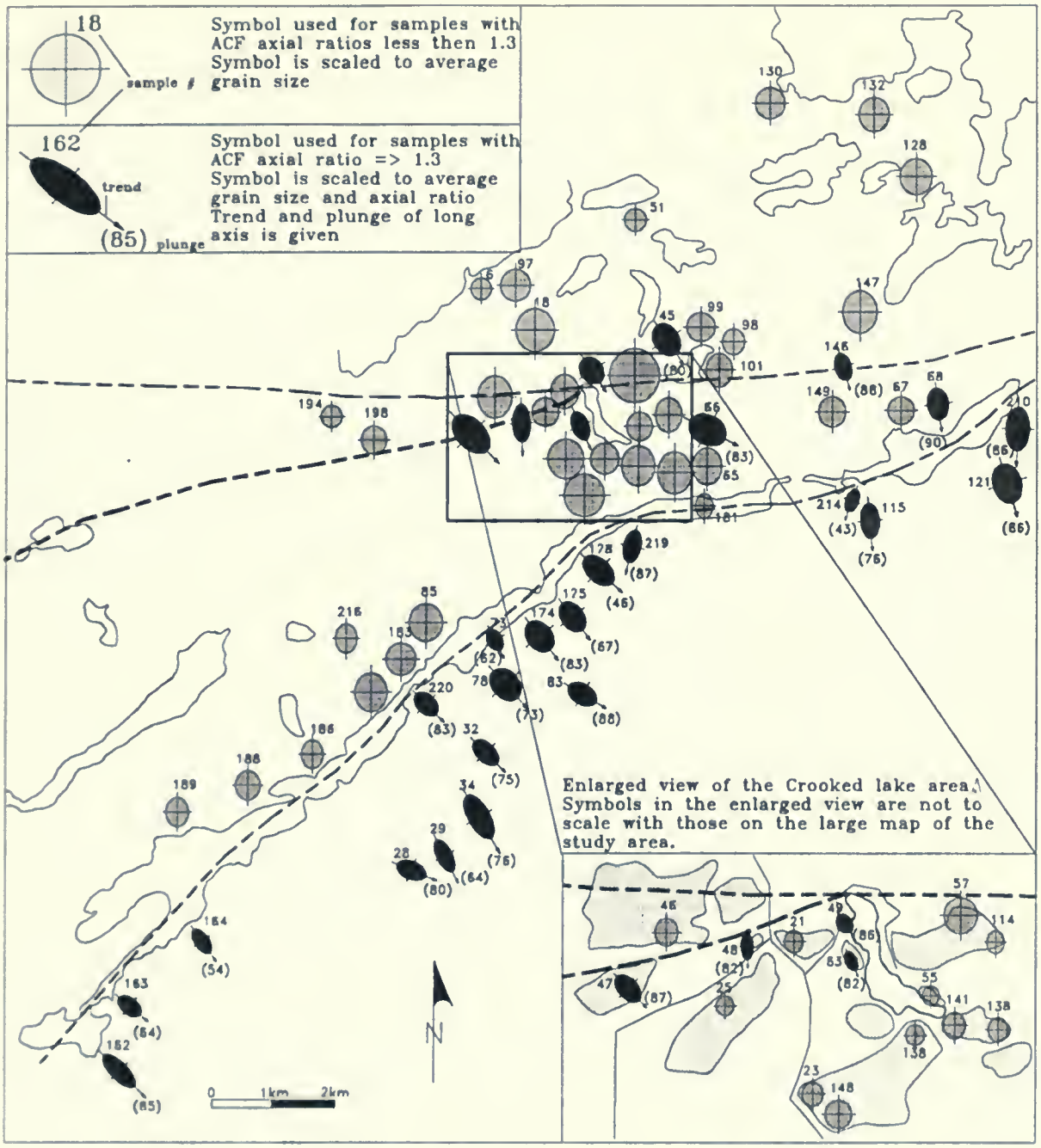

Figure 7-1: Regional ACF analysis of 65 samples of Mississagi quartzite

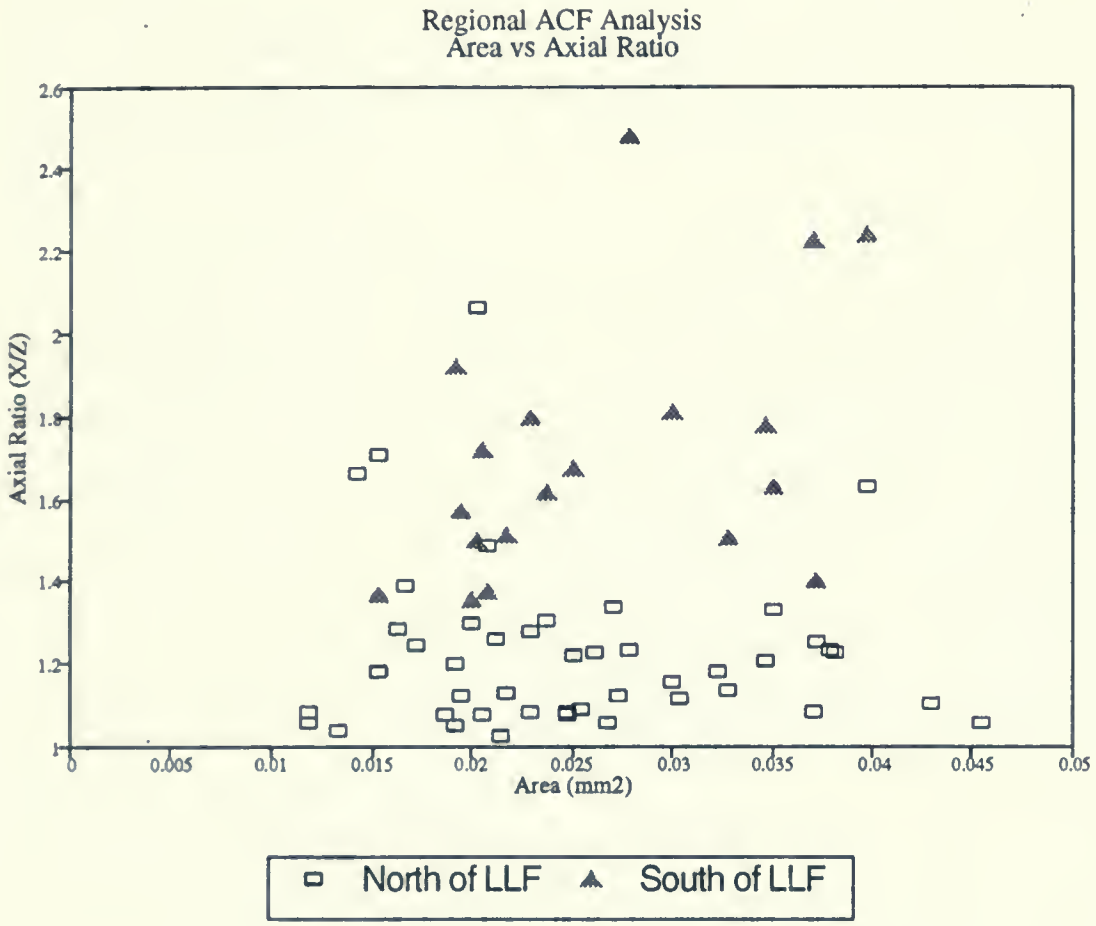

Figure 7-2: Graph plotting average grain size versus axial ratio

grains.

7.3.2 Axial Ratio

All samples of Mississagi quartzite south of the LLF have axial ratios greater then 1.3. Values range from 1.38 to 2.48 with an average of the 20 samples south of the LLF equal to 1.72. The elongation of the quartz grains increases approaching the Chief Lake batholith as samples with axial ratio greater than 2.0 are in close proximity to the contact with the batholith.

In contrast to Mississagi quartzite south of the LLF, rocks north of the fault are dominated by average grain axial ratios less than 1.3. The only exceptions to this are isolated occurrences of lineated rocks adjacent to the MFZ. The average axial ratios for samples with axial ratios less than 1.3 is equal to 1.15 and the average of the 7 samples north of the LLF with an axial ratio greater than 1.3 is 1.59. Eight of the samples with axial ratios greater than 1.3 are located on splay faults of the MFZ and not on the actual plane of the MF as defined by Dressler (1984b). The most notable of these splay faults is the Naughton Fault in which samples DR47 and DR48 were taken.

7.3.3 Long Axis Orientation

Consistent orientations of the long axis are observed in the rocks south of the LLF. Based on ACF determination of long axis orientation of quartz grains, the lineated rocks south of the LLF can be divided into two groups based on the regional orientation of the quartz grain long axis which defines the lineation. The variation in regional lineation orientation appear in the LLF just south of Crooked Lake (Figure 7-1).

Rocks to the west of this boundary have a consistent lineation trend in a southeasterly direction. The plunge of the lineation ranges from 46 to 87°. In the southeastern section of the study area the regional trend of the lineation rotates approximately 40° and trends in a

south to southwest orientation which reflects the bend in the LLF. As the thin sections were cut parallel to the observed lineation, changes in the trend of the long axis is directly related to changes in the orientation of the lineation. The trend of the long axis for the deformed samples in the MFZ is in a south to southeast direction and the plunge is subvertical with angles between 80 and 90°.

7.4 3-D Grain Shape Analysis Using ACF

ACF analysis can be used to determine the 3 dimensional characteristics of quartz grains. If the grain dimensions are the result of strain, it can provide a minimum value for the finite strain ellipse. Detailed 3-D shape analysis was performed on 9 samples of ductily deformed Mississagi Formation quartzite. Eight of the samples were from south of the LLF and one was taken from the MFZ.

Thin sections used in the regional ACF analysis were oriented such that the long axis of the grain, as determined by ACF represents the X axis or the direction of maximum extension. The mutually perpendicular short axis represents the Z kinematic axis or direction of minimum extension. The section therefore lies within the X-Z kinematic plane. Quartz c-axis fabric analysis revealed that the plane of principal shear is slightly oblique to the X axis.

To determine the three dimensional shape of average grains, a thin section for each of the 9 samples was cut perpendicular to both foliation and lineation. This thin section was oriented in the Y-Z plane, with Y being the axis of intermediate extension. In the two mutually perpendicular thin sections, all three axes could be examined. ACF analysis was performed on the Y-Z plane thin section and combined with the data for the X-Z plane.

The length of the Z axis which is present in both sections was then set at a value of

1 which allowed for the calculation of the relative values for the X and Y axis with respect to a fixed value for Z. A single numeric value for the Z axis could not be determined from the 2 thin sections as they were analyzed at different magnification. This was done to ensure an accurate ACF output as the surface area of a specific grain can vary greatly depending on the surface which is being viewed. It was determined in Chapter 6 that the surface area of individual grains must be between 0.5 and 1% of the total ACF analysis area for accurate results. X/Y and Y/Z ratios and k values were calculated and plotted on a Flinn diagram (Figure 7-3). Statistical information for the 9 samples is given in Table (7-2). Sample locations with corresponding ACF analysis output are plotted in Figure (7-4).

The 3-D shape of the deformed quartz grains can be described as triaxial ellipsoids with (X>Y>Z) (Ramsay and Huber. 1983) where X is parallel to the observed lineation, Y is normal to lineation and lies in the plane of the foliation and Z is normal to the plane of the foliation. Based on the position of the 9 samples on a Flinn diagram and corresponding k values, the samples can be divided into two groups. The first group includes those samples with $k > 1$ (1.17 to 1.62) (DR29, DR83, DR115, DR219 and DR220). These samples lie in the field of constrictional strain ($X/Z > Y/Z$) resulting in the development of a stretching lineation which plunges between 65 and 88° in a south to southeast direction. The second group which includes samples DR34, DR48, DR73 and DR162 lie in the field of flattening strain ($X/Z < Y/Z$) with k values ranging from 0.68 to 0.89.

A possible explanation for the presence of the flattening strain fabrics is that samples DR162 and DR34 are located within a southwest trending shear zone that was mapped by Henderson (1967) while the other samples are distant from this shear zone. This shear zone forms the contact between much of the Chief Lake batholith and lithologies of the Huronian Supergroup. Deferential straining along these narrow shear zones could explain the apparent

change in the 3-D grain shape for these samples.

Figure 7-3: Flinn diagram plot of 9 samples of deformed Mississagi quartzite. Data based on 3-D ACF analysis. Statistical information of each sample given in Table 7-2

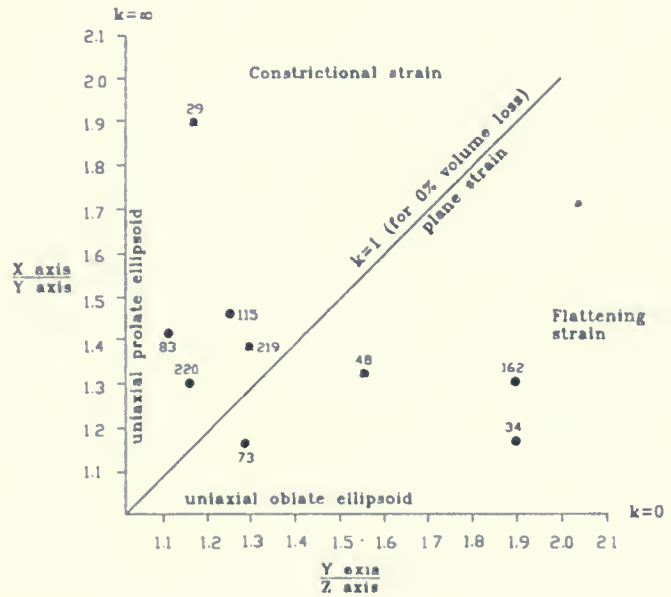

Table (7-2) Statistical information for 3-D ACF Analysis of 9 samples of Mississagi Quartzite

Sample #	X-Z plane axial ratio	Y-Z plane axial ratio	X	Y	Z	X/Y	Y/Z	k
DR162	2.48	1.90	2.48	1.90	1	1.30	1.90	0.68
DR29	2.32	1.17	2.23	1.17	1	1.90	1.17	1.62
DR34	2.24	1.90	2.24	1.90	1	1.17	1.90	0.61
DR220	5.51	1.16	1.51	1.16	1	1.30	1.16	1.21
DR83	1.57	1.11	1.57	1.11	1	1.41	1.11	1.27
DR73	1.50	1.29	1.50	1.29	1	1.16	1.29	0.89
DR219	1.81	1.30	1.81	1.30	1	1.39	1.30	1.06
DR115	1.83	1.25	1.83	1.25	1	1.46	1.25	1.17
DR48	2.07	1.56	2.07	1.56	1	1.32	1.56	0.84

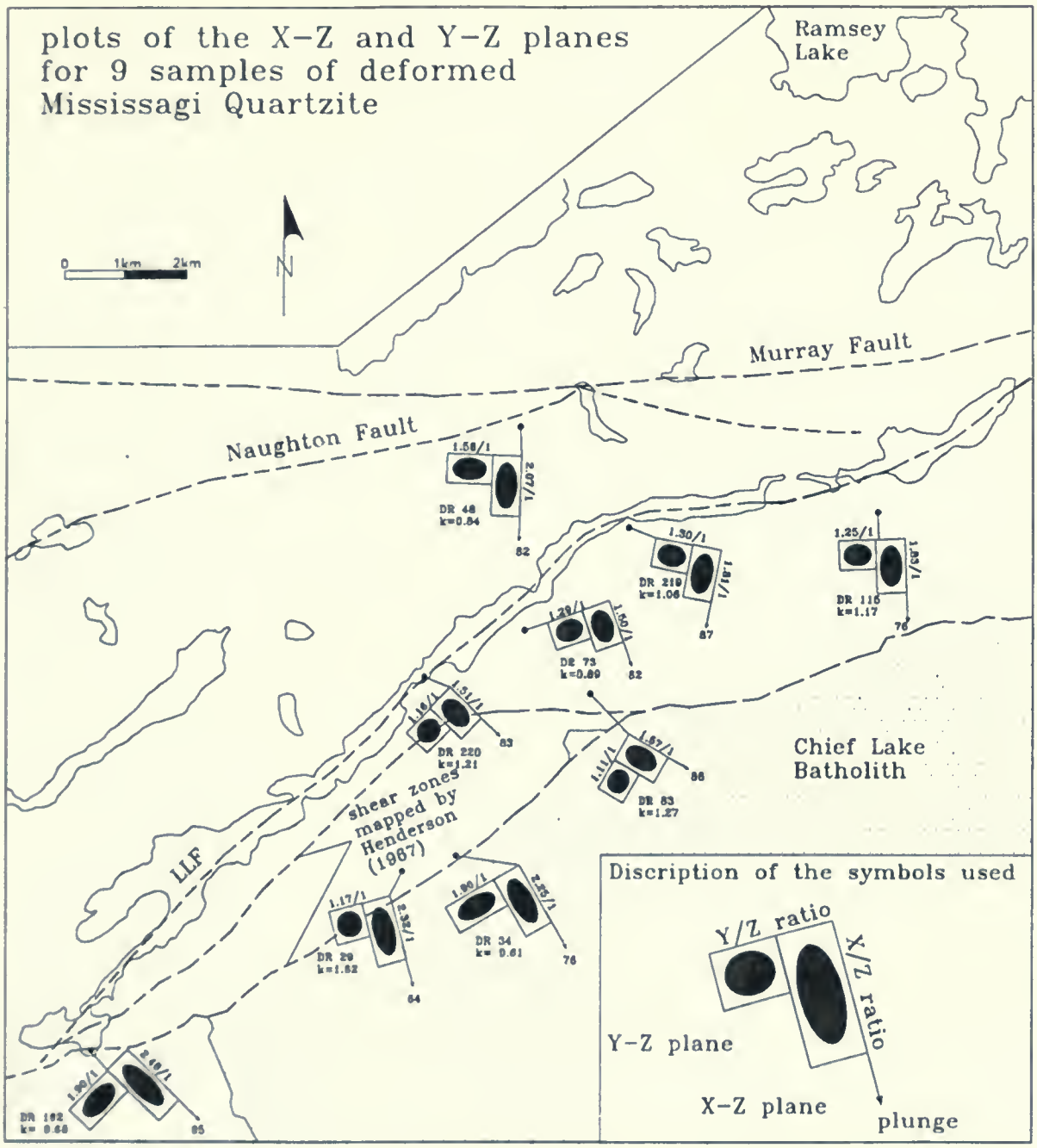

Figure 7-4: 3-D grain shape analysis of 9 samples of deformed Mississagi Quartzite

The flattening strain ellipse of DR48, which is located adjacent to the Naughton Fault of the MFZ could have been produced by a component of strike slip strain during south over north high angle reverse shear along the MFZ or may indicate that total strain intensity was less along the MFZ during deformation.

7.4 Summary of Regional Grain Shape Analysis using ACF

Based on regional ACF analysis of grain shapes in the quartzites of the Mississagi Formation, the LLF is a major structural feature that separates rocks of contrasting grain shape. Rocks north of the LLF have for the most part not undergone extensive ductile deformation directed from the southeast. Limited evidence of ductile deformation in the Mississagi quartzite north of the LLF is restricted to rocks immediately adjacent to the MFZ. The resulting finite strain ellipse in the MFZ is a triaxial form ($X > Y > Z$) with $k < 1$ indicating that the rocks underwent flattening strain. The finite strain X axis plunges subvertically to the south with the mutually perpendicular Y axis trending east-west and plunging subhorizontally.

In contrast lithologies south of the LLF have undergone regional penetrative ductile deformation as all samples have axial ratios in the X-Z plane greater than 1.3 with a average of 1.72. The reduction in average grain surface area in the X-Z plane south of the LLF is attributed to partial recrystallization of quartz. 3-D ACF analysis of samples of quartzite south of the LLF indicate that the rocks underwent regional constrictional style deformation represented by a triaxial strain ellipse.

Chapter 8

Discussion and Tectonic Synthesis

8.1 Correlation of Lithologic Units

In order to fully reconstruct the deformational history associated with the major structural features in the study area, it is important that the stratigraphic correlation of the Huronian Supergroup be properly understood. This has been a topic of much debate since the area was first mapped in detail by Collins (1938). The most notable area of controversy is the formational correlation of the occurrences of gritty quartz-rich conglomeritic rocks that crop out in several locations along the LLF. In this study they have been correlated with the Lauzon Member which forms the base of the Bruce Formation. This correlation was based on the sharp lithologic contact with the underlying Mississagi Formation. The pink granite clasts are absent in the Ramsay Lake Formation but have been documented in the Lauzon Member. The identification of large Mississagi quartzite clasts within the conglomerate indicates that the unit postdates the Mississagi Formation and that the Mississagi was lithified prior to deposition of the Lauzon Member. The quartz rich mineralogy of the matrix contrasts with that of either the Bruce or Ramsay Lake Formations in the study area.

Although outcrops of the Lauzon conglomerate form a northeasterly trending belt across the area, it is clear that the present configuration of Lauzon Member outcrops have been affected by displacement along the LLF. It is most likely that much of the Mississagi quartzite south of the LLF was stratigraphically lower than the conglomerate prior to deformation.

In a regional context the rocks of the Huronian Supergroup in the area become

younger from north to south and are correlated with the Hough Lake and lower Quirke Lake Groups. This regional southerly dipping configuration of the lithologies appears to predate the Sudbury event and is remnant of the large scale folding that affected Huronian rocks in the Manitoulin area to the west. This is based on the fact that the northeasterly trending belt of each Huronian formation in the study area can be correlated with some confidence to similar less deformed areas of Huronian strata to the east and west of the study area.

Occurrences of the Lauzon Member can be correlated with a belt of Bruce Formation conglomerates along the north shore of Panache Lake to the southwest and to the Quirke Lake Group rocks in Dryden and Falconbridge Townships to the northeast. Structural blocks of Quirke Lake and Cobalt Group rocks have been identified at the contact with the Chief Lake batholith just outside the southwest corner of the study area (Henderson 1967).

Another interesting feature was a small outcrop of monomictic conglomerate that clearly was deposited on vertical beds of Mississagi Formation. The unit differs in mineralogy from that of the underlying quartzite, and based on thin section analysis has undergone less deformation than the underlying rocks. The recognition of this unit indicates that the present erosional surface of the rocks was once the surface of sediment deposition. This unit was most likely deposited after the first major deformational period but may predate the Grenvillian Orogeny as it has undergone some deformation.

Rocks in the study area have been intruded by felsic dykes that strike in a southwest direction. Dykes of this type have not been reported in previous literature for the region. In thin section, the dyke appears undeformed, indicating that felsic dyke intrusion occurred after much of the deformation that affected the area. Possible disruption of the dyke across the major structural features in the area could not be determined.

8.2 Deformation in the Study Area

Rocks in the area have undergone significant deformation which appears to post-date the regional folding documented in comparable rocks to the southwest and northeast. Two major structural features cut across the study area, namely the well documented MFZ and the previously undocumented LLF. Evaluation of deformation was completed using three different methods, 1) field observations, 2) fabric analysis of quartz crystallographic preferred orientations and 3) grain shape analysis using the computer based autocorrelation function. Based on field mapping and microstructural studies the LLF was a more significant plane of displacement then the MFZ as it separated rocks that have undergone noticeably different deformation styles.

8.2.1 South of the Long Lake Fault

A regional grain shape analysis using ACF determined that the LLF represents the northern limit of regional penetrative elongation of quartz grains in the Mississagi Formation. The finite strain ellipse determined using three dimensional ACF grain shape analysis defines a triaxial ellipsoid with an average k value = 1.27 (for no volume loss). This places the samples in the constrictional strain field. Although the regional strain was constrictional, local occurrences of flattening strain occur south of the LLF and may be related to changes in strain intensity along narrow shear zones at the contact of the Chief Lake batholith and the Huronian metasediments.

ACF determined k values represent a minimum value for strain as they are based on the three dimensional shape of deformed quartz grains. Petrographic examination of thin sections revealed that pressure solution was minimal during deformation. Grain volume loss determined for rocks south of the LLF is approximately 25% for an average grain volume determined from rocks north of the LLF. This is based on regional grain size values

determined from ACF analysis. Much of this average grain volume loss can be attributed to increased levels of dynamic recrystallization in the rocks south of the LLF and not to a net loss of silica from the system or a smaller initial grain size.

Quartz c-axis fabric analysis in the area revealed that the LLF represents the northern limit of consistent fabric development in samples of Mississagi quartzite. Well developed quartz c-axis fabrics south of the LLF indicate that the rock deformed in a plastic nature by dislocation glide. There is evidence that quartz grains south of the LLF have accommodated the imposed strain by active glide on the prism plane in the <a> direction which is widely believed to produce a fabric dominated by development of the Maxima I. Limited development of the Maxima III and no development of the Maxima I position north of the LLF indicate that prism glide was restricted to south of the LLF. This is a key indicator that differences in deformation occur across the LLF. Two possible parameters that could explain this distribution are the temperature and strain rate. It is well documented that temperature during deformation can influence the ease with which active dislocation glide can occur along a specific crystallographic plane. As the LLF separates rocks to the south that were most likely at P-T conditions characteristic of amphibolite facies metamorphism during deformation from rocks with greenschist facies P-T conditions, increased temperature could be the important factor for active glide on the prism plane. Similar fabrics to those from samples south of the LLF have been documented by Shanks and Schwerdtner (1990) in the amphibolite facies South Range Shear Zone within the Sudbury Structure.

Kinematic interpretation using the asymmetric development of the Type I crossed girdle in the deformed samples south of the LLF reveal a south over north sense of shear. A similar kinematic conclusion was determined from 2 samples in the MFZ. No other kinematic indicators were found to confirm this sense of shear; however it would seem

logical to ascribe a south over north sense of shear on the LLF as it has juxtaposed ductily deformed amphibolite grade rocks to the south with non-ductily deformed, lower grade rocks to the north.

8.2.2 North of Long Lake Fault

Deformation north of the LLF contrasts greatly with that south of the fault. North of the LLF, deformation is characterized by distinct structural block being juxtaposed to form angular discordances. In several locations vertically bedded lithologies appear to have been thrust onto shallow dipping rocks. On previous maps of the area many of these angular discordances have been interpreted as folds. Prior to deformation related to the MFZ these rocks may have been in a similar configuration to those distant from the MFZ and resulted from folding. It is clear that their present configuration was not produced during a period of folding but rather a period of brittle faulting and therefore fold axes were not assigned to these changes in bedding orientation. Thrusting of structural blocks most likely resulted during the south or north reverse faulting along the LLF. As rocks south of the LLF fault were brought to the surface, rocks north of the LLF underwent compression in a southeast-northwest direction. Approaching the MFZ clasts of Sudbury-Type breccia show a strong alignment in a northeast direction. This alignment can be attributed to the southeast-northwest compression. Occurrences of cataclastic breccia are well developed in the MF. Thin section analysis of the breccia revealed that previously ductily deformed quartzites were incorporated into the breccia indicating that a period of ductile deformation limited to the MFZ predated the brecciation.

Evidence for a stretching lineation is restricted to rocks immediately adjacent to the major structural features of the MFZ; however in many localities along the MF no lineation is developed. No variation in metamorphic grade occurs across the MF as previously

interpreted on the metamorphic compilation map of Card (1978) indicating that in this area the MF was not a plane of significant vertical displacement.

8.3 Timing of Geological Events in Area

Rocks in the study area have been affected by several deformational and metamorphic events. To understand the present configuration of the rocks and to develop a tectonic synthesis for the southern Sudbury region, timing of different events is critical.

The ductile deformational event which effected the rocks south of the LLF postdates intrusion of the 1750 Ma Chief Lake batholith. Ductile deformation of the Huronian rocks characterized by the south east trending mineral lineation and a constrictional triaxial strain ellipse mimics that described in the deformed rocks of the Chief Lake batholith (Henderson, 1972). Studies in the Proterozoic granites north of the Grenville Front by Krogh (1970) concluded that the rocks were lineated between 1750 and 1590 Ma. For the purpose of this study, the Grenville Front is defined as the northwestern limit of 1.1 to 1.0 radiometric rock ages and is indicated on Figure (8-1).

Resent structural investigations within the Sudbury Structure by Shanks and Schwerdtner (1989) have concluded that significant south over north reverse displacement occurred along the South Range Shear Zone resulting in significant shortening of the Sudbury Structure in a southeast northwest direction. Shanks and Schwerdtner (1989) determined that the dominantly ductile deformation and corresponding amphibolite facies metamorphism occurred between 1600 and 1238 Ma and therefore postdated the Sudbury event. The timing, deformational style, and regional orientation of Shanks and Schwerdtner's (1989) deformational event is similar to that documented in this study. It is concluded that they are most likely the same event. The 1100-1000 Ma Grenville orogeny has a tectonic front which

parallels the 1600 Ma penetrative deformation that has effected the Huronian aged rocks but is located to the southeast of the LLF.

North of the LLF much of the deformation which resulted in the thrusting of structural blocks postdates the 1850 Ma Sudbury event indicated by the alignment of Sudbury-Type breccia clasts parallel to the regional foliation. It is likely that deformation north of the LLF can be correlated in time with that of the ductile deformation south of the LLF. However it appears that during this deformational event rocks that underwent ductile deformation were juxtaposed along the LLF against rocks that underwent dominantly brittle deformation. The absence of Sudbury-Type breccia south of the LLF can best be explained by the fact that the rocks were deeper and more distant from the location of the Sudbury Structure during the 1850 Ma Sudbury event than their present location.

Much of the ductile deformation in the area can not be attributed to the 950-1100 Ma Grenvillian Orogeny for several reasons. Olivine diabase dykes (1250 Ma) south of the LLF have not been affected by ductile deformation or metamorphism. This sets the minimum age of the ductile deformation at 1250 Ma. To support this, structural analysis by Henderson (1967, 1972), Davidson (1992) and Phemister (1961) immediately east of the study area where high grade gneisses of the Grenville Province are juxtaposed directly against Huronian sediments indicate that the mineral lineation which has deformed 1250 olivine diabase dykes and is therefor indicative of the Grenvillian Orogeny is limited in Huronian rocks to within 1 km of the Grenville Front. Many of the lineated samples in the study area are 20 km from the Grenville Front and none are closer than 8 km. North of the LLF, olivine diabase dykes can be traced across many of the structural blocks without disruption indicating that most of the deformation north of the LLF predates olivine dyke intrusion.

Dextral offsetting of olivine diabase dykes across the MF has been documented by

Davidson (1992) just east of the study area. He estimated a 700 m dextral offset of a distinct pair of dykes. Although no olivine dykes could be traced across the MF in the study area, olivine diabase dyke mapped by Thompson (1962) northeast of Crooked Lake appears to be offset dextrally along the MF on the order of 1500 m. A post 1250 Ma period of deformation was most likely responsible for the brecciation of ductily deformed rocks within the MFZ. Davidson (1992) also noted that the MF cuts through high grade gneisses of the Grenville Province. This would indicate that the MF was active after the Grenvillian Orogeny if the Grenville Front is defined by the transition from lower grade to higher grade metamorphism, rather than the development of a southeast trending down-dip mineral lineation.

One interesting feature that was observed on a radar image of the region was an apparent southeast trending zone of structural deflection (Figure 8-1). Many of the northeast trending structural features appear to be reoriented into a more easterly trend within this zone of deflection. Structures that have been affected include the LLF and the Grenville Front. Within the study area this zone of deflection bisects the LLF in the same location that the regional trend in lineation shifts from southeast to south. Within the Grenville Province, high grade gneisses on strike with this zone of deflection have been folded about an axis that parallels the trend of the zone of deflection (Card 1978). Since rocks of the Grenville Province appear to have been affected, active deformation in this zone of deflection postdates much of the Grenvillian Orogeny. The northern limit of the zone of deflection was the LLF as rocks north of the LLF appear not to have been affected. This zone of deflection could possibly be related to deformation during the post Grenvillian displacement along the MFZ described above. Alternatively the southerly trending lineation in the zone of deflection was produced during the Grenvillian and overprinted the pre-1250 Ma southeast trending lineation

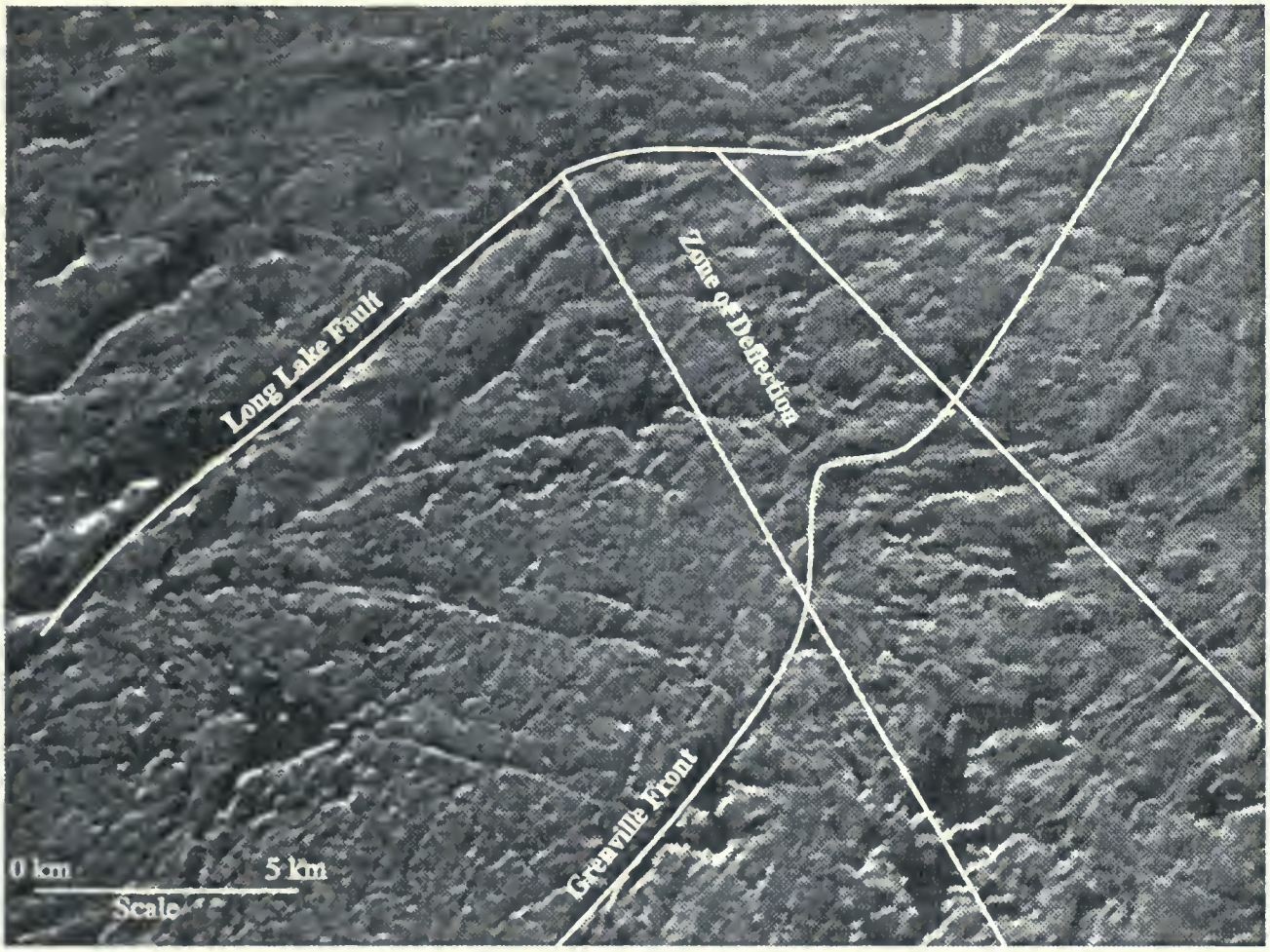

Figure 8-1: Copy of a radar image of the southeast section of the study area showing the south east trending zone of deflection. Not the apparent deflection of both the Long Lake Fault and the Grenville Front. Many of the linear features within the Grenville province appear to have been deflected in the zone (CCRS Airborn SAR, 1990. South Sudbury Line)

observed west of the zone of deflection. If this is the case then deformation attributed to the Grenville Orogeny could have extended for several kilometres beyond the Grenville Front in some isolated areas.

It is apparent that significant south over north reverse shear occurred along the LLF between 1750 and 1250 Ma and was part of a regional reverse faulting deformational event in the southern Sudbury area. Vertical displacement along the LLF resulted in the juxtaposing of rocks that underwent ductile deformation to the south with similar rocks that underwent brittle deformation to the north. There is evidence for a post-1250 Ma strike slip sense of displacement along the MFZ and possibly the LLF. As well there is some evidence that post-Grenvillian deformation may have had a limited effect in the area.

Chapter 9

Conclusions

Metasedimentary rocks in the study area have been correlated with the Hough Lake and Quirke Lake Groups of the Huronian Supergroup and form the southern section of a northeast trending and southeast younging corridor that separates the Proterozoic granites of the Chief Lake batholith to the south from the mafic intrusive rocks of the Sudbury Igneous Complex to the north.

Two major structural features cut across the study area, namely the MFZ and the LLF. Based on structural investigation, the Long Lake Fault was a more significant plane of displacement during post Sudbury event deformation. Huronian rocks south of the LLF are characterized by a southeast trending down dip lineation. In addition these rocks display a well developed quartz c-axis fabric characterized by the development of a strong Maxima I position which is attributed to glide along the prism plane in the <a> axis direction. No evidence for prism glide was found in the rocks north of the LLF. Possible kinematic interpretation of quartz c-axis fabrics indicate that the rocks south of the LLF underwent south over north reverse shearing during amphibolite facies metamorphic conditions.

Computer based ACF analysis was found to be a useful tool in the determination of deformed quartz grain characteristics, including average grain size, shape and long axis orientation. Regional ACF analysis of the Mississagi quartzite revealed that the LLF represents the northern limit of penetrative ductile deformation resulting in the elongation of quartz grains parallel to the stretching lineation. 3-D grain shape analysis using ACF provided a minium estimate of the finite strain ellipse. The strain ellipse is of the triaxial form ($X > Y > Z$) with k values equal to 1.27 and was produced by a period of constrictional

strain. Displacement along the LLF was one of high angle reverse shear in which rocks south of the LLF were raised relative to the rocks north of the LLF. This is based on the fact that at the surface, the LLF separates rocks to the south that have undergone significant ductile deformation and were metamorphosed to amphibolite facies conditions from similar lithologies that have undergone dominantly brittle deformation at greenschist facies to the north.

North of the LLF evidence for ductile deformation is restricted the rocks immediately adjacent to the MFZ. Deformation north of the LLF is characterized by the angular juxtaposing of structural blocks by faulting and not a series of folds as indicated in previous studies in the area. Brittle faulting and the juxtaposing of structural blocks is attributed to southeast-northwest compression of the rocks north of the LLF during the south over north reverse faulting along the LLF.

In a regional context, much of the southern Sudbury region underwent south over north reverse faulting about 1600 Ma. Postdating this deformational event was a period of sediment deposition and intrusion of both felsic and mafic dykes. Dextral strike slip offsetting of these dykes indicate that a late period of deformation occurred along the major structural features in the area. There is indirect evidence that this event post dated the Grenvillian Orogeny dated at 1.1 Ma (Davidson 1986).

References

Baker, M.B. 1917. Long Lake gold mine, Sudbury District. Ontario Burrow of Mines, **XXVI**: 157-162.

Burrows, A.G. and Rickaby, H.C. 1935. Sudbury Nickel Field Restudied. Ontario Department of Mines, **43**: Part 2

Brocoum, S.T. and Dalziel, I.W.D. 1974. The Sudbury Basin, the Southern Province, the Grenville Front and the Penokean Orogeny. Geological Society of America Bulletin, **85**: 1571-1580.

Card, K.D. 1968. Geology of Denison-Waters area, Ontario Deptartment of Mines, Geological Report, **60**: 63 p.

Card, K.D. 1978. Metamorphism of the Middle Precambrian (Aphebian) rocks of the Eastern Southern Province. *In* Metamorphism in the Canadian Shield. Geological Survey of Canada, Paper, **78-10**: 269-282.

Card, K.D., and Hutchinson, R.W. 1972. The Sudbury Structure: its regional geologic setting. *In* New Developments in Sudbury Geology, ed. J.V. Guy-bray, Geological Association of Canada, Special Paper, **10**: 67-78.

Card, K.D., Gupta, V.K., McGrath, P.H. and Grant F.S. 1984. The Sudbury Structure: its regional geological and geophysical Setting, *In* The Geology and Ore Deposits of the Sudbury Structure, eds. E.G. Pye, A.J. Naldrett and P.E. Giblin; Ontario Geological Survey, Special Volume, **1**: 25-45.

Card, K.D., Innes, D.G., and Deblicki, R.L. 1977: Stratigraphy, Sedimentology and Petrology of the Huronian Supergroup in the Sudbury - Espanola Area. Ontario Division of Mines Geoscience Study, **16**: 99 p.

Collins, W.H. 1938. Copper Cliff sheet, Geological Survey of Canada Map No. **292** A.

Cooke, H.C. 1946. Problems of Sudbury Geology, Ontario. Geological Survey of Canada Bulletin, **3**: 77 p.

Corfu, F., and Andrews, J.A. 1986. A U-Pb age for the mineralized Nipissing diabase, Gowganda, Ontario. Canadian Journal of Earth Sciences, **23**: 107-109.

Dalziel, I.W.D., Brown, J.M.and Warren, T.E. 1969. The structural and metamorphic history of the rocks adjasent to the Grenville Front near Sudbury, Ontario, and Mount Wright, Quebec. *In* Age relations in high-grade metamorphic terrains, ed. by H.R. Wynne-Edwards. Geological Association of Canada Special paper, **5**: 207-224.

Davidson, A. 1986. A New Look at the Grenville Front in Ontario. Geological Association of Canada, Field Trip **15**: Guidebook, 31 p.

Davidson, A. 1992. Relationship between faults in the Southern Province and the Grenville Front southeast of Sudbury, Ontario. *In* Current Research, Part C, Geological Survey of Canada, Paper, **92-1C**: 121-127.

Debicki, R.L. 1990. Stratigraphy, Palenvironment and Economic Potenial of the Huronian Supergroup in the Southern Cobalt Embayment. Ontario Geological Survey, **148**: 154p.

Deitz, R.S. 1964. Sudbury Structure as an Astrobleme. Journal of Geology, **72**: 412-434.

Dressler, B.O. 1984a: Sudbury Geological Compilation. Ontario Geological Survey Map 2491, Precambrian Geology Series, 1:50,000 scale.

Dressler, B.O. 1984b. The effects of the Sudbury event and the intrusion of the Sudbury Igneous Complex on the footwall rocks of the Sudbury structure. *In* The Geology and Ore Deposits of the Sudbury Structure, eds. E.G. Pye, A.J. Naldrett and P.E. Giblin; Ontario Geological Survey, Special Volume, **1**: 97-136.

Fairbairn, H.W. 1949. Structural petrology of deformed rocks. Addison Wesley press, Cambridge, Mass.

Flinn, D. 1962. On folding during three-dimentional progressive deformation. Geological Society of London Quarterly Journal, **75**: 385-433.

Fueten F. 1989. Deformation of the quartzo-feldspathic gneisses in the Thompson Belt, Manitoba. Ph.D. thesis, University of Toronto, Ontario, Canada.

Fueten, F. 1992. Tectonic interpretation of systematic variations in quartz c-axis fabrics across the Thompson Belt. Journal of Structural Geology, **14**: 775-789.

Fueten, F., Robin, P-Y-F., and Stephens, R. 1991. A model for the development of a domainal quartz c-axis fabric in a coarse grained gneiss. Journal of Structural Geology, **13**: 1111-1124.

Fueten, F. and Redmond, D.J. 1992. Structural studies in the Southern Province, south of Sudbury, Ontario. *In* Current Research, Part C, Geological Survey of Canada Paper, **92-1C**: 179-187.

Gapais, D., Bale, P., Choukroune, P., Cobbold, P.R., Mahjoub, Y., Marquer, D. 1987. Bulk kinematics from shear zone patterns: some field examples. Journal of Structural Geology, **9**: 635-646.

Grant, J.A., Pearson, W.J., Phemister, T.C., and Thomson, J.E. 1962. Geology of Bi der, Dill, Neelon, and Dryden Townships, District of Sudbury. Ontario Department of Mines Geological Report, **9**: 1-24.

Heilbronner, R.P. 1992. The autocoorelation function: an image processing tool for fabric analysis. Tectonophysics, **212**: 351-370.

Henderson, J.R. 1967. Structural and petrologic relations across the Grenville Province - Southern Province Boundary, Sudbury District, Ontario; unpublished Ph.D. thesis, McMaster University, 119 p.

Henderson, J.R. 1972. Deformation of the Killarney Granite, Ontario, Canada; 24th IGC-Section, **3**: 505-515

Hobbs, B.E. 1968. Recrystallization of single srystals of quartz. Tectonophysics, **6**: 353-401.

Krogh, T.E. 1967. Rb/Sr chronology of the granitic rocks southeast of Sudbury, Ontario. *In* Davis, G.L., Hart, S.R., Aldrich, L.T., Krogh, T.E. and Munizaga, F., Geochronology, Carnegie Institution of Washington. Yearbook, **65**: 1965-1966.

Krogh, T.E. 1970. Isotopic ages along the Grenville Front in Ontario. Carnegie Institution of Washington Yearbook, **68**: 309-313.

Krogh, T.E., Corfu, F., Davis, D.W., Dunning, G.R., Heaman, L.M., Kamo, S.L., Machado, N., Greenough, J.D., and Nakamura, E.1987. Precise U-Pb isotopic ages of diabase dykes and mafic to ultramafic rocks using trace amounts of baddeleyite and zircon, *In* Mafic Dyke Swarms, eds. H.C. Halls and W.F. Fahrig; Geological Association of Canada, Special Paper, **34**: 147-152.

Krogh, T.E., McNutt, R.H., and Davis, G.L. 1982: Two high precision U-Pb zircon ages for the Sudbury Nickel Irruptive. Canadian Journal of Earth Sciences, **19**: 723-728.

Lister, G.S. and Dornsiepen, U.F. 1982. Fabric transition in the Saxony Granulite Terrane. Journal of Structural Geology, **4**: 81-92.

Lister, G.S., and Hobbs, B.E. 1980. The simulation of Fabric Development During Plastic deformation and its Application to Quartzite: the influence of deformation history. Journal of Structural Geology, **2**: 335-370.

Lister, G.S., and Williams, P.F. 1980. Fabric Development in Shear Zone: Theoretical Control and Observed Phenomena. Journal of Structural Geology, **1**: 283-297.

Long, D.G.F. 1977. Resedimented conglomerates of Huronian (lower Aphebian age), from the north shore of lake Huron, Ontario, Canada. Canadian Journal of Earth Sciences, **14**: 2495-2509.

Misyashiro, A. 1961. Evolution of metamorphic belts, Journal of Petrology, **16**: 1-21.

Pfeiderer, S., Ball, D.G.A and Bailey, R.C. 1992. A comuter program for the determination of the two-dimensional auto-correlation function of digital images. Computers and Geosciences (in press).

Phemister, T.C. 1961. The boundary between the Timiskaming and grenville subprovinces in the township of Neelon, Dryden, Dill and Broder, district of Sudbury, Ontario Department of Mines preliminary Report, **1961-5**.

Poirier, J.P. 1985. Creep of Crystals. Cambridge Earth Science Series, Cambridge University Press, Cambridge.

Price, G.P. 1985. Preferred orientation in Quartzites. in Preferred Orientations in Deformed Metals and Rocks: An Introduction to Modern Textural Analysis, ed. H-R. Wenk, Academic Press, Orlando: 385-406.

Ramsay, J.G. and Huber, M.I. 1983. The techniques of Modern Structural Geology, Volume 1: Strain analysis. 303p.

Ransom, D.M. 1971. Host Control of Recrystallized Quartz Grains. Mineralogical Magazine, **38**: 26-29.

Robin, P-Y-F. (in prep). Strain analysis from closed passive markers of any shape, the inertia tensor method.

Robin, P-Y-F., and Jowett, C.E. 1986. Computerized Density Countuoring and Statistical Evaluation of Orientation Data using Counting Circles and Continuous Weighting Function. Tectonophysics, **121**: 207-223.

Seabright, R. 1992. Structural Analysis of Anastomosing Shear Zones along the Murray Fault, Sudury area, Ontario. unpublished Bsc thesis, Brock University, St Catharines, Ontario.

Shanks, W.S., and Schwerdtner, W.M. 1989. Deformation of the Sudbury Structure and its Footwall. *In* Geoscience Research Grant Program, Summary of Research 1988-1989, ed. V.G. Milne, Ontario Geological Survey, Miscellaneous Paper, **144**: 4-17

Spaven, H,R. 1966. Granite tectonics in part of the Eden township, Sudbury district of Ontario. unpublished Master's thesis, McMaster University, Hamilton Ontario.

Speers, E.C. 1957. The age relationship and origin of the common Sudbury breccia. Journal of Geology, **65**: 497-514.

Starkey, J., and Cutforth, C. 1979. A Demonstration of the Interdependence of the Degree of Quartz Preferred Orientation and the Quartz Content of Deformed Rocks. Canadian Journal of Earth Science, **15**: 841-847.

Thompson, J.E. 1962. Broder, Dill, Neelon and Dryden Township, District of Sudbury, Ontario Department of Mines compalation Map, **2017**, scale 1:31 680.

Turner, F.J. 1980. Metamorphic Petrology: mineralogical, field and tectonic aspects, second edition. International series in the earth and planetary sciences. Hemishere publishing company.

Urai, J.L., Means, W.D., and Lister, G.S. 1986. Dynamic Recrystallization of Minerals. Geophysical Monograph, **36**: 161-199.

Van Schmus, W.R. 1965. The geochronology of the Blind River-Bruce Mines area. Ontario, Canada; Journal of Geology, **73**: 755-780.

Van Schmus, W.R. 1976. Early and Middle Proterozoic history of the Great Lakes area, North America. Royal Society of London, Philosophical Transactions, **12**: 1175-1189.

Woodcock, N.H. 1977. Specification of fabrics shapes using an eigenvalue method. Geological Society of America Bulletin, **88**: 1231-1236.

Yates, A.B. 1948. Properties of the International Nickel Company of Canada. in Structural Geology of Canadian Ore deposits, Canadian Institute of Mining and Metallurgy, Jubile Volume, **7**: 596-617.

Yardley, B.W.D. 1989. An introduction to Metamorphic Petrology. Longman Earth Science Series.

Zolnai, A.I., Price, R.A., and Helmstaedt, H. 1984. Regional cross section of the Southern Province adjacent to Lake Huron, Ontario: implications for the tectonic significance of the Murray Fault Zone. Canadian Journal of Earth Sciences, **21**: 447-456.

Appendix 1

Contoured plots and statistical information
for bedding plots used in Figure 4-1

Pole of Bedding plot for rocks north of the MFZ

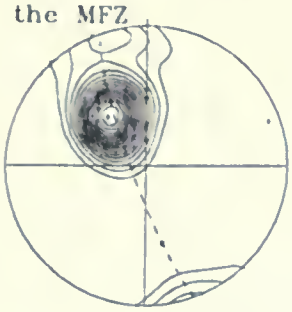

Pole of Bedding plot for rocks within the MFZ

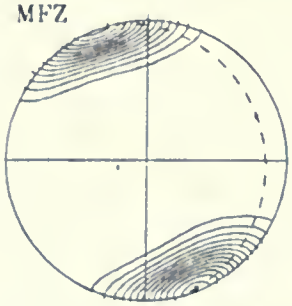

Pole of Bedding plot for rocks between the MFZ and the LLF

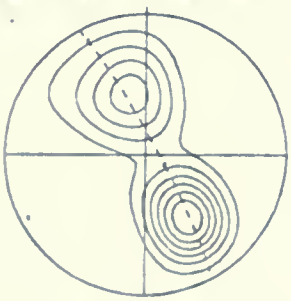

Pole of Bedding plot for rocks north of the LLF

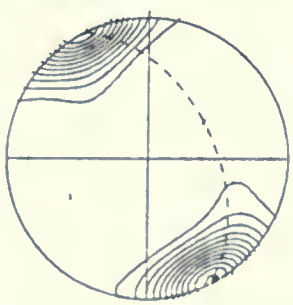

Pole of Bedding plot for rocks south of the LLF

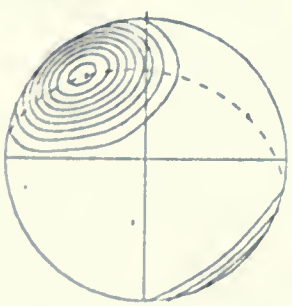

Trend of lineation plot for rocks south of the LLF

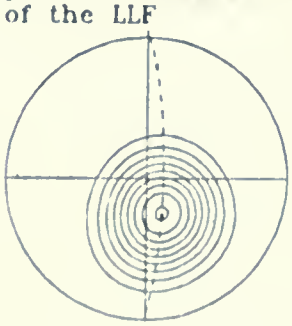

Appendix 2

Contoured plots and statistical information
for quartz c-axis fabrics in Figure 5-5

DR 162

N = 150 E = 4.25
k = 35.33 Sigma = 1.42
(Peak - E)/Sigma = 11.6
Peak position : 97.6 / 17.1

DR 163

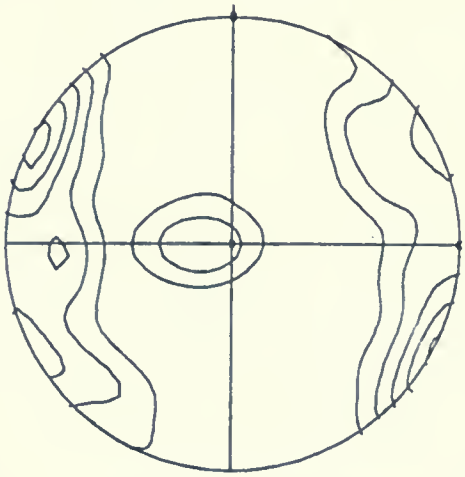

N = 150 E = 4.25
k = 35.33 Sigma = 1.42
(Peak - E)/Sigma = 8.8
Peak position : 299.4 / 2.3

DR 164

N = 150 E = 4.25
k = 35.33 Sigma = 1.42
(Peak - E)/Sigma = 7.6
Peak position : 277.1 / 11.4

DR 169

N = 150 E = 4.25
k = 35.33 Sigma = 1.42
(Peak - E)/Sigma = 7.8
Peak position : 270.0 / 85.5

DR 28

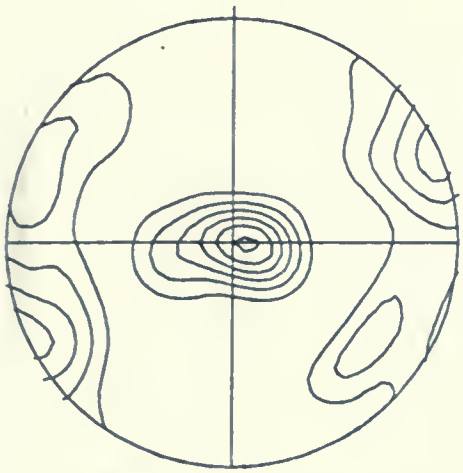

N = 150 E = 4.25
k = 35.33 Sigma = 1.42
(Peak - E)/Sigma = 10.6
Peak position : 90.0 / 85.5

DR 32

N = 150 E = 4.25
k = 35.33 Sigma = 1.42
(Peak - E)/Sigma = 6.7
Peak position : 90.0 / 90.0

DR 220

N = 150 E = 4.25
k = 35.33 Sigma = 1.42
(Peak - E)/Sigma = 10.8
Peak position : 90.0 / 90.0

DR 83

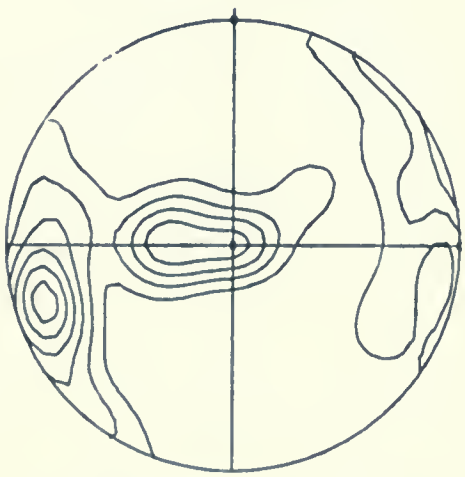

N = 150 E = 4.25
k = 35.33 Sigma = 1.42
(Peak - E)/Sigma = 11.3
Peak position : 251.6 / 13.2

DR 174

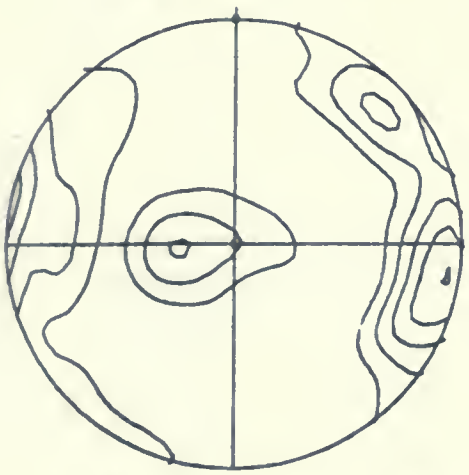

N = 150 E = 4.25
k = 35.33 Signa = 1.42
(Peak - E)/Signa = 8.1
Peak position : 100.0 / 4.6

DR 73

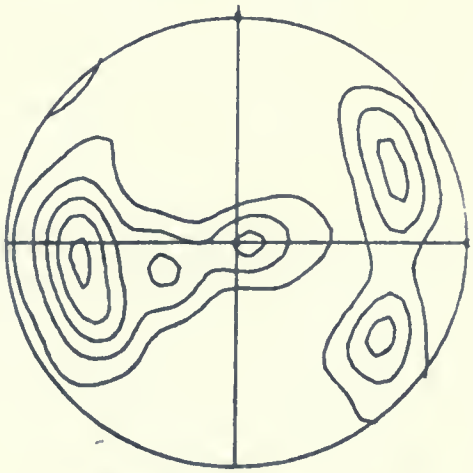

N = 150 E = 4.25
k = 35.33 Signa = 1.42
(Peak - E)/Signa = 8.6
Peak position : 265.2 / 33.5

DR 219

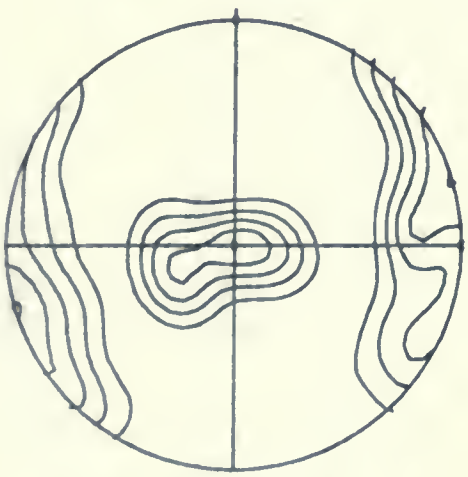

N = 150 E = 4.25
k = 35.33 Signa = 1.42
(Peak - E)/Signa = 8.1
Peak position : 253.6 / 1.8

DR 214

N = 149 E = 4.24
k = 35.11 Signa = 1.41
(Peak - E)/Signa = 11.2
Peak position : 47.7 / 18.5

DR 210

N = 150 E = 4.25
k = 35.33 Sigma = 1.42
(Peak - E)/Sigma = 10.8
Peak position : 251.6 / 75.7

DR 149

N = 150 E = 4.25
k = 35.33 Sigma = 1.42
(Peak - E)/Sigma = 6.0
Peak position : 116.6 / 37.9

DR 146

N = 150 E = 4.25
k = 35.33 Sigma = 1.42
(Peak - E)/Sigma = 5.2
Peak position : 243.4 / 26.4

DR 128

N = 150 E = 4.25
k = 35.33 Sigma = 1.42
(Peak - E)/Sigma = 8.7
Peak position : 93.8 / 17.6

DR 47

N = 150 E = 4.25
k = 35.33 Sigma = 1.42
(Peak - E)/Sigma = 5.6
Peak position : 298.6 / 31.8

DR 48

N = 150 E = 4.25
k = 35.33 Sigma = 1.42
(Peak - E)/Sigma = 7.2
Peak position : 53.1 / 17.8

DR 139

N = 150 E = 4.25
k = 35.33 Sigma = 1.42
(Peak - E)/Sigma = 6.8
Peak position : 58.4 / 16.3

DR 49

N = 150 E = 4.25
k = 35.33 Sigma = 1.42
(Peak - E)/Sigma = 2.8
Peak position : 116.6 / 26.4

DR 186

N = 150 E = 4.25
k = 35.33 Signa = 1.42
(Peak - E)/Signa = 4.9
Peak position : 285.9 / 20.2

DR 216

N = 150 E = 4.25
k = 35.33 Signa = 1.42
(Peak - E)/Signa = 6.9
Peak position : 104.9 / 14.8

DR 85

N = 150 E = 4.25
k = 35.33 Signa = 1.42
(Peak - E)/Signa = 7.9
Peak position : 270.8 / 33.7

DR 18

N = 150 E = 4.25
k = 35.33 Sigma = 1.42
(Peak - E)/Sigma = 6.0
Peak position : 246.8 / 16.5

DR 46

N = 150 E = 4.25
k = 35.33 Sigma = 1.42
(Peak - E)/Sigma = 3.8
Peak position : 55.0 / 32.7

D. Redmond

1